VOLUME 84 NO. WW2
MARCH 1958

# JOURNAL of the

# Waterways and Harbors Division

PROCEEDINGS OF THE

AMERICAN SOCIETY OF CIVIL ENGINEERS

## BASIC REQUIREMENTS FOR MANUSCRIPTS

This Journal represents an effort by the Society to deliver information to the reader with the greatest possible speed. To this end the material herein has none of the usual editing required in more formal publications.

Original papers and discussions of current papers should be submitted to the Manager of Technical Publications, ASCE. The final date on which a discussion should reach the Society is given as a footnote with each paper. Those who are planning to submit material will expedite the review and publication procedures by complying with the following basic requirements:

1. Titles should have a length not exceeding 50 characters and spaces.

2. A 50-word summary should accompany the paper.

3. The manuscript (a ribbon copy and two copies) should be double-spaced on one side of 8½-in. by 11-in. paper. Papers that were originally prepared for oral presentation must be rewritten into the third person before being submitted.

4. The author's full name, Society membership grade, and footnote reference stating present employment should appear on the first page of the paper.

5. Mathematics are reproduced directly from the copy that is submitted. Because of this, it is necessary that capital letters be drawn, in black ink, ⅛-in. high (with all other symbols and characters in the proportions dictated by standard drafting practice) and that no line of mathematics be longer than 6½-in. Ribbon copies of typed equations may be used but they will be proportionately smaller in the printed version.

6. Tables should be typed (ribbon copies) on one side of 8½-in. by 11-in. paper within a 6½-in. by 10½-in. invisible frame. Small tables should be grouped within this frame. Specific reference and explanation should be made in the text for each table.

7. Illustrations should be drawn in black ink on one side of 8½-in. by 11-in. paper within an invisible frame that measures 6½-in. by 10½-in.; the caption should also be included within the frame. Because illustrations will be reduced to 69% of the original size, the capital letters should be ⅛-in. high. Photographs should be submitted as glossy prints in a size that is less than 6½-in. by 10½-in. Explanations and descriptions should be made within the text for each illustration.

8. Papers should average about 12,000 words in length and should be no longer than 18,000 words. As an approximation, each full page of typed text, table, or illustration is the equivalent of 300 words.

Further information concerning the preparation of technical papers is contained in the "Technical Publications Handbook" which can be obtained from the Society.

---

Reprints from this Journal may be made on condition that the full title of the paper, name of author, page reference (or paper number), and date of publication by the Society are given. The Society is not responsible for any statement made or opinion expressed in its publications.

This Journal is published by the American Society of Civil Engineers. Publication office is at 2500 South State Street, Ann Arbor, Michigan. Editorial and General Offices are at 33 West 39 Street, New York 18, New York. $4.00 of a member's dues are applied as a subscription to this Journal.

AT,BD,CP,CO,IIW,IR,SU,WW,PL.

Journal of the

# WATERWAYS AND HARBORS DIVISION

Proceedings of the American Society of Civil Engineers

WATERWAYS AND HARBORS DIVISION
EXECUTIVE COMMITTEE
Roger H. Gilman, Chairman; Lawrence B. Feagin, Vice-Chairman;
Lewis C. Coxe; Joe W. Johnson; Evan W. Vaughan, Secretary

COMMITTEE ON PUBLICATIONS
Jay V. Hall, Jr., Chairman; Joseph M. Caldwell;
Ellsworth I. Davis; James W. Dunham

CONTENTS

March, 1958

Papers

| | Number |
|---|---|
| Selection of Design Wave for Offshore Structures by Charles L. Bretschneider | 1568 |
| Shipboard Hydraulic Breakwater by R. A. Dilley | 1569 |
| The Welland Canal by W. A. O'Neil | 1570 |
| Forces Induced on a Large Vessel by Surge by John T. O'Brien and D. I. Kuchenreuther | 1571 |
| Contractor's Planning for Navigation Locks by F. J. Larkin | 1572 |
| Breaking Wave Force Prediction by R. L. Wiegel and R. E. Skjei | 1573 |
| Discussion | 1579 |

Copyright 1958 by the American Society of Civil Engineers.

Paper 1568 March, 1958 WW 2

Journal of the
WATERWAYS AND HARBORS DIVISION
Proceedings of the American Society of Civil Engineers

# SELECTION OF DESIGN WAVE FOR OFFSHORE STRUCTURES[a]

Charles L. Bretschneider,* A.M. ASCE
(Proc. Paper 1568)

## ABSTRACT

Methods are presented for selecting for offshore structures the design wave, crest elevation, wave length and the maximum horizontal particle velocity at the crest. The problem is somewhat different in regards to coastal structures—sea walls, rubble mound breakwaters, levees, etc., and will not be discussed in this paper. Essentially, this paper is the third of a series intended to supplement the information presented in an earlier report on Surface Waves and Offshore Structures by Reid and Bretschneider.(1) The first paper "Hurricane Design Wave Practices" by Bretschneider(2) presents methods for computing the significant and maximum waves for a hurricane moving from deep water over the Continental Shelf to the coast. The second paper "Approximate Response of Water Level on a Sloping Shelf to a Wind Fetch which Moves Towards Shore" by Reid(3) presents methods for obtaining hurricane storm surge.

Wave data from various sources, supplemented by a limited amount of wave theory required for the development of generalized graphs are given in Appendix I. This information is used to revise some of the original graphs of reference (1). The wave data include some from the large tank at the Beach Erosion Board; some hurricane wave data from Lake Okeechobee, Florida;(4) model data by Danel(5) of France; that summarized by Munk;(6) and that reported by Mason(7) from the small tank at the Beach Erosion Board.

Much of the material in the present paper was originally initiated by Professor Robert O. Reid of Texas A. & M. as presented in reference (1), and therefore, should be credited accordingly.

Note: Discussion open until August 1, 1958. A postponement of this closing date can be obtained by writing to the ASCE Manager of Technical Publications. Paper 1568 is part of the copyrighted Journal of the Waterways and Harbors Division, Proceedings of the American Society of Civil Engineers, Vol. 84, No. WW 2, March, 1958.

a. Presented at ASCE Convention, New York, N. Y., October, 1957.

* Hydraulic Engr. (Research), Beach Erosion Board, Corps of Engrs., U. S. Dept. of the Army, Washington, D. C.

## INTRODUCTION

Methods of predicting maximum waves for hurricane design wave problems have been presented in reference (1). In regards to both the design of offshore structures and coastal structures, it is important to realize a design wave height, period, crest elevation and wave length. In many cases there may be a number of waves for selection. For the design of an offshore platform supported by piling, it is necessary that the underside of the deck clear the crest of the wave. The wave length and surface profile are important when computing total forces and overturning moments induced by the wave on a series of supporting piles. The maximum horizontal particle velocity at the crest gives a check against the wave theory used to compute the internal velocity field.

The selection of the design wave consists of the following steps:

I. Calibration
   (a) Storm Surge Formulae
   (b) Wave Forecasting Formulae and Techniques

II. Frequency Study
   (a) Wave Statistics
   (b) Hurricane Frequency Study

III. Predictions for Design
   (a) Storm Surge
   (b) Significant Wave Height and Period
   (c) Maximum Wave Height and Corresponding Wave Period
   (d) Crest Elevation of Maximum Wave
   (e) Wave Length of Maximum Wave

The above steps are discussed below:

### Calibration

It is necessary to calibrate storm surge prediction formulae and techniques to take into account deviations between observed and predicted high water levels. This is particularly evident in and near coastal areas where irregularities in both bottom topography and coastal features play important roles in modification of storm surges.

Methods of predicting storm surges on the open coast are given by Reid[3] and Freeman et al,[8] among others. In using any method, storm surge hydrographs should be used where available for calibration, such that when applied to the design storm, a reasonable estimate of storm surge is obtained. This requires the analysis of all past hurricanes, where such data are available. In those cases where no data are available, a nearby and similar location where data are available may be used. As a first approximation to the solution of the storm surge one may use directly the method proposed by Reid.[3]

Calibration of wave forecasting formulae and techniques is also necessary to take into account variabilities in individual techniques and locations. A number of methods are available for predicting waves both in deep and shallow water. In the case of deep water there are four methods generally used: Sverdrup-Munk-Bretschneider method,[9] Pierson-Neumann-James method,[10] Darbyshire method[11] and Suthon-Braceline method.[12] All the

above have incorporated therein inherent characteristics associated with both the procurement of data from various locations and also the method of analysis and interpretation of these data by the individual contributors. A very objective verification study of the above methods was made by Roll,[13] and the general conclusion was that each method works better for the particular region from which the principal data were obtained. Perhaps, even better verification might have been made provided the individual contributors made the forecast, each using their own methods and techniques. The graphical approach method, utilized by Wilson,[14] should be a useful tool for calibration purposes.

For wind waves in shallow water, there exist two methods: Thijsse[15] and Bretschneider,[16] each giving reasonably consistent results for shallow water of constant depth. The method of Bretschneider,[17] extended to the Continental Shelf, is calibrated, based on hurricane wind and wave data from Lake Okeechobee, Florida,[4] and some ordinary wind wave data from the Gulf of Mexico.[18] Although this method is used to predict hurricane waves over the Continental Shelf, improvements in the techniques can be expected when hurricane wave data become available from the Continental Shelf for a refined calibration. An example of computations illustrating this method is given in reference 2.

## Frequency Study

Much data on wave statistics for various locations along the United States shores have been compiled by use of wave hindcasting techniques. The data, summarized in various Beach Erosion Board Technical Memoranda, are given in terms of the significant height and period. The importance of these wave statistics can be considered, where hurricanes are not a menace, for certain design problems other than offshore structures, and for planning marine operations. It must be emphasized that the maximum wave may be as much as 1.87 times the significant height.

To date, little information is available on the frequency of hurricane waves, as far as actual observations are concerned. However, hurricane wave statistics for deep water of the Gulf of Mexico have recently been compiled by Wilson[19] using the graphical approach to wave forecasting.[14] For most design problems these data must be brought across the Continental Shelf taking bottom friction and refraction into account as further generation takes place. This report might be a source for obtaining the design wave for locations in the Gulf of Mexico.

The selection of the design wave can be obtained by use of an alternate method, wherein the design storm is first selected. This method consists of a frequency study of all hurricanes and other major storms passing a given length of coastline. Generally a 300 to 400-mile section of coastline is selected in order to obtain a sufficient number of hurricanes for a frequency study. The frequency study is then normalized in terms of 100 miles of coastline. For example, consider the hurricanes of record which entered the United States coast between Jacksonville, Florida and Cape Hatteras, North Carolina. The distance between Jacksonville and Cape Hatteras is close to 430 nautical miles. Between 1893 and 1955, 17 hurricanes entered this part of the coast. Insufficient data are available for hurricanes occurring before 1893. These 17 hurricanes are summarized in Table A in descending order of

TABLE A

Frequency of 17 Hurricanes Between Cape Hatteras and Jacksonville (1893 - 1955)

| | Date | R Nautical Miles | $\Delta P$ Inches of Mercury | $R\Delta P$ | f (percent) |
|---|---|---|---|---|---|
| 1 | 9/31/99 | 110 | 1.22 | 134.2 | 2.94 |
| 2 | 10/15/54 | 36 | 2.31 | 83.2 | 8.82 |
| 3 | 9/19/55 | 50 | 1.46 | 73.0 | 14.71 |
| 4 | 8/12/55 | 45 | 1.40 | 63.0 | 20.59 |
| 5 | 12/ 2/25 | 54 | 1.02 | 55.1 | 26.47 |
| 6 | 8/27/93 | 34 | 1.64 | 50.8 | 32.35 |
| 7 | 9/13/13 | 39 | 1.16 | 45.2 | 38.23 |
| 8 | 9/ 2/98 | 32 | 1.40 | 44.8 | 44.12 |
| 9 | 8/17/55 | 45 | 0.82 | 36.9 | 50.00 |
| 10 | 9/17/06 | 37 | 0.99 | 36.6 | 55.88 |
| 11 | 9/13/93 | 23 | 1.59 | 36.5 | 61.76 |
| 12 | 8/11/40 | 27 | 1.19 | 32.1 | 67.64 |
| 13 | 8/28/11 | 27 | 1.05 | 28.4 | 73.53 |
| 14 | 8/14/53 | 30 | 0.79 | 23.7 | 79.41 |
| 15 | 10/15/47 | 12 | 1.38 | 16.6 | 85.29 |
| 16 | 8/11/14 | 19.5 | 0.76 | 14.8 | 91.17 |
| 17 | 8/30/52 | 20 | 0.95 | 11.4 | 97.05 |

(Values R and $\Delta P$ were furnished by Hydrometeorological Section, U. S. Weather Bureau)

the Energy Index, $R\Delta P$. The frequency of occurrence of the above hurricanes is obtained by use of the Beard's formula.(2)

$$f = \frac{100\ (N-\frac{1}{2})}{M}\ , \text{ where}$$

$f$ = percent of occurrence (frequency)

$N$ = the order of $R\Delta P$ (1 to 17)

$M$ = the total number of hurricanes, 17

The information from Table A is plotted on the log-probability graph, Figure 1, and it is seen that the intensity along this part of the coast is slightly greater than for the United States as a whole (as given by Reid; see Figure 7, reference 2).

Since 17 hurricanes entered a 430 mile section of coast in 62 years, one obtains $\frac{62}{17} \times \frac{430}{100} = 15.7$ years as a hurricane recurrence interval, which means on the long run average that the center of a hurricane will enter a 100 mile section of the east coast between Cape Hatteras and Jacksonville once in 15.7 years. The recurrence interval for any particular strength of storm for Figure 1 is obtained from

$$I = \frac{15.7}{f}\ 100, \text{ or } f = \frac{1570}{I}$$

Figure 1 can be used to obtain the Energy Index $R\Delta P$ for a particular recurrence interval, say once in 100 years, whence $f = 1570/100 = 15.7$ percent, and from Figure 1 $R\Delta P = 69$. From Table I it is seen that the radius of maximum wind will be between 45 and 50 nautical miles and $\Delta P$ between 1.46 and 1.40 inches of mercury. Further investigations reveal that such a hurricane may have a forward speed $V_F$ between 7 and 14 knots (Table I, reference 2). Hence the design storm is selected for a recurrence interval of once in 100 years, per one hundred miles of coast:

$R$ = 48 nautical miles

$\Delta P$ = 1.44 inches of mercury

$R\Delta P$ = 69

$V_F$ = 10.5 knots

## Design Wave Predictions

Once the design storm has been determined and the prediction formulae calibrated, computations are made for storm surge and significant waves. Methods used are given in the references. An example is worked out in reference 2 based on Hurricane Hazel of October 15, 1954. For this example $R\Delta P = 83.2$, corresponding to $f = 9.0$ percent from Figure 1. The recurrence interval in years per 100 miles of coast is $I = 1570/9 = 175$ years. In this example it was found for a mean low water depth, $d_o = 74$ feet, the total depth

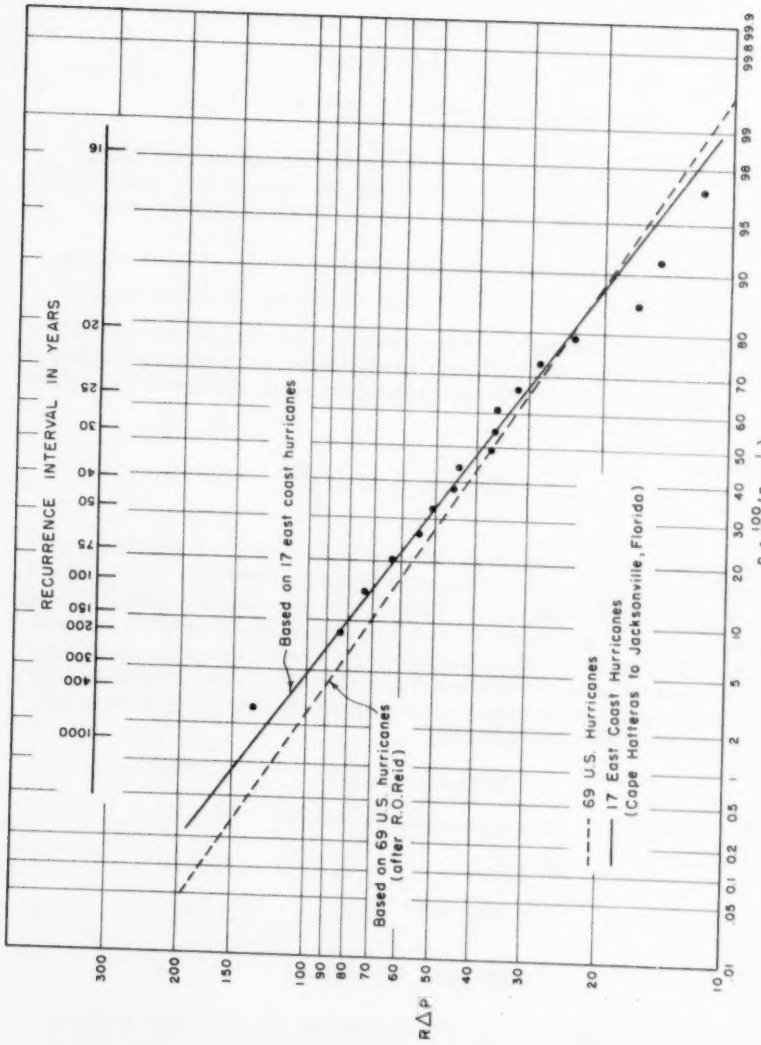


FIGURE 1 FREQUENCY OF HURRICANE RΔP VS PERCENT OF OCCURRENCE
(R in nautical miles ΔP in inches of mercury)

with surge applied d = 85.3, and $H_{max}$ = 39.6 feet and T = 11.63 seconds.

The crest elevation above d = 85.3 feet is obtained by use of Figure 2.* Compute $H/T^2 = .293$ and $d/T^2 = .63$, and read from Figure 2, $\eta_o/H = .69$. Hence $\eta_o = (39.6)(.69) = 27.3$ feet, and the crest elevation will be 85.3 + 27.3 = 112.6 feet above sea bottom.

The wave length is obtained from

$$L = \left(\frac{L}{L_A}\right) \frac{gT^2}{2\pi} \tanh \frac{2\pi d}{L_A}, \text{ where}$$

$L_A$ is the Airy Wave Length and $L/L_A$ is a correction factor for wave steepness and is obtained by use of Figure 3. The deep water Airy Wave Length is $L_o = 5.12\ T^2 = 693$ feet. Compute $d/L_o = \frac{85.3}{693} = .123$ and from Tables** by Wiegel,(21) $\tanh \frac{2\pi d}{L_A} = \frac{L_A}{L_o} = .7656$ (or from Figure 4 $\frac{L_A}{L_o} = .77$). From Figure 3 for $d/T^2 = .63$ and $H/T^2 = .293$ read $L/L_A = 1.06$.

Thus L = 1.06 (693)(.77) = 565 feet. The wave celerity $C = L/T = 565/11.63$ = 48.5 feet/second.

The maximum horizontal particle velocity at the crest can be obtained from Figure 5. Compute, $\frac{2g\eta_o}{C^2} = \frac{(64.4)(27.3)}{C^2} = .75$. From Figure 5 read $u_{max}/C = 0.5$. Thus $u_{max} = 0.5\ (48) = 24$ feet/second.

It is interesting to compare the above values with those obtained by use of the Airy(22, 23) Wave Theory. $\eta_o = \frac{H}{2} = (39.6)/2 = 19.8$ feet, or 7.5 feet lower than that given for this example. The Airy Wave Length is $L_A = 693\ (.7656) = 531$ feet or 32 feet shorter. The wave speed is $C = L/T = 45.6$ feet/seconds. The maximum horizontal particle velocity is given by $u_{max} = \frac{gH}{2C} = 13.8$ feet/second. The Airy theory is usually extended to include the finite height, from which $u_{max}$ is given by

$$u_{max} = \frac{\pi H}{T} \frac{\cosh \frac{2\pi (d+.5H)}{L}}{\sinh \frac{2\pi d}{L}} = 17.0 \text{ feet/second}$$

which is 40 percent less than that obtained by use of Bernoulli's equation (Figure 5). Since the force on a pile is proportional to the velocity squared one obtains $(24/17)^2 = 2.0$ as the ratio of maximum crest force obtained by the two methods, assuming the same drag coefficient in either case.

Thus if the Airy Wave Theory is used for design conditions, an added safety

---

* See Appendix I for development of Figures 2, 3 and 5.

** The solution of $L_A/L_o \tanh 2\pi d/L_A$ is given in Figure 4 in terms of $d/T^2$.

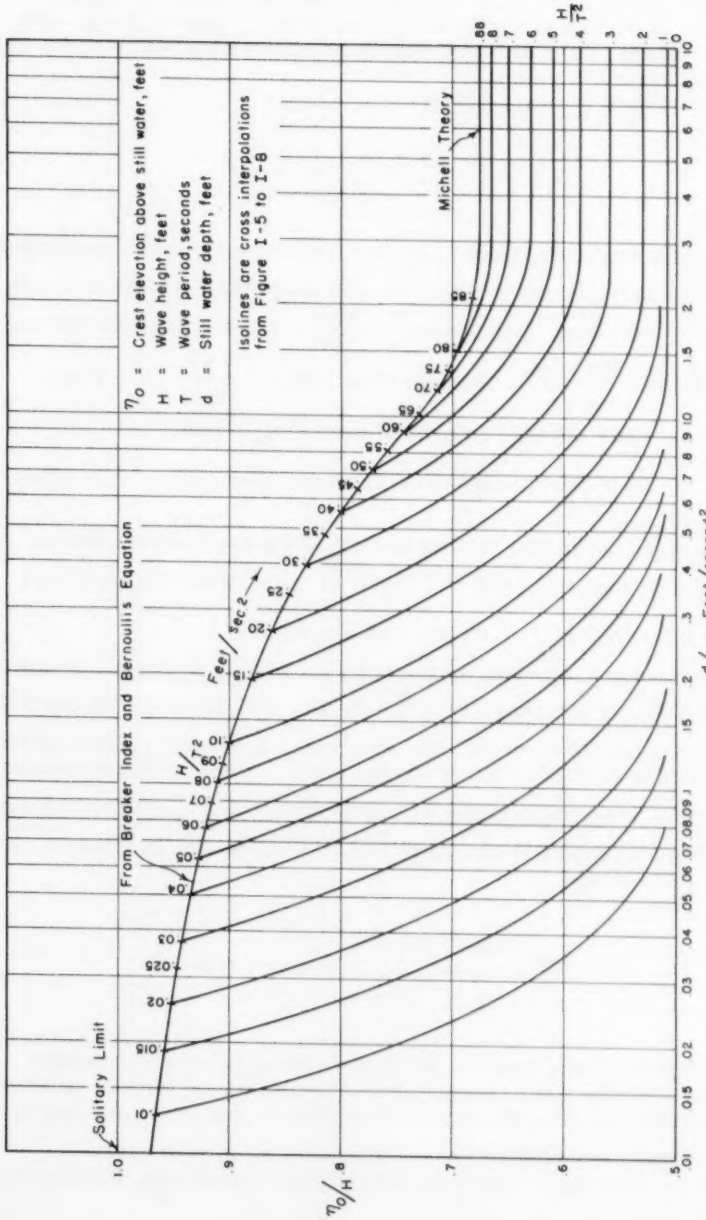


FIGURE 2. RATIO OF CREST ELEVATION ABOVE STILL WATER TO WAVE HEIGHT

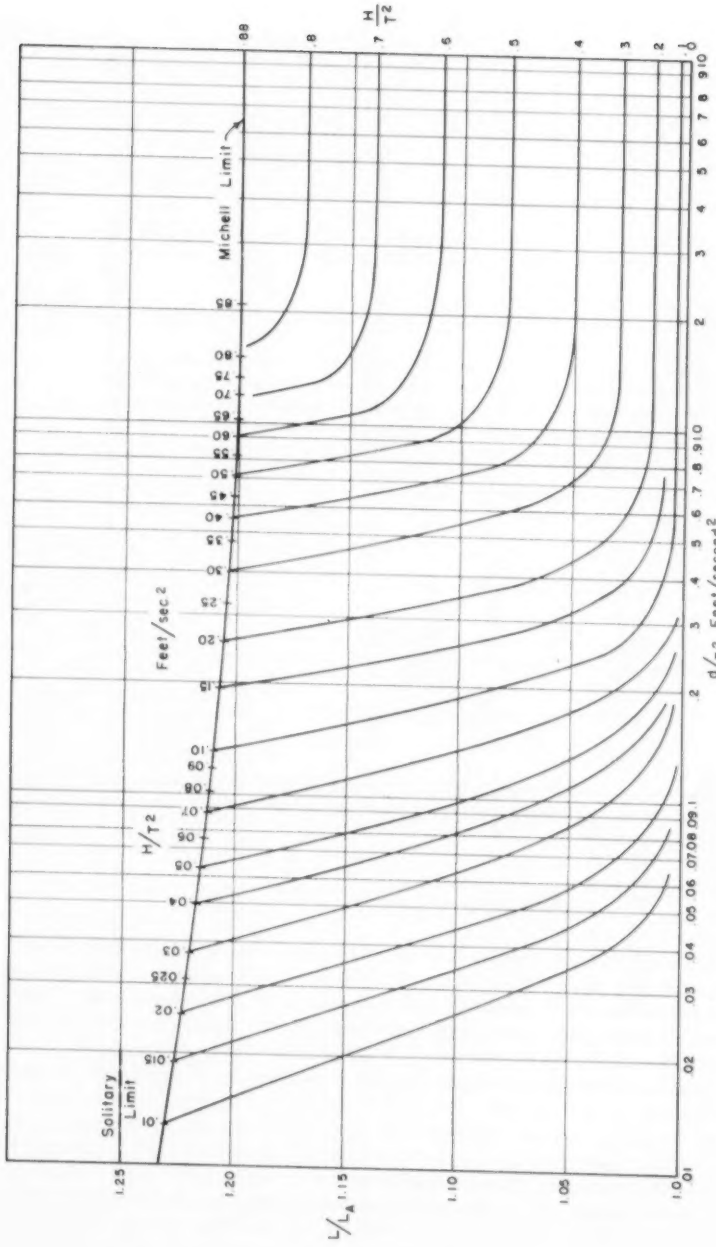


FIGURE 3. CORRECTION FACTOR FOR WAVE LENGTH DUE TO STEEPNESS

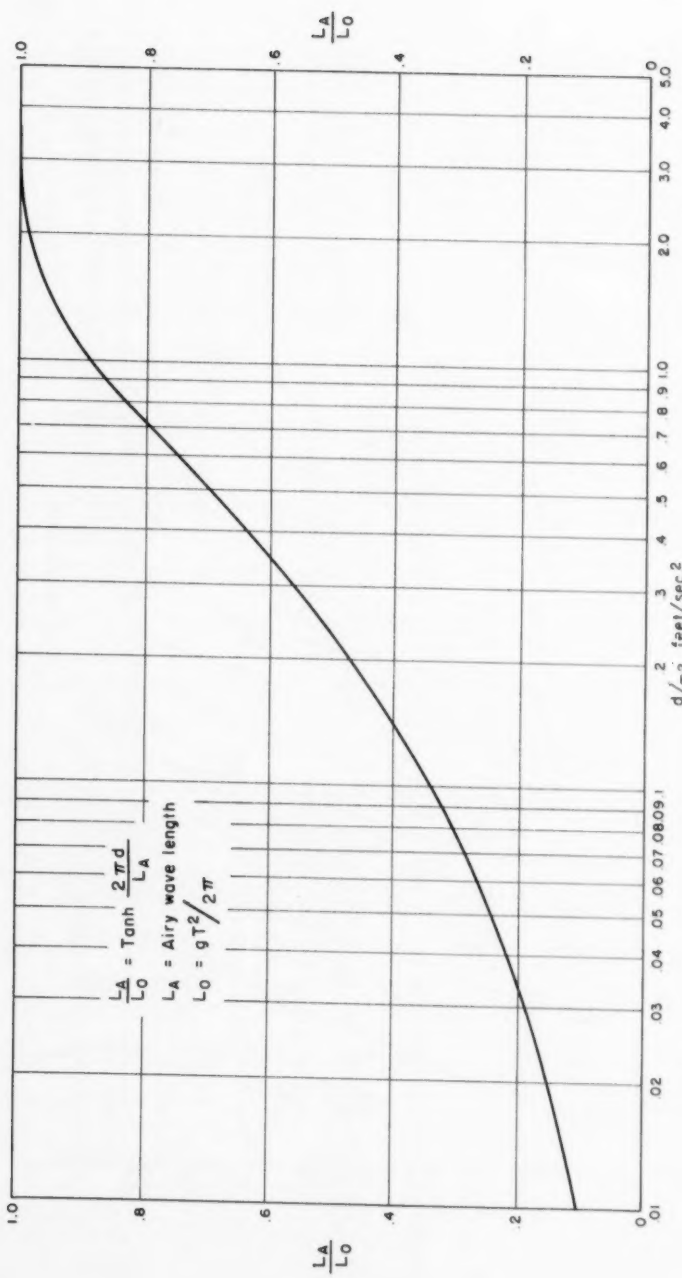


FIGURE 4. $L_A/L_O$ VS $d/T^2$

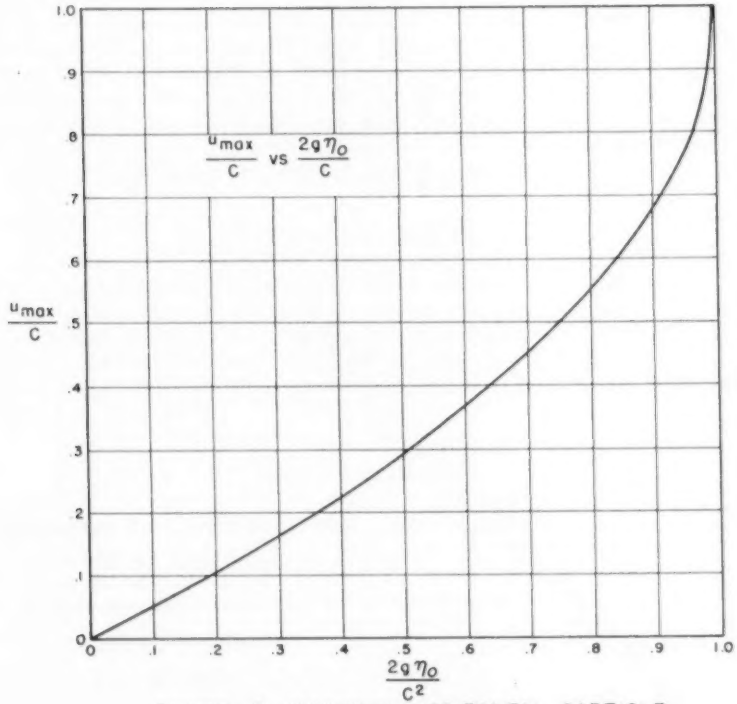


FIGURE 5. MAXIMUM HORIZONTAL PARTICLE VELOCITY AT CREST

factor is mandatory for both the crest elevations and the velocity and acceleration fields. Use of the Airy Theory in the above sense is not a recommended practice.

## Application to Hurricane Wind Waves

The preceding discussion is applicable to regular and simple waves, unaffected by strong winds. Figure 2 (and also 3) does not take into account any change in wave characteristics due to strong winds. This can best be studied by use of emperical data. Hurricane wave data from Lake Okeechobee, Florida,[4] have been analyzed for H, T, d, and $\eta_o$ (Table I-3). Figure 2, with the aid of $H/T^2$ and $d/T^2$ computed from Table I-3 was used to obtain the predicted value of $\eta_o$ also presented in Table I-3. Figure 6 is a comparison between observed $\eta_o$ and predicted $\eta_o$. Much of the scatter is due to the inability of obtaining exactly, H, T, and d, and long run averages are more significant. Even under controlled laboratory conditions one experiences considerable scatter of individual data. The regression line of observed $\eta_o$ to predicted $\eta_o$ has an intercept at .052 and a slope of 1.045 as determined by the least squares techniques. If it is assumed that Figure 2 is correct for waves unaffected by wind, then the effect of hurricane winds is to increase on

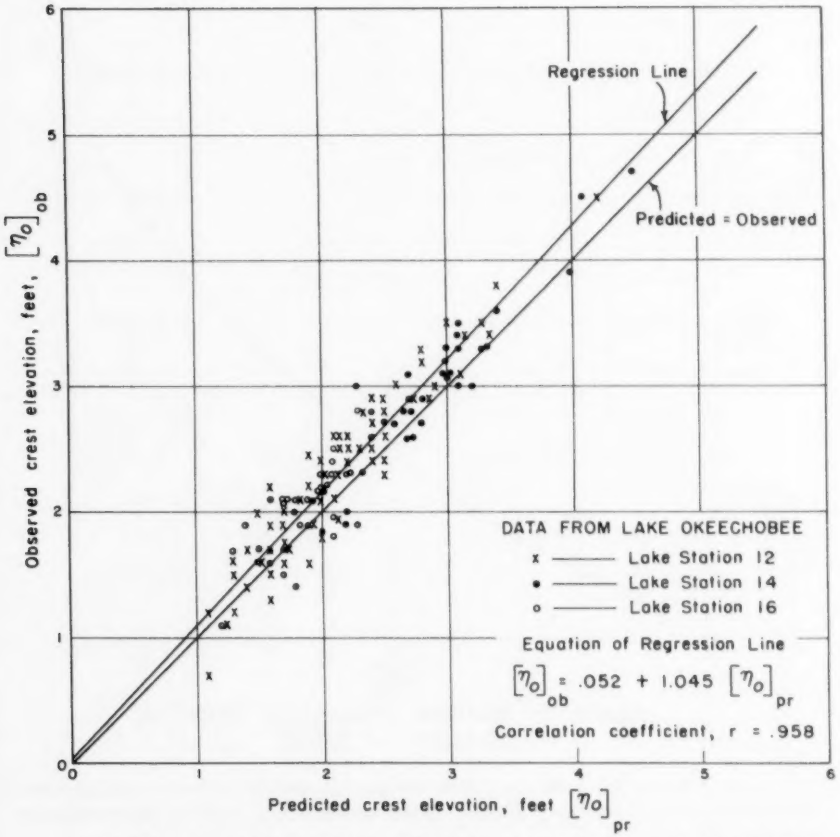


FIGURE 6. COMPARISON BETWEEN OBSERVED AND PREDICTED CREST ELEVATION ABOVE STILL WATER

(Predictions by use of Figure 2)

long run averages the crest elevation above still water by about 5 percent. Because of the scatter of data, perhaps a 10 percent increase in some cases is justified for the design wave. This, of course, needs further study, using possible wave data of the Gulf of Mexico.

## SUMMARY AND CONCLUSIONS

This paper represents the latest revision for obtaining for the design wave height, crest elevation, wave length, and maximum horizontal particle velocity at the crest of the design wave, and is intended to supplement the information presented in reference 1, as well as to be a continuation of reference 2.

Two generalized graphs are prepared using wave theory, Bernoulli's equation and wave data. Figure 2 is for obtaining the crest elevation and Figure 3

for obtaining the wave length of the design wave. A fourth graph, Figure 5, can be used in conjunction with Figures 2 and 3 for predicting the maximum horizontal particle velocity at the crest. The effect of hurricane winds has been considered. Based on Lake Okeechobee hurricane wave data it was found that the crest elevations were about 5 percent greater than that predicted from Figure 2. The scatter of data shows that perhaps a 10 percent increase may be justified, but this needs further investigation of larger hurricane waves, such as might be obtained in the Gulf of Mexico.

## ACKNOWLEDGMENTS

The author extends his appreciation to the Beach Erosion Board for sponsoring personnel and time used in the preparation of this paper. In particular, this includes Mr. F. W. Kellum for computations, Mr. V. E. Dahlin for drafting, and others. Much credit is also extended to Professor R. O. Reid of Texas A. & M. College, who initiated much of the original work presented in reference 1.

## LIST OF SYMBOLS

| | |
|---|---|
| A | wave amplitude above still water, feet |
| $A_o$ | $H/_2$, half the wave height, feet |
| b | used as a subscript to denote a breaking wave |
| C | wave celerity feet/second |
| $C_A$ | wave celerity of the Airy wave, feet/second |
| $C_b$ | wave celerity of breaking waves, feet/second |
| d | depth of water, feet |
| f | frequency of occurrence, percent |
| g | acceleration of gravity, 32.16 feet/second$^2$ |
| h | trough elevation above bottom, feet |
| H | wave height, feet |
| $H_b$ | breaking wave height, feet |
| I | recurrence interval, years |
| k | wave number, $k = 2\pi/L$ |
| L | wave length, feet |
| $L_o$ | deep water Airy wave length, feet |
| $L_A$ | Airy wave length, feet |
| R | radius of maximum wind, nautical miles |
| T | wave period, second |
| $u_s$ | horizontal particle velocity along the free surface of gravity wave (stationary coordinate system), feet/second |

$u_o$ horizontal particle velocity at crest ($\theta$ = 0), feet/second

$u_{max}$ maximum horizontal particle velocity at the crest, feet/second

$V_A$ absolute particle velocity, feet/second

$V_F$ forward speed of hurricane, knots

$w_s$ vertical particle velocity, feet/second

$w_m$ particle velocity at still water elevation at the free surface, feet/second

$\pi$ 3.1416

$\sigma$ angular frequency, radians/second

$\eta$ elevation of free surface of wave measured from still water, feet

$\eta_o$ crest elevation above still water, feet

$\eta_b$ crest elevation of breaking wave above still water, feet

$\theta$ phase position, degrees

## REFERENCES

1. Reid, R. O. and C. L. Bretschneider, "Surface Waves and Offshore Structures: The Design Wave in Deep or Shallow Water, Storm Tide, and Forces on Vertical Piling and Large Submerged Objects," Technical Report, Texas A. & M. Research Foundation, October 1953, 36 pp.

2. Bretschneider, C. L., "Hurricane Design Wave Practices," Paper 1238 WW2, Journal of the Waterways and Harbors Division, Proceedings ASCE, 1957, pp. 1238-1, 1238-33.

3. Reid, R. O., "Approximate Response of Water Level on a Sloping Shelf to a Wind Fetch which Moves Towards Shore," Beach Erosion Board Technical Memorandum No. 83, June 1956, 47 pp.

4. Corps of Engineers, U. S. Army, Hurricane Data, October 17-18, 1950, Proj. Bull. No. 5 (Project CWI-167: Waves and Wind Tides in Inland Waters; Lake Okeechobee, Florida), Office of the District Engineer, Jacksonville.

5. Danel, Pierre, "On the Limiting Clopotis," National Bureau of Standards, Circular 521, Gravity Waves, Ch. 6, November 28, 1952, pp. 35-45.

6. Munk, W. H., "Solitary Wave Theory," Annals New York Academy of Sciences, Vol. 51, New York, May 13, 1949, pp. 376-424.

7. Mason, Martin A., "A Study of Progressive Oscillatory Waves in Water," Beach Erosion Board Technical Report No. 1, Office of the Chief of Engineers, Washington, D. C., 1948, 39 pp.

8. Freeman, John C., Jr., Ledolph Baer, and Glen H. Jung, "The Bathystrophic Storm Tide," presented at the 150th National Meeting of the American Meteorological Society, January 28-31, 1957, New York, New York.

9. Bretschneider, C. L., "Revised Wave Forecasting Relationships," Proceedings of Second Conference on Coastal Engineering, 1952. Also see "Revisions in Wave Forecasting," to be presented at the Sixth Conference on Coastal Engineering, December 1957.

10. Pierson, W. J., Jr., Gerhard Neumann, and R. W. James, "Practical Methods for Observing and Forecasting Ocean Waves by Means of Wave Spectra and Statistics," H. O. Pub. No. 603, 1955, 284 pp.

11. Darbyshire, J., "An Investigation of Storm Waves in the North Atlantic Ocean," Proceedings Royal Society, A230, 1955.

12. Suthons, Commander C. T., "The Forecasting of Sea and Swell Waves," p. 20, Naval Met. Branch, 1945.

13. Roll, H. U., "Forecasting Surface Gravity Waves," Conference on Long Waves and Storm Surges, National Institute of Oceanography, Wormley, England, May 27-31, 1957.

14. Wilson, B. W., "Graphical Approach to the Forecasting of Waves in Moving Fetches," Beach Erosion Board Technical Memorandum No. 73, April 1955, 31 pp.

15. Thijsse, J. Th., "Growth of Wind-Generated Waves and Energy Transfer," Gravity Waves, Circular 521, National Bureau of Standards, Washington, 1952, pp. 281-287.

16. Bretschneider, C. L., "Generation of Wind Waves in Shallow Water," Beach Erosion Board Technical Memorandum No. 51, 1954.

17. Bretschneider, C. L., "Wave Forecasting Relationships for the Gulf of Mexico," Beach Erosion Board Technical Memorandum No. 84, December 1956, 28 pp.

18. Bretschneider, C. L., "Field Investigation of Wave Energy Loss in Shallow Water Ocean Waves," Beach Erosion Board Technical Memorandum No. 46, September 1954.

19. Wilson, B. W., "Hurricane Wave Statistics for the Gulf of Mexico," Beach Erosion Board Technical Memorandum No. 98, June 1957, 61 pp. and table.

20. Beard, L. R., "Statistical Methods in Hydrology," Office, Chief of Engineers, Department of the Army, Washington, D. C., July 1952, 35 pp. and figure.

21. Wiegel, R. L., "Tables of the Functions $^{d}/_{L}$ and $^{d}/_{L_0}$," Technical Report No. H.E.-116-265, Department of Engineering, University of California, Berkeley, January 1948, 58 pages.

22. Airy, G. B., "On Tides and Waves," Encyclopedia Metropolitana, Vol. 5 (Mixed Science) London, pp. 241-396, 1845.

23. Lamb, Horace, Hydrodynamics, 6th Ed., Dover Pub., New York XV, 1945, 738 pp.

24. Michell, J. H., "On the Highest Waves in Water," Philosophical Mag., Vol. 36, No. 5, 1893, pp. 430-435.

25. Stokes, Sir G. G., "On the Theory of Oscillatory Waves," Transactions, Cambridge Philosophical Society, Vol. 8, pp. 441-455, 1847.

26. Keulegan, G. H., "Wave Motion," Engineering Hydraulics, Proceedings of the Fourth Hydraulics Conference, Iowa Institute of Hydraulic Research, June 1949, Ch. II, pp. 711-768.

27. Chappelear, J. E., "An Investigation of the Solitary Wave," Transactions A.G.U., Vol. 37, No. 6, December 1956, pp. 726-734.

28. Bretschneider, C. L., and E. K. Rice, "The Generation and Decay of Wind Waves in a Sixty-foot Channel," Technical Report HE-116-327, Institute of Engineering Research, University of California, Berkeley, July 1951, (unpublished), 3 pp.

## APPENDIX I

The following material is limited to the development and application of Figures 2, 3, and 5. This requires only a brief summary of wave theory, the use of Bernoulli's equation, and the source and nature of the wave data. The section on wave theory does not consider the internal velocity and acceleration fields usually reserved for papers on wave forces. If necessary, such information may be obtained from the cited references and numerous other sources.

### Brief Summary of Wave Theory
### (As applicable to Figures 2, 3, and 5)

#### Airy Wave Theory

The Airy Wave Theory[7, 8] is applicable to very low steepness waves in deep or shallow water ($H/L$ and $H/d$ small). The surface profile is given by

$$\eta = \frac{H}{2} \cos \Theta \text{ , where} \qquad (1)$$

$\Theta = kx - \sigma t$ is the phase position

$H$ = wave height, vertical distance between crest and trough

$k = \frac{2\pi}{L_A}$ wave number

$\sigma = \frac{2\pi}{T}$ angular frequency

$x$ = horizontal distance from crest

$t$ = time position from crest

$T$ = wave period

$L_A$ = Airy wave length

The Airy wave length is given by

$$L_A = \frac{gT^2}{2\pi} \tanh \frac{2\pi d}{L_A} \text{ , where} \qquad (2)$$

g = acceleration of gravity

d = mean water depth

The wave celerity, $C_A$ is given by

$$C_A = \frac{L_A}{T} \tag{3}$$

The Airy theory is used for the lower boundary limit (Figures 2 and 3) in the field of wave theories.

Solitary Wave Theory (for breaking waves)

The solitary theory[6] for non-breaking waves will not be discussed. The highest wave in shallow water is governed by the solitary wave theory[6] and is a wave of elevation entirely. The height of the breaking wave is obtained from $H_b = 0.78d$.

The celerity $C_b$ is given by

$$C_b = \sqrt{2g\,H_b} \tag{4}$$

The crest of the breaking wave is cusp shape with angle of 120° and the crest elevation $\eta_{o/H} = 1.0$.

This theory is used for the upper boundary limit for $d/L \to 0$

Modified Solitary Theory

The modified solitary theory discussed in great detail by Munk,[6] is applicable to breaking waves in very shallow water. The breaking wave height is obtained from $H_b = 0.78h$, where, h = elevation of trough above bottom, given by

$$\frac{d}{h} = 1 + \frac{4}{3}\sqrt{\frac{3h}{h+H} \cdot \frac{H}{gT^2}} \tag{5}$$

The wave celerity of the breaking wave is given approximately by equation 4, and more exactly by equation 18. The wave celerity for a non-breaking solitary wave is given by $C = \sqrt{g(H+h)}$, and applies only for moderate or low values of $h/H$. The wave length is obtained from $L = CT$.

The elevation of crest above still water is obtained from

$$\frac{\eta_o}{H} = 1 - \frac{(d-h)}{(H)} \tag{6}$$

This theory is used as the upper limit in very shallow water, small $d/L$.

Michell - Havelock Theory

The Michell-Havelock theory[24] is applicable to breaking waves in deep

water. The breaking wave height is given by, $H_b = L/7$, where L is the wave length, given by

$$L = 1.20 \frac{g}{2\pi} T^2 \tag{7}$$

The crest elevation above still water is obtained from $\eta_o/H = 0.676$. This theory is used for the upper limit in deep water, $d/L = 0.5$.

Stokes Theory (second approximation)(25)

This is a second order theory, one order above the Airy theory, and applies for waves of small finite steepness. The wave length is given by

$$L = \frac{g}{2\pi} T^2 (\tanh)\ kd \left[1 + \left(\frac{\pi H}{L}\right)^2 f_1 \left(\frac{d}{L}\right)\right], \text{ where} \tag{8}$$

$$f_1\left(\frac{d}{L}\right) = \frac{5 + 2\cosh 2kd + 2\left[\cosh [2kd]\right]^2}{8\left[\sinh kd\right]^4}$$

The surface profile is given by

$$\eta/H = \frac{1}{2}\left[\cos\theta + \frac{1}{2}\frac{\pi H}{L} f_2\left(d/L\right) \cos 2\theta, \text{ where}\right] \tag{9}$$

$$f_2\left(d/L\right) = \frac{1}{2}\frac{(\cosh kd)(2 + \cosh 2kd)}{[\sinh kd]^3}$$

The elevation of crest $\eta_o$ above still water is obtained from 9 for $\theta = 0$. This theory is used next to the boundary of the Airy theory.

Stokes Theory (third approximation for deep water)

The third approximation for deep water has a surface profile given by

$$\eta/H = \cos\theta + \frac{\pi A}{L}\cos 2\theta + \frac{3}{2}\left(\frac{\pi A}{L}\right)^2 \cos 3\theta \quad \text{where} \tag{10}$$

A is related to $A_o = \frac{H}{2}$ according to Keulegan(26)

$$A_o = \left[A\left[1 + \frac{3}{2}\left(\frac{\pi A}{L}\right)^2\right]\right] \tag{11}$$

and the celerity is given by

$$C^2 = \frac{gL}{2}\left[1 + \left(\frac{2A}{L}\right)^2\right] \tag{12}$$

This theory is used as the boundary for deep water, for waves of finite height, but is adjusted slightly as $H/L$ approached $1/7$.

The solution of equations 11 and 12 is given in Table I-1. Equation 10 for $\eta_o/H$ breaks down sooner than 12, and is adjusted by use of wave data.

TABLE I-1

Solution of Stokes Third Approximation

for Wave Length in Deep Water

| $A_o/A$ | $H/L$ | $L/L_A$ | $H/T^2$ (ft/sec$^2$) |
|---|---|---|---|
| 1.01 | .0524 | 1.027 | .275 |
| 1.02 | .0748 | 1.054 | .397 |
| 1.03 | .0925 | 1.083 | .513 |
| 1.04 | .1079 | 1.112 | .614 |
| 1.05 | .1217 | 1.141 | .711 |
| 1.06 | .1346 | 1.172 | .808 |
| 1.07 | .1468 | 1.203 | .900 |

The above theories are those used, together with wave data to prepare a set of useful graphs for determining wave characteristics for most design waves. The Cnoidal wave theory might also be mentioned, since it represents waves in the intermediate zone between Stokian and solitary waves. However, this theory is a little difficult to use in its present form, and instead is replaced by wave data as far as Figures 2 and 3 are concerned.

Application of Bernoulli's Equation

Wave data with the aid of Bernoulli's equation can be used to obtain best fit numerical relationships for wave characteristics in the intermediate zone where no simple wave theory exists. The problem of wave motion can be reduced to one of steady state by use of the Rayleigh principle wherein a steady current equal to the wave celerity is superimposed thereon in an opposite direction to wave motion. The free surface profile then becomes a streamline. The pressure along this streamline is constant atmospheric, or in reference to the atmosphere is zero. Using the mean water depth as a reference and applying Bernoulli's equation along the free surface of the now stationary wave, one obtains

$$\left[\frac{v_s - C}{C}\right]^2 + \left[\frac{w_s}{C}\right]^2 + \frac{2g}{C^2}\eta = K \text{ , where} \qquad (13)$$

($u_s$-C) is the horizontal particle velocity along the free wave surface in the moving coordinate system, ft./sec.

$u_s$ = the horizontal particle velocity along the free wave surface in the stationary coordinate system, ft./sec.

C = the wave speed, ft./sec.

$w_s$ = the vertical particle velocity at the free surface, ft./sec.

$\eta$ = elevation of free surface measured from still water (positive above and negative below still water), feet.

g = acceleration of gravity 32.2 ft./sec.$^2$

K = the constant of Bernoulli's equation

The absolute velocity $V_a$, is obtained from

$$V_a^2 = (u_s - C)^2 + w_s^2 \tag{14}$$

The constant K can be evaluated at any number of known positions of the free surface. For the purpose of this discussion, the constant will be evaluated at still water, where $\theta = 0$. At this point $u_s = 0$, but $w_s$ has a finite value which will be termed $w_m$, not necessarily the maximum vertical particle velocity. Hence the constant becomes

$$K = 1 + \left(\frac{w_m}{C}\right)^2 \tag{15}$$

Thus

$$\left[\frac{u_s - C}{C}\right]^2 + \left[\frac{w_s}{C}\right]^2 + \frac{2g\eta}{C^2} = 1 + \left(\frac{w_m}{C}\right)^2 \tag{16}$$

The above expression relates the surface profile to the wave celerity, horizontal particle velocity $u_s$ and $w_m$.

The crest elevation $\eta_o$ above still water can be determined, since at $\theta = 0$, $u_s = u_o$ and $w_s = 0$, whence

$$2g\,\eta_o = 2\,u_o C - u_o^2 + w_m^2\ , \tag{17}$$

Breaking Waves

For the special case of breaking waves (deep or shallow)

$$u_o = C = C_b \text{ and } \eta_o = \eta_b$$

thus

$$C_b^2 = 2g\,\eta_b - w_m^2 \tag{18}$$

Equation 18 can be written in the following form

$$\frac{\eta_{b/H}}{(L/L_A)^2} = \frac{g}{2\pi^2} \frac{\left[\tanh \frac{2\pi d}{L_A}\right]^2}{H/T^2} \left[1 + (\frac{w_m}{C_b})^2\right] \quad (19)$$

Where $L_A$ is the Airy wave length given by equation 2.
For the special case of the solitary breaker in shallow water,

$$\eta_{b/H} = 1.0,\ w_m^2 = 0,\ \tanh \frac{2\pi d}{L_A} \longrightarrow \frac{2\pi d}{L_A}$$

and $H/d = .78$, whence from equation 19, $L/L_A = 1.25$.

For the special case of the highest wave in deep water, according to the Michell Theory, $\eta b/H = .676$, $L/L_A = 1.20$ and $H/L = 1/7$ and since $\tanh \frac{2\pi d}{L} \rightarrow 1.0$, whence from equation 19, $(\frac{w_m}{C_b})^2 = .0113$.

If it is assumed that $(\frac{w_m}{C_b})^2$ varies from 0 is shallow water to a maximum of .0113 in deep water, then its contribution in equation 19 is negligible for all breaking waves.

Thus

$$C_b = \sqrt{2g\eta_b} \quad \text{for all breaking waves.} \quad (20)$$

Maximum Horizontal Particle Velocity

The maximum horizontal particle velocity, $u_{max}$, occurs at the crest position $\theta = 0$ ($u_{max} = u_o$, and $\eta = \eta_o$). $u_{max}$ can be investigated by use of Bernoulli's equation, provided one has previously determined $\eta_o$ and L, say from Figures 2 and 3 of the text, respectively. Solving equation 17 for $u_{max}/C$ one obtains

$$\frac{u_{max}}{C} = 1 - \sqrt{1 - \frac{2g\eta_o}{C^2} + (\frac{w_m}{C})^2} \quad (21)$$

It was shown that for all breaking waves deep or shallow water $(w_m/C)^2$ can be neglected. This is also probably true for all non-breaking waves, whence,

$$\frac{u_{max}}{C} = 1 \sqrt{1 - \frac{2g\eta_o}{C^2}} \quad (22)$$

$u_{max}$ can never be greater than given by the above approximation.

Equation 22 can be investigated for the Airy Wave Theory, H/L very small. If $H/L$ is very small, $\eta_o = \frac{H}{2}$ and $gH/C^2 \ll 1.0$. Hence an expansion of equation 22 by the Binominal theorm leads to

$$u_{max} = \frac{gH}{2C^2} \quad (23)$$

which is the same as that predicted from the Airy theory for $H/L$ very small. consider also equation 21, for the Airy Wave Theory, $(w_m)^2 = (u_{max})^2$ and one obtains exactly equation 23. Thus equation 22 is a very good approximation for obtaining the maximum horizontal particle velocity at the crest. The solution of equation 22 is given in Figure 5 of the text.

## Source and Nature of Wave Data

Wave data used in this paper consists of both breaking and non-breaking waves. Breaking waves from various sources have been summarized by Munk(6) in terms of $H_b/L_o$, and $d/H_b$, where $L_o = \frac{g}{2\pi} T^2$. This information in terms of $H_b/T^2$ and $d/T^2$ is given below in Table I-2.

TABLE I-2
(After Munk)

Summary of Observations of Depth of Breaking Location

| | Number of Observations Which Were Averaged | $H/T^2$ feet/sec$^2$ | $d/T^2$ feet/sec$^2$ | Symbol In Fig. 1 |
|---|---|---|---|---|
| Estero Bay | 244 | .026 | .034 | ○ |
| SIO Daily | 238 | .041 | .053 | △ |
| SIO Leica | 56 | .067 | .081 | △ |
| WHOI | 17 | .072 | .079 | ⊡ |
| Berkeley Tank | 2 | .123 | .157 | ● |
| B.E.B. Tank | 27 | .205 | .267 | ⊖ |
| Lake Superior | 134 | .358 | .558 | ⊕ |

The above information is presented in Figure I-1, Breaking Index Curve, for $H/T^2$ versus $d/T^2$. At the far right of Figure I-1 are two points; (symbol $\phi$), wind obtained in the Berkeley tank by Bretschneider and Rice.(28)

The other symbols (·) are data from Danel,(5) originally given in terms of $H/L$ and $d/L$, but transformed approximately to $H/T^2$ and $d/T^2$. The lower portion of the curve is governed by the Solitary theory ($H = .78d$) and the deep water portion by the Michell theory ($H/L = 1/7$, or $H/T^2 = .88$). The transition is governed by wave observations, imposing Bernoulli's equation and the other figures to be discussed.

Figure I-2 is the Breaking Index Curve in terms of $H/L$ versus $d/L$ and is similar to that of Figure I-1. The dashed curve is the relationship given by Danel(5) and corresponds to $H/L = 1/7 \tanh \frac{2\pi d}{L}$. At about $d/L = 0.1$ the curve by Danel intersects and crosses the solitary limit $H = .78d$. The solid curve is a continuous curve from $d/L = 0$ to $d/L =$ deep water, and is based on the imposing solution of Bernoulli's equation using Figure I-1 and others following.

Figure I-3 is a plot of the breaking crest elevation above bottom $Y_c/T^2$ versus $d/T^2$, and the data is that obtained from Lake Okeechobee, Florida. This curve is obtained by use of Figure I-1 and Figure 2 of the text, where

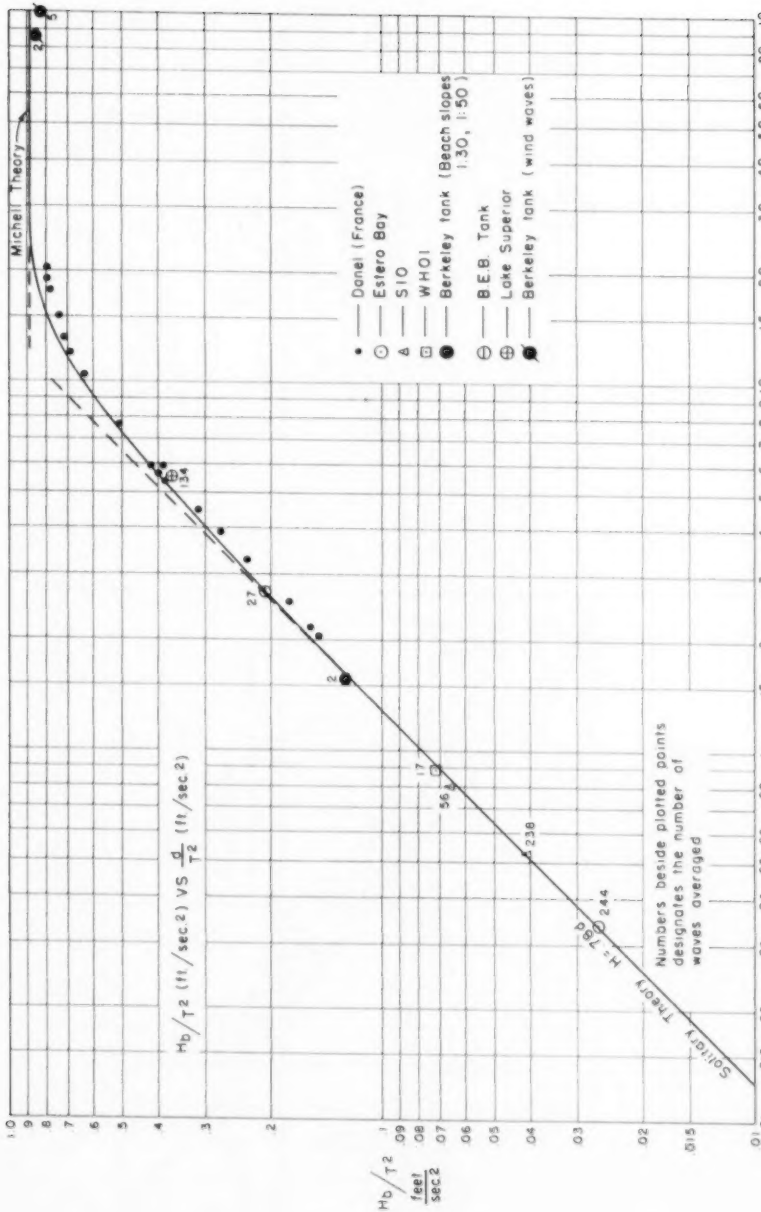


FIGURE I-1. BREAKING INDEX CURVE

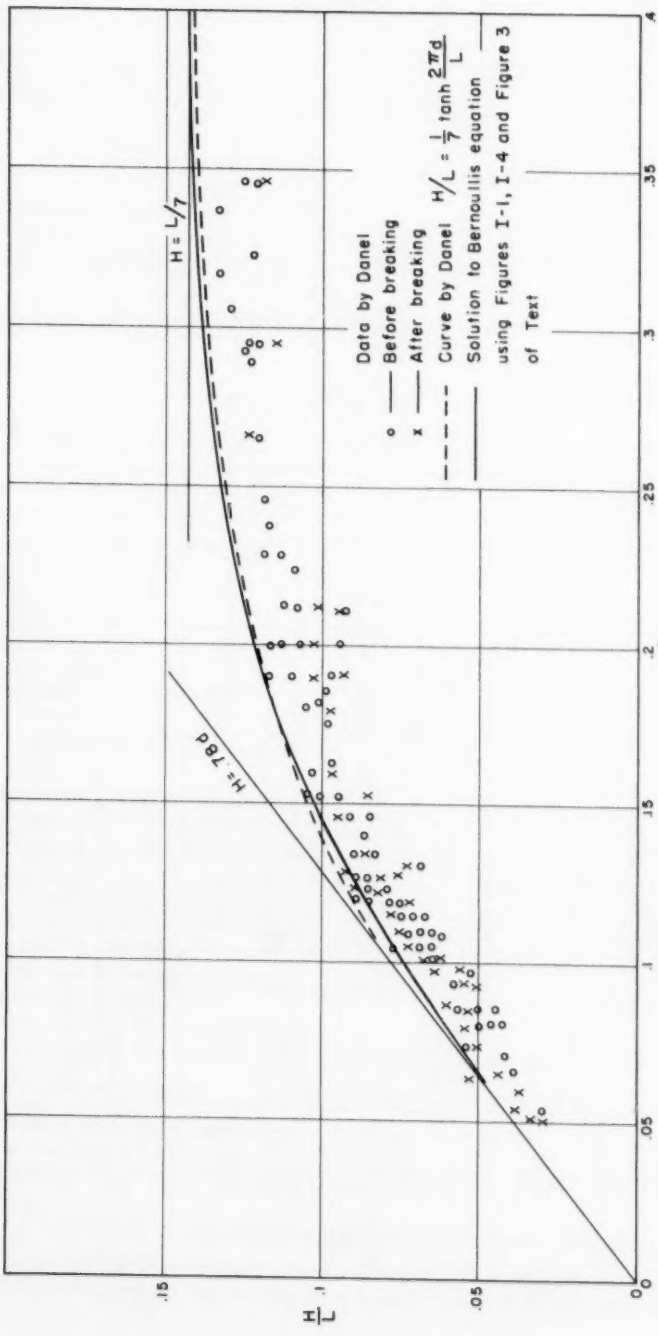


FIGURE I-2. H/L VERUS d/L FOR MAXIMUM WAVES

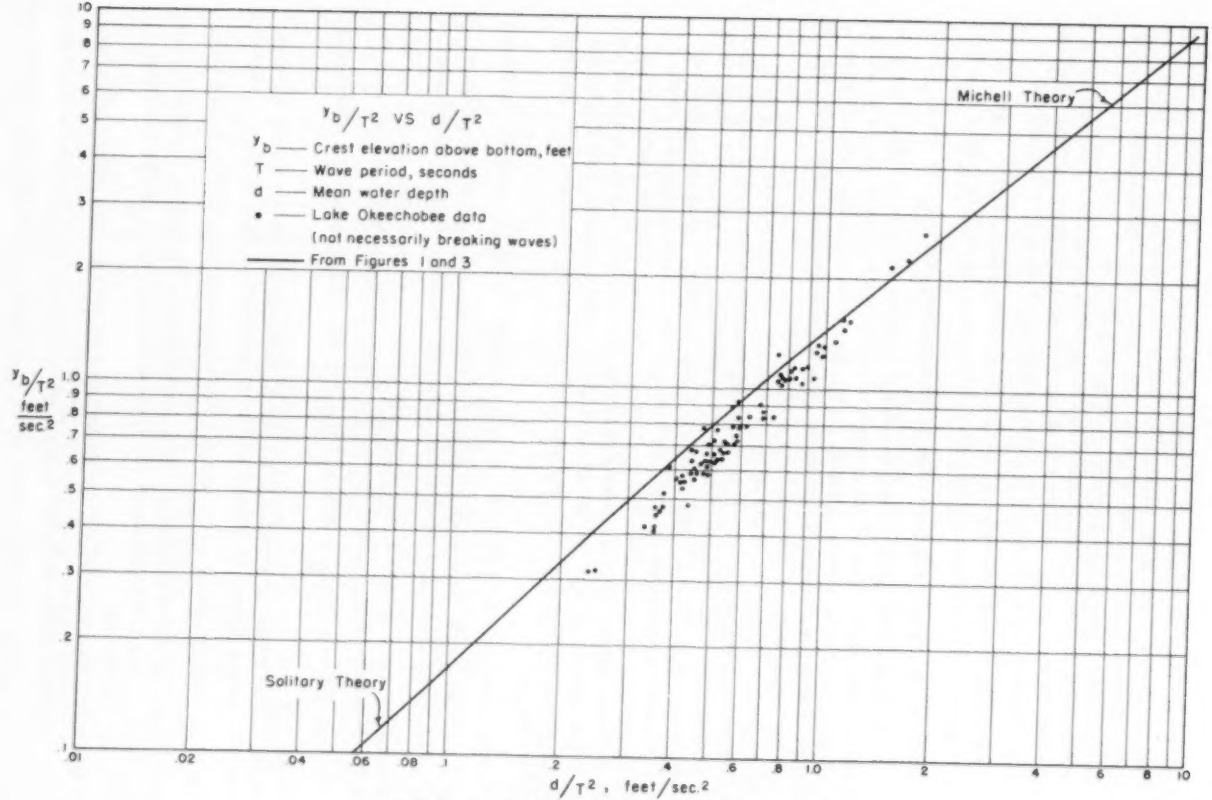


FIGURE 1-3. BREAKING WAVE CREST ELEVATION

$Y_c/_T2 = d/_T2 + \frac{\eta_o}{H} (H/_T2)$. The data consists of maximum waves of the October 17-18, 1950 hurricane.(4) These waves are not necessarily breaking and there is no way of knowing which waves were breakers. Hence, the envelope curve and not a mean curve is used. The data are summarized in Table I-3, and not all the points are plotted in Figure I-3.

In order to tie in the breaker index relationships, with the figures following, equation 19 was used. Figure I-4 is an imposing solution of this equation assuming Figures I-1 to be correct, and assuming $(w_m/C_b)^{2*}$ varies as shown from 0 at $H_b/_T2 = d/_T2 = 0$, to .0113 at deep water, $H/T^2 = .88$. Assuming Figure I-2 to be correct permits determination of $L/L_A$ as a function of either $d/T^2$ or $H/_T2$, and hence the determination of $\eta_b/_H$ for all breaking waves in the transition zone. Perhaps other representations of these figures could have been made, thus altering each of the corresponding figures. However, there is one best solution which gives the most accurate overall relationships. A trial and error process was used to obtain this best solution. In addition use was made of the non-breaking waves.

Figures I-5, -6, and -7, plots of $\eta_o$ versus H, are wave data for non-breaking waves obtained in the large tank of the Beach Erosion Board. The depth of the water was 15 feet. Three wave periods, T = 5.6, 7.87, and 11.33 seconds, were tested for a wide range in wave heights. Each wave record was 15 minutes in duration and the highest and the lowest individual wave of each record was determined. These data are summarized in Table I-4 according to the highest and the lowest wave of each record. The termination point of the curves of each of the above figures is obtained by the Breaking Index Curve of Figure I-1. These data are truly in the intermediate zone of $d/_T2$ and $H/_T2$.

Figure I-8 is a plot of data of $\eta_{o/H}$ versus $H/T^2$ for deep water waves obtained in the small tank of the Beach Erosion Board, and reported by Mason.(7) Since these are deep water data the variable $d/_T2$ is eliminated. However, the wave period T was different under each test run, hence the plot is given in terms of $\eta_{o/H}$ versus $H/T^2$. The breaking point corresponds to the Michell Theory, $\eta o/_H = .676$ and $H/_T2 = .88$. These data are summarized in Table I-5.

Using cross plots of Figures I-5, -6, -7, and -8 and the previous figures discussed, it is possible to construct the generalized graph of $\eta_{o/H}$, Figure 2 of the text. The graph of $\eta_{o/H}$ versus $d/_T2$ with isolines of $H/_T2$, are tied together as best fit relationships using wave theory, Bernoulli's equation and wave data. Table I-6 represents the final selected values of the breaking wave characteristics.

Figure 3 of the text, $L/L_A$, needs some discussion. The envelope curve of $L/L_A$ is related to the Breaker Index Curve, Figure I-1. Bernoulli's equation Figure I-4, and the envelope curve of $\eta_{o/H}$ of Figure 2 of the text. These are

* It would have made very little difference in the final results if it had been assumed $(w_m/C_b)^2 = 0$ for all breaking waves.

TABLE I-3

Hurricane Wind Wave Data Lake Okeechobee, Florida
(Highest Waves of each 1-Minute Run)
October 17-18, 1950

Lake Station 16

| H(feet) | T(Sec) | d(feet) | Observed $\eta_o$(feet) | Predicted $\eta_o$(feet) | H(feet) | T(Sec) | d(feet) | Observed $\eta_o$(feet) | Predicted $\eta_o$(feet) |
|---|---|---|---|---|---|---|---|---|---|
| 3.3 | 3.8 | 8.7 | 2.0 | 2.2 | 2.6 | 4.7 | 9.5 | 2.1 | 1.6 |
| 3.5 | 2.9 | 8.7 | 2.3 | 2.3 | 2.5 | 3.3 | 9.6 | 1.7 | 1.5 |
| 2.3 | 3.7 | 8.9 | 1.9 | 1.4 | 2.9 | 4.3 | 9.6 | 1.9 | 1.9 |
| 3.1 | 3.9 | 8.9 | 2.2 | 2.0 | 2.8 | 3.5 | 9.6 | 2.1 | 1.8 |
| 2.7 | 3.7 | 9.0 | 2.1 | 1.7 | 2.8 | 3.7 | 9.6 | 1.9 | 1.8 |
| 2.3 | 4.9 | 9.0 | 2.3 | 2.2 | 2.1 | 3.8 | 9.6 | 1.7 | 1.3 |
| 3.6 | 4.0 | 9.3 | 2.8 | 2.4 | 2.8 | 5.4 | 9.7 | 2.1 | 1.7 |
| 3.2 | 3.0 | 9.3 | 2.2 | 2.0 | 3.2 | 4.0 | 9.7 | 2.2 | 2.0 |
| 3.5 | 3.9 | 9.3 | 1.9 | 2.3 | 2.1 | 4.9 | 9.7 | 1.1 | 1.2 |
| 2.5 | 4.2 | 9.3 | 1.4 | 1.8 | 3.6 | 4.5 | 9.7 | 2.6 | 2.4 |
| 2.5 | 4.0 | 9.4 | 1.7 | 1.7 | 3.5 | 2.7 | 9.7 | 3.0 | 2.3 |
| 3.2 | 3.4 | 9.3 | 2.2 | 2.0 | 3.3 | 3.4 | 9.7 | 2.5 | 2.1 |
| 2.5 | 4.1 | 9.3 | 1.5 | 1.7 | 3.0 | 4.4 | 9.7 | 2.1 | 1.9 |
| 3.0 | 3.4 | 9.3 | 2.1 | 1.9 | 3.5 | 3.6 | 9.7 | 2.8 | 2.3 |
| 2.5 | 3.7 | 9.2 | 1.6 | 1.5 | 3.4 | 3.4 | 10.0 | 2.3 | 2.2 |
| 2.6 | 3.9 | 9.3 | 1.7 | 1.6 | 3.1 | 4.8 | 10.0 | 2.3 | 2.0 |
| 2.6 | 3.7 | 9.3 | 1.6 | 1.6 | 3.3 | 3.0 | 10.0 | 2.4 | 2.1 |
| 3.2 | 3.3 | 9.3 | 2.2 | 2.0 | 2.7 | 3.3 | 10.0 | 1.8 | 1.7 |
| 2.8 | 4.0 | 9.3 | 1.9 | 1.8 | 2.8 | 4.6 | 10.0 | 2.1 | 1.7 |
| 2.7 | 4.7 | 9.3 | 2.1 | 1.7 | 2.9 | 3.2 | 9.7 | 2.0 | 1.8 |
| 3.2 | 4.8 | 9.5 | 2.2 | 2.0 | 3.3 | 3.2 | 9.3 | 1.9 | 2.1 |
| 3.2 | 4.4 | 9.5 | 2.3 | 2.1 | 3.2 | 4.4 | 9.3 | 1.8 | 2.1 |
| 2.9 | 4.8 | 9.5 | 2.1 | 1.8 | | | | | |

TABLE I-3 (Continued)

Hurricane Wave Data Lake Okeechobee, Florida
(Highest Waves of each 1-Minute Run)
October 17-18, 1950

Lake Station 12

| H(feet) | T(Sec) | d(feet) | Observed $\eta_o$(feet) | Predicted $\eta_o$(feet) | H(Feet) | T(Sec) | d(feet) | Observed $\eta_o$(feet) | Predicted $\eta_o$(feet) |
|---|---|---|---|---|---|---|---|---|---|
| 2.7 | 2.6 | 8.8 | 2.0 | 1.7 | 3.1 | 2.5 | 8.2 | 2.1 | 2.0 |
| 2.6 | 2.8 | 8.6 | 2.1 | 1.7 | 3.2 | 3.0 | 8.1 | 2.6 | 2.1 |
| 2.2 | 3.2 | 8.6 | 1.5 | 1.3 | 4.3 | 2.9 | 8.1 | 3.1 | 3.1 |
| 2.3 | 2.7 | 8.6 | 1.4 | 1.4 | 3.4 | 3.2 | 8.1 | 2.8 | 2.3 |
| 2.2 | 3.5 | 8.5 | 1.2 | 1.3 | 3.5 | 2.9 | 8.1 | 2.5 | 2.4 |
| 1.8 | 3.4 | 8.5 | 1.2 | 1.1 | 3.9 | 3.0 | 8.1 | 2.9 | 2.7 |
| 2.4 | 2.7 | 8.5 | 1.6 | 1.5 | 2.2 | 3.0 | 8.0 | 1.7 | 1.4 |
| 2.7 | 3.2 | 8.6 | 1.6 | 1.7 | 2.8 | 3.8 | 7.7 | 2.1 | 1.8 |
| 1.9 | 3.7 | 8.6 | .7 | 1.1 | 3.1 | 3.7 | 7.7 | 2.3 | 2.1 |
| 3.6 | 2.6 | 8.6 | 2.9 | 2.4 | 3.9 | 3.8 | 7.7 | 3.3 | 2.8 |
| 2.6 | 3.0 | 8.5 | 1.7 | 1.6 | 5.3 | 4.0 | 7.7 | 4.5 | 4.2 |
| 2.5 | 3.0 | 8.5 | 1.3 | 1.6 | 4.5 | 3.2 | 7.7 | 3.5 | 3.3 |
| 2.9 | 2.8 | 8.5 | 2.2 | 1.9 | 3.2 | 3.2 | 7.7 | 2.4 | 2.2 |
| 2.2 | 2.8 | 8.4 | 1.6 | 1.3 | 3.9 | 3.7 | 7.7 | 2.9 | 2.8 |
| 3.2 | 2.9 | 8.4 | 2.1 | 2.1 | 4.3 | 3.0 | 7.6 | 3.4 | 3.1 |
| 2.6 | 2.9 | 8.4 | 1.7 | 1.7 | 4.7 | 2.6 | 7.6 | 3.8 | 3.4 |
| 3.6 | 3.7 | 8.3 | 2.3 | 2.5 | 4.1 | 3.0 | 7.6 | 3.5 | 3.0 |
| 3.5 | 3.5 | 8.3 | 2.4 | 2.4 | 3.2 | 3.0 | 7.6 | 2.5 | 2.2 |
| 2.7 | 3.5 | 8.3 | 1.8 | 1.7 | 3.9 | 3.1 | 7.6 | 3.2 | 2.8 |
| 3.0 | 3.7 | 8.3 | 2.3 | 2.0 | 2.8 | 4.1 | 7.6 | 1.8 | 1.9 |
| 2.6 | 2.6 | 8.3 | 2.2 | 1.6 | 2.8 | 2.4 | 7.9 | 2.4 | 2.0 |

TABLE I-3 (Continued)

Hurricane Wave Data Lake Okeechobee, Florida
(Highest Waves of each 1-Minute Run)
October 17-18, 1950

Lake Station 12 (Continued)

| H(feet) | T(Sec) | d(feet) | Observed $\eta_o$(feet) | Predicted $\eta_o$(feet) | H(feet) | T(Sec) | d(feet) | Observed $\eta_o$(feet) | Predicted $\eta_o$ (feet) |
|---|---|---|---|---|---|---|---|---|---|
| 3.2 | 2.8 | 8.0 | 2.6 | 2.1 | 2.8 | 3.7 | 10.8 | 2.0 | 1.7 |
| 2.0 | 4.7 | 8.0 | 1.1 | 1.2 | 3.5 | 3.5 | 10.6 | 2.6 | 2.2 |
| 2.9 | 4.8 | 8.8 | 1.6 | 1.9 | 3.7 | 4.9 | 10.6 | 2.4 | 2.5 |
| 3.2 | 4.7 | 8.8 | 2.1 | 2.1 | 3.0 | 3.1 | 10.4 | 2.4 | 1.9 |
| 2.9 | 3.4 | 8.8 | 1.9 | 1.8 | 3.1 | 3.8 | 10.4 | 1.8 | 2.0 |
| 3.3 | 3.0 | 9.2 | 2.1 | 2.1 | 3.7 | 4.4 | 10.3 | 2.9 | 2.5 |
| 3.2 | 4.2 | 9.5 | 1.9 | 2.1 | 2.8 | 3.8 | 10.3 | 1.8 | 1.7 |
| 3.7 | 3.7 | 9.5 | 2.6 | 2.5 | 2.5 | 3.9 | 10.3 | 1.7 | 1.5 |
| 3.3 | 3.0 | 9.6 | 2.5 | 2.1 | 2.7 | 4.0 | 10.3 | 1.7 | 1.6 |
| 4.2 | 4.3 | 9.6 | 3.0 | 2.9 | 3.9 | 3.4 | 10.3 | 3.0 | 2.6 |
| 3.2 | 4.1 | 9.6 | 2.4 | 2.1 | 2.5 | 3.2 | 10.3 | 2.0 | 1.5 |
| 3.6 | 3.7 | 9.6 | 2.7 | 2.4 | 3.0 | 4.6 | 10.2 | 1.9 | 1.9 |
| 3.2 | 3.3 | 9.6 | 2.3 | 2.0 | 2.7 | 4.3 | 10.2 | 1.9 | 1.6 |
| 3.3 | 3.7 | 9.6 | 2.5 | 2.1 | 3.7 | 3.9 | 10.2 | 2.8 | 2.5 |
| 3.8 | 3.6 | 10.4 | 2.6 | 2.5 | 2.8 | 3.9 | 10.2 | 1.9 | 1.7 |
| 3.2 | 3.7 | 10.4 | 2.3 | 2.0 | 3.5 | 2.9 | 10.0 | 2.5 | 2.3 |
| 2.6 | 5.0 | 10.8 | 1.5 | 1.6 | 3.1 | 3.4 | 10.0 | 2.1 | 1.9 |

TABLE I-3 (Continued)

Hurricane Wave Data Lake Okeechobee, Florida
(Highest Waves of each 1-Minute Run)
October 17-18, 1950

Lake Station 14

| H(feet) | T(Sec) | d(feet) | Observed $\eta_o$(feet) | Predicted $\eta_o$(feet) | H(feet) | T(Sec) | d(feet) | Observed $\eta_o$(feet) | Predicted $\eta_o$(feet) |
|---|---|---|---|---|---|---|---|---|---|
| 4.3 | 2.8 | 8.6 | 3.1 | 3.0 | 4.3 | 3.7 | 9.3 | 3.3 | 3.0 |
| 3.9 | 3.8 | 8.7 | 3.1 | 2.7 | 4.5 | 4.8 | 9.5 | 3.3 | 3.3 |
| 2.9 | 3.5 | 8.7 | 1.9 | 1.8 | 4.4 | 4.1 | 9.6 | 3.3 | 3.1 |
| 3.8 | 3.4 | 8.7 | 2.7 | 2.6 | 4.4 | 2.7 | 9.7 | 3.2 | 3.0 |
| 4.1 | 3.2 | 8.7 | 2.9 | 2.8 | 6.0 | 3.3 | 9.7 | 4.7 | 4.5 |
| 4.1 | 3.9 | 8.8 | 2.7 | 2.8 | 4.0 | 3.8 | 9.7 | 2.9 | 2.7 |
| 4.1 | 3.2 | 8.9 | 2.6 | 2.8 | 4.8 | 3.4 | 9.7 | 3.6 | 3.4 |
| 3.9 | 3.7 | 8.9 | 2.8 | 2.7 | 4.4 | 4.2 | 9.7 | 3.4 | 3.1 |
| 3.4 | 3.4 | 8.9 | 1.9 | 2.2 | 3.1 | 3.6 | 9.7 | 1.8 | 2.0 |
| 3.5 | 2.7 | 8.9 | 2.3 | 2.3 | 5.3 | 5.0 | 9.7 | 3.9 | 4.0 |
| 3.9 | 3.7 | 9.0 | 2.8 | 2.7 | 4.5 | 4.7 | 9.5 | 3.0 | 3.2 |
| 4.6 | 2.2 | 9.0 | 3.5 | 3.1 | 4.5 | 5.1 | 9.3 | 3.3 | 3.3 |
| 3.7 | 2.4 | 8.9 | 2.7 | 2.5 | 5.7 | 3.0 | 9.4 | 4.5 | 4.1 |
| 3.9 | 3.6 | 8.9 | 2.6 | 2.7 | 4.4 | 2.4 | 9.4 | 3.1 | 3.0 |
| 4.3 | 2.9 | 9.3 | 3.1 | 3.0 | 4.5 | 3.2 | 9.5 | 3.0 | 3.1 |

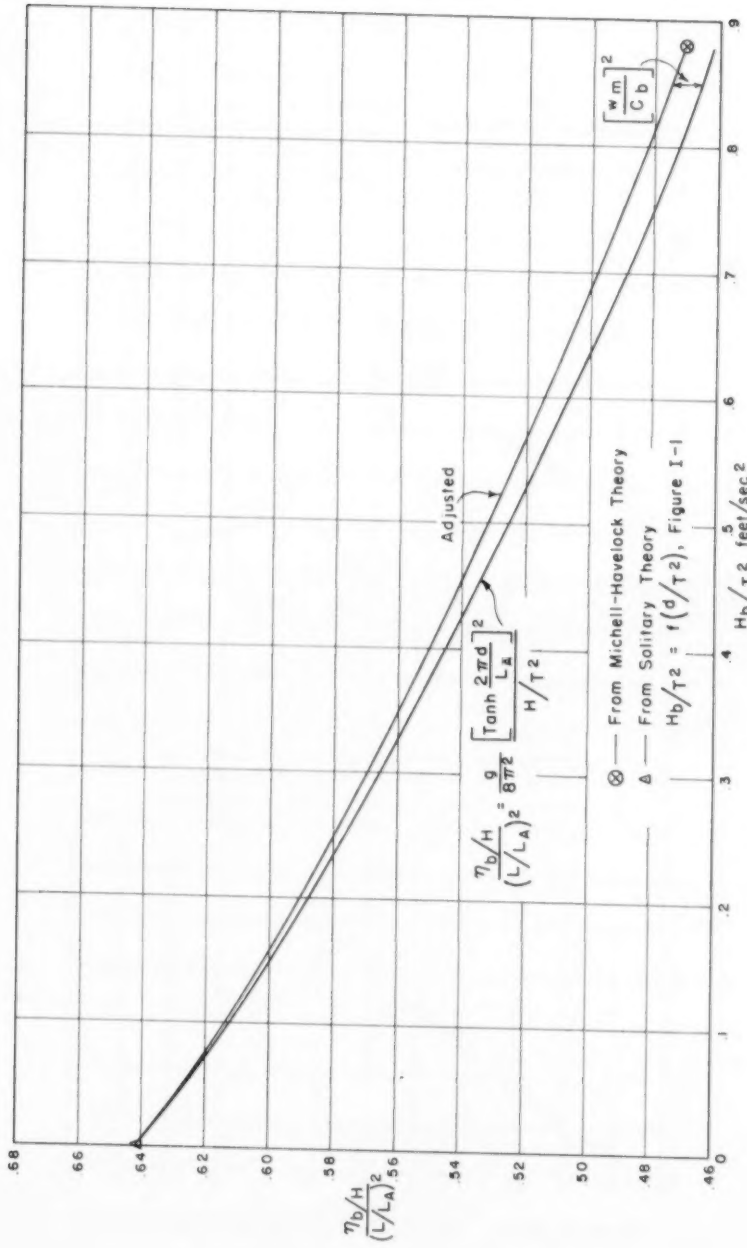


FIGURE I-4. SOLUTION OF BERNOULLI'S EQUATION

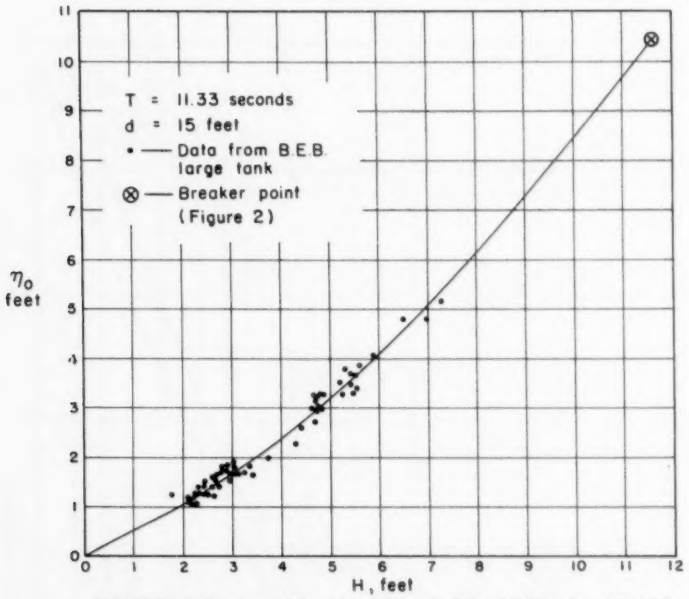


FIGURE I-5. $\eta_o$ VS H FOR 11.33 SECOND WAVES IN 15 FEET OF WATER

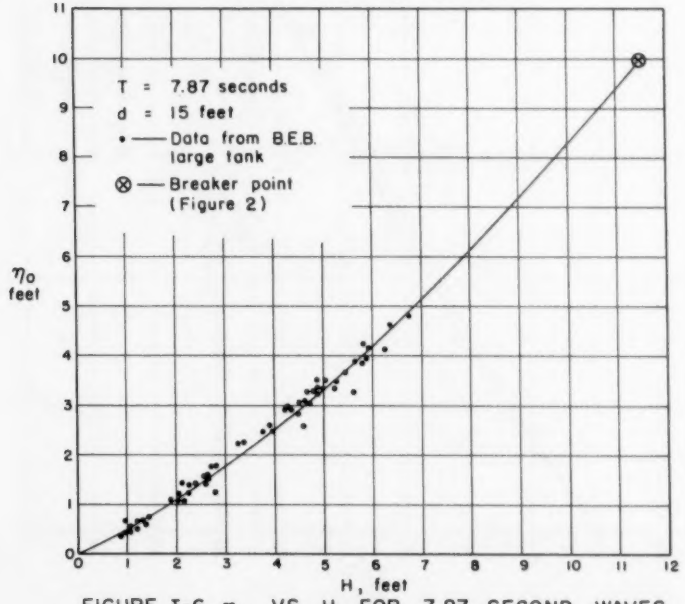


FIGURE I-6. $\eta_o$ VS H FOR 7.87 SECOND WAVES IN 15 FEET OF WATER

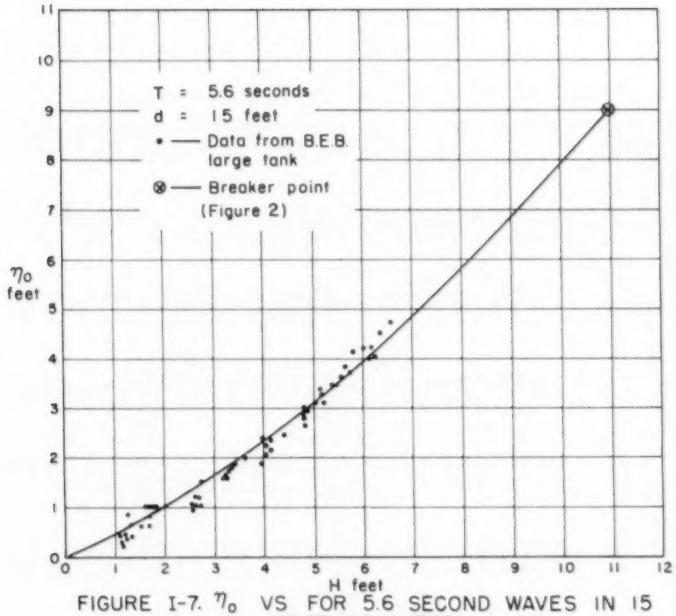


FIGURE I-7. $\eta_0$ VS FOR 5.6 SECOND WAVES IN 15 FEET OF WATER

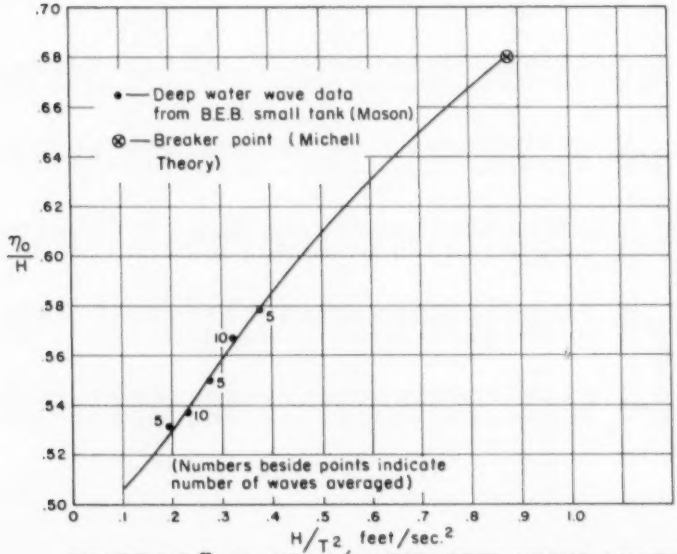
• — Deep water wave data from B.E.B. small tank (Mason)
⊗ — Breaker point (Michell Theory)
(Numbers beside points indicate number of waves averaged)
$\frac{\eta_0}{H}$
$H/T^2$ feet/sec.$^2$

FIGURE I-8. $\eta_0$ H VS $H/T^2$ FOR DEEP WATER WAVES

TABLE I-4

Summary of Wave Data Large Tank Beach Erosion Board (Depth = 15 feet)

| T = 7.87 Seconds | | | | T = 11.33 Seconds | | | | T = 5.6 Seconds | | | |
|---|---|---|---|---|---|---|---|---|---|---|---|
| Highest Wave | | Lowest Wave | | Highest Wave | | Lowest Wave | | Highest Wave | | Lowest Wave | |
| H | $\eta_o$ | H | $\eta_o$ | H | $\eta_o$ | H | $\eta_o$ | H | $\eta_o$ | H | $\eta_o$ |
| feet | feet | feet | feet | feet | feet | feet | feet | feet | feet | feet | feet |
| 5.82 | 3.85 | 5.45 | 3.65 | 6.57 | 4.79 | 4.70 | 2.72 | 6.18 | 4.04 | 5.45 | 3.48 |
| 5.90 | 3.93 | 5.30 | 3.48 | 7.00 | 4.80 | 4.88 | 3.29 | 6.35 | 4.52 | 5.72 | 3.85 |
| 5.85 | 3.85 | 5.27 | 3.36 | 5.37 | 3.79 | 4.82 | 3.29 | 6.20 | 4.04 | 5.45 | 3.48 |
| 5.67 | 3.85 | 5.09 | 3.48 | 5.26 | 3.48 | 4.73 | 3.12 | 6.18 | 4.23 | 5.52 | 3.67 |
| 5.86 | 4.22 | 5.62 | 3.24 | 7.31 | 5.18 | 5.26 | 3.28 | 6.20 | 4.04 | 5.45 | 3.47 |
| 6.36 | 4.60 | 4.70 | 3.10 | 5.65 | 3.85 | 4.89 | 3.29 | 6.35 | 4.52 | 5.66 | 3.85 |
| 6.75 | 4.80 | 4.84 | 3.29 | 5.45 | 3.66 | 4.43 | 2.61 | 6.02 | 4.23 | 5.45 | 3.48 |
| 6.26 | 4.13 | 4.89 | 3.33 | 5.55 | 3.66 | 4.31 | 3.29 | 6.56 | 4.79 | 5.80 | 4.19 |
| 5.92 | 4.13 | 4.85 | 3.29 | 5.45 | 3.48 | 4.75 | 3.03 | 4.86 | 2.82 | 3.98 | 2.40 |
| 4.68 | 3.27 | 4.55 | 3.10 | 5.52 | 3.37 | 4.79 | 2.95 | 5.12 | 3.38 | 3.98 | 2.35 |
| 5.00 | 3.33 | 4.50 | 2.81 | 5.90 | 4.04 | 4.72 | 3.29 | 5.06 | 3.11 | 4.04 | 2.22 |
| 4.89 | 3.48 | 4.60 | 2.57 | 5.45 | 3.66 | 4.82 | 2.95 | 5.15 | 3.34 | 4.42 | 2.44 |
| 4.68 | 3.10 | 3.99 | 2.63 | 5.49 | 3.29 | 4.70 | 2.93 | 4.87 | 2.67 | 4.09 | 2.06 |
| 4.70 | 3.25 | 3.98 | 2.48 | 2.87 | 1.66 | 2.25 | 1.18 | 4.85 | 2.82 | 3.94 | 1.88 |
| 4.25 | 2.91 | 3.76 | 2.48 | 2.95 | 1.79 | 2.35 | 1.22 | 4.87 | 2.92 | 4.15 | 2.16 |
| 4.27 | 2.93 | 3.36 | 2.28 | 3.06 | 1.79 | 2.14 | 1.05 | 5.22 | 3.10 | 4.15 | 2.35 |
| 4.31 | 2.92 | 3.38 | 2.26 | 2.63 | 1.41 | 2.18 | 1.15 | 3.29 | 1.60 | 2.63 | 1.22 |
| 2.63 | 1.60 | 2.39 | 1.43 | 2.82 | 1.79 | 1.79 | 1.22 | 3.22 | 1.60 | 2.57 | 1.08 |
| 2.61 | 1.58 | 2.16 | 1.41 | 2.72 | 1.41 | 2.23 | 1.22 | 3.34 | 1.74 | 2.63 | 1.22 |
| 2.76 | 1.79 | 2.28 | 1.41 | 2.78 | 1.60 | 2.29 | 1.05 | 3.38 | 1.78 | 2.72 | 1.03 |
| 2.80 | 1.29 | 2.24 | 1.22 | 3.08 | 1.79 | 2.49 | 1.41 | 3.66 | 1.98 | 2.54 | .94 |
| 2.78 | 1.79 | 2.16 | 1.04 | 2.78 | 1.54 | 2.12 | 1.03 | 3.47 | 1.88 | 2.64 | 1.04 |
| 2.63 | 1.41 | 2.09 | 1.04 | 2.96 | 1.75 | 2.34 | 1.32 | 3.25 | 1.60 | 2.44 | 1.04 |
| 2.65 | 1.62 | 2.11 | 1.22 | 2.98 | 1.60 | 2.44 | 1.41 | 3.38 | 1.74 | 2.76 | 1.50 |
| 2.59 | 1.50 | 1.95 | 1.05 | 3.00 | 1.60 | 2.51 | 1.22 | 1.67 | 1.03 | 1.24 | .85 |
| 1.26 | .66 | .92 | .38 | 3.26 | 1.65 | 2.44 | 1.22 | 1.69 | 1.06 | 1.26 | .39 |
| 1.43 | .72 | .98 | .66 | 3.38 | 1.80 | 2.68 | 1.22 | 1.69 | .66 | 1.19 | .33 |
| 1.32 | .68 | 1.09 | .57 | 3.04 | 1.82 | 2.42 | 1.22 | 1.69 | .83 | 1.30 | .66 |
| 1.24 | .51 | .98 | .47 | 3.42 | 1.60 | 2.25 | 1.22 | 1.82 | 1.04 | 1.18 | .28 |
| 1.35 | .66 | 1.09 | .47 | 3.02 | 1.58 | 2.25 | 1.03 | 1.67 | 1.04 | 1.17 | .47 |
| 1.34 | .70 | .99 | .47 | 3.72 | 1.97 | 2.46 | 1.48 | 1.73 | 1.04 | 1.09 | .47 |
| 1.34 | .68 | 1.04 | .47 | 2.93 | 1.56 | 2.52 | 1.22 | 1.51 | .66 | 1.30 | .47 |
| | | | | 2.94 | 1.60 | 2.28 | 1.03 | | | | |
| | | | | 3.13 | 1.62 | 2.52 | 1.22 | | | | |
| | | | | 3.00 | 1.60 | 2.62 | 1.22 | | | | |

TABLE I-5

Summary
Deep Water Waves (Beach Erosion Board Small Tank)

| Run | H(feet) | T(sec) | $H/T^2$ | $\eta_o/H$ |
|---|---|---|---|---|
| 1 | .293 | .850 | .406 | .543 |
| 1 | .279 | .850 | .387 | .548 |
| 18 | .272 | .847 | .378 | .585 |
| 3 | .264 | .848 | .367 | .610 |
| 1 | .259 | .850 | .359 | .602 |
| Average | | | .379 | .578 |
| 18 | .249 | .847 | .347 | .570 |
| 13 | .236 | .848 | .328 | .533 |
| 18 | .236 | .847 | .328 | .610 |
| 4 | .234 | .860 | .316 | .556 |
| 4 | .233 | .860 | .315 | .579 |
| 13 | .225 | .848 | .313 | .587 |
| 23 | .305 | .988 | .311 | .587 |
| 4 | .223 | .860 | .302 | .548 |
| 23 | .296 | .988 | .302 | .571 |
| 23 | .287 | .988 | .293 | .540 |
| Average | | | .323 | .567 |
| 19 | .203 | .842 | .286 | .589 |
| 19 | .196 | .842 | .276 | .541 |
| 19 | .192 | .842 | .270 | .542 |
| 22 | .178 | .843 | .251 | .539 |
| 2 | .248 | 1.003 | .248 | .581 |
| Average | | | .275 | .550 |
| 2 | .242 | 1.003 | .242 | .538 |
| 14 | .226 | .969 | .241 | .487 |
| 22 | .170 | .843 | .240 | .530 |
| 14 | .218 | .969 | .233 | .550 |
| 14 | .214 | .969 | .228 | .509 |
| 5 | .217 | .985 | .225 | .535 |
| 2 | .220 | 1.003 | .220 | .563 |
| 22 | .155 | .843 | .218 | .555 |
| 5 | .207 | .985 | .214 | .522 |
| 17 | .192 | .966 | .204 | .551 |
| Average | | | .231 | .537 |
| 17 | .190 | .966 | .203 | .516 |
| 5 | .195 | .985 | .202 | .543 |
| 17 | .186 | .966 | .198 | .506 |
| 20 | .176 | .996 | .178 | .547 |
| 20 | .161 | .996 | .162 | .528 |
| Average | | | .197 | .532 |

TABLE I-6

Summary of Breaking Index Relationships

| $d/T^2$ | $H/T^2$ | $H/d$ | $d/L_A$ | $H/L_A$ | $L_A/L_o$ | $\eta_{b/H}$ $\overline{(L/L_A)^2}$ | $\eta_{b/H}$ $\overline{(L/L_A)^2}$ | $\eta_{b/H}$ | $L/L_A$ | $d/L$ | $H/L$ | $Y_o/T^2$ |
|---|---|---|---|---|---|---|---|---|---|---|---|---|
| | | | | | | * | ** | | | | | |
| 0 | 0 | .780 | 0 | 0 | 0 | .6410 | .641 | 1.000 | 1.249 | 0 | 0 | |
| .01 | .0078 | .780 | .0177 | .0138 | .1106 | .6383 | .639 | .970 | 1.232 | .0144 | .0112 | .0176 |
| .02 | .0156 | .779 | .0251 | .0195 | .1561 | .6357 | .637 | .957 | 1.227 | .0205 | .0159 | .0349 |
| .03 | .0233 | .778 | .0307 | .0239 | .1907 | .6352 | .636 | .951 | 1.223 | .0251 | .0195 | .0522 |
| .04 | .0311 | .777 | .0356 | .0276 | .2197 | .6317 | .634 | .941 | 1.219 | .0292 | .0226 | .0693 |
| .05 | .0389 | .777 | .0399 | .0310 | .2452 | .6291 | .631 | .934 | 1.217 | .0328 | .0255 | .0863 |
| .06 | .0466 | .776 | .0438 | .0340 | .2679 | .6268 | .628 | .926 | 1.214 | .0361 | .0280 | .1032 |
| .08 | .0620 | .775 | .0507 | .0393 | .3081 | .6231 | .624 | .918 | 1.213 | .0418 | .0324 | .1369 |
| .10 | .0774 | .774 | .0569 | .0440 | .3431 | .6190 | .621 | .911 | 1.212 | .0469 | .0363 | .1706 |
| .15 | .1154 | .770 | .0705 | .0542 | .4158 | .6098 | .611 | .896 | 1.210 | .0583 | .0448 | .2534 |
| .20 | .1532 | .766 | .0823 | .0630 | .4753 | .6002 | .601 | .877 | 1.208 | .0681 | .0522 | .3344 |
| .25 | .1900 | .760 | .0930 | .0707 | .5253 | .5911 | .593 | .865 | 1.207 | .0771 | .0586 | .4144 |
| .30 | .2266 | .755 | .1029 | .0777 | .5695 | .5826 | .585 | .852 | 1.207 | .0853 | .0644 | .4931 |
| .35 | .2622 | .749 | .1123 | .0841 | .6083 | .5744 | .578 | .842 | 1.206 | .0931 | .0697 | .5708 |
| .40 | .2973 | .743 | .1215 | .0903 | .6432 | .5664 | .570 | .829 | 1.206 | .1007 | .0749 | .6465 |
| .45 | .3312 | .736 | .1303 | .0959 | .6745 | .5591 | .564 | .819 | 1.205 | .1081 | .0796 | .7213 |
| .50 | .3645 | .729 | .1389 | .1013 | .7031 | .5520 | .557 | .808 | 1.204 | .1154 | .0841 | .7945 |
| .60 | .4274 | .712 | .1557 | .1109 | .7535 | .5407 | .548 | .794 | 1.203 | .1294 | .0922 | .9394 |
| .70 | .4864 | .695 | .1721 | .1196 | .7941 | .5277 | .534 | .776 | 1.202 | .1432 | .0995 | 1.0774 |
| .80 | .5404 | .675 | .1884 | .1273 | .8289 | .5175 | .525 | .756 | 1.200 | .1570 | .1061 | 1.2085 |
| 1.00 | .6339 | .634 | .2211 | .1402 | .8832 | .5008 | .510 | .732 | 1.198 | .1846 | .1170 | 1.4640 |
| 1.20 | .7075 | .590 | .2544 | .1500 | .9215 | .4885 | .497 | .712 | 1.197 | .2125 | .1253 | 1.7037 |
| 1.40 | .7628 | .545 | .2883 | .1571 | .9482 | .4797 | .489 | .700 | 1.197 | .2409 | .1312 | 1.9340 |
| 1.60 | .8025 | .502 | .3234 | .1622 | .9662 | .4735 | .483 | .693 | 1.197 | .2702 | .1355 | 2.1561 |
| 2.00 | .8492 | .425 | .3960 | .1681 | .9847 | .4647 | .476 | .684 | 1.198 | .3306 | .1403 | 2.5809 |
| 2.40 | .8691 | .362 | .4712 | .1706 | .9947 | .4633 | .474 | .682 | 1.199 | .3930 | .1423 | 2.9927 |
| 3.00 | .8770 | .292 | .5867 | .1713 | .9987 | .4629 | .473 | .681 | 1.200 | .4889 | .1427 | 3.5924 |
| 5.12 | .8800 | .172 | 1.0000 | .1720 | 1.0000 | .4625 | .470 | .677 | 1.200 | .8333 | .1428 | 5.7184 |

* First approximation, Figure I-4
** Adjusted, Figure I-4

terminating points. The starting point for low but finite steepness is given by Stokes' theory equation 8. For waves of finite height in deep water, Stokes' third approximation is used, equations 11 and 12. The values given in Table I are very slightly adjusted such that $L/L_A = 1.20$ at $H/T^2 = .88$. These are used to obtain the isolines of $H/T^2$ at the far right of Figure 3. To obtain the continuation of these isolines of $H/T^2$ to the breaking limit established along the envelope curve one could make use of Figure 2 and solving equation 16 for non-breaking waves. This would require the knowledge of the horizontal particle velocity at the crest, since $u_o \neq C$ for non-breaking waves. At present there is no suitable wave theory for obtaining $u_o$ for large non-breaking waves. However, one could start with an assumed velocity field based on an approximation of wave theory, using Figures 2 and 3 as first approximations and employ relaxation techniques to obtain the complete picture. Such a procedure has been set up (Chappelear)[27] in case of the Solitary theory. The isolines of $H/T^2$ in Figure 3 have been assumed as shown, but have not been checked and adjusted according to relaxation techniques. It is believed that the assumed isolines of $H/T^2$ of Figure 3 are sufficiently accurate for design purposes, but if greater accuracy is required one may refer to the work by Chappelear.[27] Hence the design wave length is given by

$$L = \left(\frac{L}{L_A}\right) \frac{gT^2}{2\pi} \tanh \frac{2\pi d}{L_A} \tag{24}$$

Figure 5 is used to predict the maximum horizontal particle velocity at the crest, the accuracy of which depends on the accuracy of Figures 2 and 3.

Paper 1569 March, 1958 WW 2

Journal of the
WATERWAYS AND HARBORS DIVISION
Proceedings of the American Society of Civil Engineers

# SHIPBOARD HYDRAULIC BREAKWATER[a]

R. A. Dilley[1]
(Proc. Paper 1569)

## SYNOPSIS

A model hydraulic breakwater was constructed on a 1:86.5 scale model Liberty Ship. The ship was moored in a model basin in seven inches of water and subjected to a series of different wave conditions. The mooring forces and wave attenuation were measured.

Graphs showing the relationship between wave attenuation and jet-flow rate and the dependence of mooring force on wave height are included. It was found that the jet-flow rate to cause a given wave attenuation increased as the ratio of wave-length to water-depth increased. There was a critical wave height for each wave period at which the mooring line forces began to increase very rapidly with increasing wave height.

The investigation was conducted in a 150 ft. x 64 ft. x 2-1/2 ft. model basin at the Engineering Field Station, University of California, Richmond, California.

## INTRODUCTION

Many investigations have been made into the problem of providing a mobile breakwater which would be effective for calming normal ocean waves. The problem is complicated by the fact that in general the area to be calmed is in an area where the water is shallow and the wave action extends over the whole depth. Model studies and some prototype installations have shown that most of the proposed types of mobile breakwaters will reduce wave heights appreciably when the ratio of wave-length to water-depth is relatively small.

Note: Discussion open until August 1, 1958. A postponement of this closing date can be obtained by writing to the ASCE Manager of Technical Publications. Paper 1569 is part of the copyrighted Journal of the Waterways and Harbors Division, Proceedings of the American Society of Civil Engineers, Vol. 84 No. WW 2, March, 1958.

a. Submitted in partial fulfillment for the Master of Science in Engineering, University of California, Berkeley, August 1957.

1. Junior Engr., Univ. of California, Inst. of Eng. Research, Berkeley, Calif.

However, the longer waves cannot be reduced in height without causing prohibitive forces on the mooring lines. Considerable study has been conducted recently on hydraulic breakwaters.[2,3] Most of the work has been done with two-dimensional models. Very little has been done in three dimensions and hardly any work has been done on the forces on the structure due to the jet action. The few studies on three-dimensional models show that the waves tend to refract around the ends of the breakwater and augment behind it.

One method of preventing this refraction would be to create currents in both directions. Instead of just directing jets into the train of waves, jets also would be directed in the opposite direction. This arrangement would have another advantage since it would eliminate the large thrust on the breakwater due to the jet action in only one direction.

## General Considerations

A portable hydraulic breakwater would be very useful for protecting a section of ocean during an amphibious landing or some other temporary operation. One way to have the hydraulic breakwater mobile would be to install it on a ship. Then it could be moved to any other location in the minimum of time. While in operation the ship would have to be moored so that it would remain in a specified position.

In order to study the feasibility of a mobile hydraulic breakwater a model was constructed and then tested in a model basin (Fig. 1). A model of a Liberty Ship hull was available for this purpose. The hydraulic breakwater equipment was installed on the model ship and a four mooring line system was designed to hold the ship in position while the jets were in operation.

The problem of mooring a mobile hydraulic breakwater is more complicated than that of mooring a standard ship due to the jet action. The complications due to the jet action will be somewhat alleviated by having jets on both sides of the ship; however, the jets could affect the resonant period of oscillation of the ship model. Also it is likely that the jets will cause net forces on the ship due to slight variations in flow rate from one side to the other.

The problem of mooring a floating structure such as a ship in the open sea where it is subjected to wave action is analogous to the problem of a mass restrained by springs and acted upon by some force which varies with time. However, due to the many degrees of freedom and the non-linearities of the mooring system no general theoretical solution has been formulated for the problem of a ship moored at any heading to the seas. Neither has there been any theoretical solutions to the relatively simpler problem of a ship in head or beam seas. The pioneer effort in a theoretical solution of this problem was made by Wilson, 1950.[6] Wilson developed a differential equation for the longitudinal motion of a ship moored alongside a dock and subjected to relatively long period harbor seiches. Wilson's analysis is considerably simpler than that which would be necessary for a vessel moored in normal sea waves, since the particle motion of a seiche is more easily described than that of a wind wave or swell and also since he only considered longitudinal motion. A ship moored in a particular heading to the waves is not limited to motion in only one direction. However, certain relationships were developed by Wilson which yield some valuable qualitative results. As would be expected the resonant period of oscillation varies inversely as the initial tension in the mooring lines. The amplitude of the seiche and consequently of the vessel motion

affects the resonant period of oscillation when the tensions are high; the greater the seiche amplitude, the lower the resonant period of the system. Wilson and Abramson, 1955,[7] have used the Ritz method to treat the Wilson equation and have shown some results for ship displacement as a function of a non-linear natural period of oscillation function for various seiche amplitudes. Although the above-mentioned problem solution is a gross simplification of the problem at hand it does show the effects of mooring line tension and possibly wave amplitude.

Several studies have been performed[1,4] with different models of existing ships with several different mooring configurations. These studies indicate that the qualitative results mentioned above hold for ships moored in normal sea waves. The natural periods of oscillation vary inversely as the tensions in the mooring lines and the resonant period of oscillation becomes lower at higher wave amplitudes.

There are many variables to be considered in the problem of mooring the mobile hydraulic breakwater. For the purpose of this first investigation only the following variables were considered and all others were held constant:

(1) Seaward wave height
(2) Leeward wave height
(3) Wave period
(4) Jet-flow rate
(5) Mooring line tension (during one special part of the tests)

## Laboratory Equipment

The experiments were conducted in a 150 ft. x 64 ft. x 2-1/2 ft. model basin at the University of California Engineering Field Station, Richmond, California. This basin is equipped with a piston-type wave generator at one end and a wave absorbing beach at the other end. A structure supporting a photographic crane spans the width of the basin affording a working platform which could be positioned over any portion of the basin. Suspended from this platform and immediately surrounding the area in which the tests were performed was a plywood and canvas wind protector. An instrument shed at the side of the basin housed the Brush Universal Analyzers and Brush Oscillograph used as recording equipment and the wave generator controls (Fig. 1).

The water surface time histories from which the wave height and wave period could be determined were recorded with parallel-wire-resistance gages.[5] There were connected in parallel with one leg of a Wheatstone Bridge which was connected to a Brush Universal Analyzer.

The model ship was a 1:86.5 scale model of a Liberty Ship which was outfitted with four mooring lines, four force meters and the pump, manifold and jets which comprised the hydraulic breakwater system. With this equipment installed on the ship it was made dynamically similar to a Liberty Ship in the loaded condition according to Froude model laws. The apparatus for determining the ship characteristics is shown in Fig. 2. The longitudinal dimension of the center of gravity was determined by suspending the ship in an upright position at two points, one near each end, and determining one reaction force. Then knowing the displacement (the ship was weighed) the horizontal position of the center of gravity could be calculated by taking moments about one point of suspension. The vertical position of the center of gravity was determined in the same manner, only the ship was supported on knife

edges on its side and the reaction force at one point was measured. The draft is the distance from the baseline of the ship to the waterline at the center of gravity and was measured directly. The draft varied along the ship because the model in the water had a slight slope downward toward the stern. The natural period of roll was measured directly by rotating the model in the water and allowing it to oscillate and timing a number of oscillations. The roll period presented is for the ship without mooring restraints. The radius of gyration for pitch was determined by suspending the model as a bifilar pendulum and allowing it to oscillate in a yawing motion. From the period of the oscillations one can determine the radius of gyration by the following equation[2] from (4):

$$r = \frac{T_p\, a}{2\pi}\sqrt{\frac{g}{l}}$$

where

$T_p$ = period of oscillation of bifilar pendulum

$g$ = acceleration of gravity

$r$ = radius of gyration

$a$ & $l$ are shown in Fig. 2a

This is actually the radius of gyration in the yawing direction but the two radii of gyration are assumed to be the same. The other characteristics tabulated were determined by direct measurement. The data for the various characteristics of the ship model are shown in Table I.

The mooring force meters were designed to serve two purposes (1) record the force in the mooring lines and (2) provide the proper mooring chain elasticity. The force meters were U shaped double cantilever type with one Baldwin-Lima-Hamilton SR-4, A-5, 120 ohm resistance type strain gage glued on each side of the two cantilever arms (Fig. 3b). The force was recorded by arranging the four resistance type strain gages in a Wheatstone Bridge so that the maximum cumulative strain could be recorded for a given force on the meter. The bridge circuit could be hooked directly to a Brush Universal Analyzer which served as a power supply and amplifier. The force meters were calibrated for deflection characteristics and force measuring sensitivity. In order to give the mooring line the correct stiffness the meter had to have a given spring constant. The spring constant could be adjusted by changing the length of the cantilever arms. This constant was checked by applying a series of known weights and recording the deflection of the force meter at the point of the mooring line attachment. When the spring constant had been adjusted to the correct value, the length of the arms was fixed securely.

In order to determine the force on the force meter from oscillograph recordings it was necessary to have a correlation between force on the meter and the deflection of the recorder pen. This was determined by statically loading the meter with known weights and observing the pen deflection.

The mooring lines were made of No. 18 steel jack chain which weighed 0.019 pounds per foot. This corresponded to a prototype 3-3/4 inch dielock chain. The stiffness of the model chain exceeded the value required as derived from model laws so that the force meter could be adjusted to give the

2. See Appendix I for List of Symbols

TABLE I

MODEL SHIP CHARACTERISTICS

| | |
|---|---|
| Center of Gravity | |
| Vertical, distance above base line, ft. | 0.266 |
| Longitudinal, distance aft of bow, ft. | 3.01 |
| Draft and Displacement | |
| Draft at center of gravity, ft. | 0.224 |
| Displacement, lb. | 33.0 |
| Natural period of roll, sec. | 1.36 |
| Radius of gyration, transverse axis, pitch, ft. | 1.04 |
| Mooring line positions | |
| Bow to bow mooring hawse pipes, ft. | 0.583 |
| Bow to stern mooring hawse pipes, ft. | 4.71 |
| Baseline to mooring hawse pipes, ft. | 0.313 |

necessary extra elasticity. This requirement governed the length of the cantilevers used in the force meters. The mooring lines were attached to the meters with a short section of 12 mil wire. These were inserted through hawse pipes made of one-eighth inch copper tubing inserted through holes drilled in the sides of the model ship a short distance above the water line and clamped to the force meter bar. The hawse pipes were drilled at 45° to the longitudinal axis of the ship and with a dip angle of 45° below horizontal (Fig. 3). The angle which the chain made with the ship varied as the ship moved, but the meter was constructed so that the force on it always acted perpendicular to the meter arm. The mooring lines were 42 inches long and had small flat plates at the anchor ends. These plates had slots in them to allow for adjusting the initial tensions. The plates were fastened securely to the basin floor with Phillips shields and screws.

The hydraulic breakwater system consisted of a small pump and direct current motor, a one-inch plastic tube manifold running the length of the ship and ten jets, one-quarter inch in diameter on each side of the model. The jets were connected to the manifold with flexible tygon tubing and were fastened to the ship with slotted plastic plates and screws so that they could be easily adjusted in the vertical direction. The jets were set to operate at the waterline during all the tests. The discharge of the jets could be varied by changing the speed of the pump which was varied by changing the input voltage to the pump motor. The pump was calibrated so that the flow rate was known as a function of motor speed and of motor input voltage. The voltage was recorded as a measure of the flow rate during the runs since the voltage was easier to measure during a run than the motor speed.

The pump used was a surplus aircraft fuel transfer pump. Flow rates from 20 to 70 gallons per minute were attainable at heads from 5 to 25 feet of water. The pump was powered by a one-half horsepower direct current motor. The direct current power was supplied by a motor-generator set with field current control to supply the variable direct current voltage source.

## Experimental Procedure

Quantitative measurements were made of the mooring line forces at the ship, the incident and transmitted wave profiles and the jet-flow rate. The surface time history recorder between the wave generator and the model was placed 21 feet from the model so that the disturbance due to the model had a negligible effect on the wave profile at the recorder. This insured that the surface time history measured was the true incident surface time history. The wave recorder located on the lee side of the breakwater was situated in what was determined by several preliminary runs to be the area of maximum wave attenuation 8 feet behind the model.

Before the tests were begun several preliminary measurements and calibrations were made. The ship model with the hydraulic breakwater on board was assembled and the ship characteristics measured. The pump and mooring force meters were calibrated. These procedures are described in the section entitled "Laboratory Equipment" above.

Besides the quantities which were measured for each run there were several quantities which were measured periodically throughout the runs. The natural periods of oscillation in the three modes of surge, sway and yaw were measured. This was done by displacing the ship model in a direction so as to

cause the desired motion. The motion induced forces in the mooring lines and made a force time history on the oscillograph from which the period of oscillation could be measured.

When the model was set up for each series of tests the initial tension in each mooring line was adjusted to a predetermined value. At intervals during these tests these tensions were checked to insure that they were maintained correct. During the tests the procedure was as follows:

1. The wave generator and recording oscillograph were started.
2. The jets were started and the motor voltage recorded. (When taking runs with jet action.)
3. The mode of oscillation experienced by the ship was observed.

The test runs covered a wave period range of 0.5 seconds to 6.5 seconds. For each wave period, wave heights ranged from 0.02 foot to 0.18 foot. For some of the wave periods the whole range of wave heights could not be tested. Enough runs were taken without jet action to establish force as a function of wave height curves. Then for each wave height and wave period for 0.6 to 1.0 seconds three or four different jet-flow rates were tested to establish wave attenuation curves.

All of these tests were run with a water depth of seven inches. This made the mooring line scope (ratio of mooring line length to water-depth) equal to six.

## Analysis of Data and Results

The wave and force data were recorded on a six-channel Brush oscillograph. The incident wave height was calculated by averaging the heights of about ten of the incident waves and multiplying the average by the calibration factor which correlated distance on the chart paper with actual wave height in feet. The transmitted wave height was not so well defined as the incident wave height. In most cases it reached a minimum shortly after the jets were started. About five of the lowest waves were averaged and multiplied by the calibration factor to get the transmitted wave height. The wave attenuation was then computed using these values and the equation

$$e = \frac{H_i - H_t}{H_i}$$

where

$e$ = wave attenuation

$H_i$ = seaward wave height

$H_t$ = leeward wave height

The wave attenuation was then plotted as a function of jet-flow rate. The flow rate was determined from the voltage reading with the aid of the calibration curve prepared before the tests were started.

In analyzing the force time records the first two peak forces which occurred after the wave reached the ship were neglected since they usually were due to some starting transient. The length of time for which the run was unaffected by side and end conditions was determined and only this length of time was considered as the run for the purpose of analysis. The four highest

forces during this time interval were averaged and multiplied by the calibration factor for the force meter to obtain the force in the mooring lines. The average of the forces in lines number 1 and 4 (Fig. 3a) were computed and plotted as a function of wave height for each different wave period (Fig. 4).

In order to show the relationship of natural period oscillation to wave amplitude resonance curves for several different wave heights are shown in Fig. 5. These curves were obtained as a cross-plot from the force as a function of wave height curves by taking the slopes of the curves for the different wave periods at the various wave heights and plotting them as a function of wave period.

The relationship between wave attenuation and jet-flow rate is given in Fig. 6 for several ratios of wave length to water depth. A cross-plot from the curves given in Fig. 6 is given in Fig. 7 to show the relationship between the ratio of wave-length to water-depth and wave attenuation, for several flow rates.

Fig. 8 shows the effect of initial tension on the natural periods of oscillation of the ship model.

## Discussion

The graphs of wave attenuation as a function of jet-flow rate (Fig. 6) show that in the range of wave heights tested and within the range of experimental error, the height of the waves at a given ratio of wave-length to water-depth does not affect the flow rate required to cause a given wave attenuation. The general shape of these curves, although not well-defined, due to the inability of obtaining data in the range from 0 to 20 gallons per minute flow rates, was known from previous work with hydraulic breakwaters.[2,3] The jet-flow rate to cause a given attenuation increases as the wave-length to water-depth ratio increases (Fig. 7). For the wave periods above 1.0 seconds the jets had no effect on the transmitted wave. This shows that the limiting L/d ratio is between 6.60 and 8.50 for the range of flow rates available. The attenuation curve in Fig. 6c for the 0.60 second period waves (L/d = 3.06) shows more scatter than those shown in Figs. 6a and 6b, especially for the condition with no jet-flow rate. It has been observed that the waves produced by the wave generator at this low period are not good cylindrical waves. This may account for some of the scatter of data for this period.

Curves are shown for the average force in lines number 1 and 4 as a function of wave height (Fig. 4). These are the mooring lines on the seaward side of the model ship. This average force was selected to use as a representative value because these two forces were generally about equal and higher than those experienced by the other two mooring lines. The forces in the mooring lines with and without jets operating were plotted on the same graph (Fig. 4). In general the jet action tended to lessen the ship motion and the mooring line forces. However, due to the scatter of data it was not possible to determine separate curves for the force as a function of wave height with and without the jets operating. The scatter of data is believed to be caused by the several modes of oscillation which the model experienced for any given wave condition, the inability to produce exactly identical waves on any two consecutive runs and the two-branch response characteristic exhibited by certain non-linear systems. Two wave trains which appeared to be the same could be slightly different and cause the model ship to experience two different modes of motion.

Some non-linear spring mass systems have a two branch response curve.(7) A description of the response of this type of system may help to describe some of the results found in these tests. For low amplitudes of the forcing function the mass will oscillate out of phase with the forcing function. As the amplitude of the forcing function increases the motion of the mass increases until a critical value of the forcing function is reached. When this critical amplitude is reached the motion changes phase and "jumps" to a higher amplitude. If the forcing function is then increased still further the motion will stay in phase and will continue to increase as the forcing function amplitude increases. However, if the forcing function decreases the amplitude of motion of the mass will decrease along a different curve and stay in phase with the forcing function until another critical point is reached. At this critical point, which is at a lower amplitude of the forcing function than the critical point mentioned above, the motion of the mass "jumps" discontinuously to a lower value and goes out of phase. Then there is one curve for a forcing function which starts low and increases and another for a forcing function which starts high and decreases.

The model hydraulic breakwater exhibited characteristics analogous to this system for the shorter period waves. In fact at all but the 6.5 second wave period condition there was a critical wave height above which the forces increased very rapidly with increase in wave height. It seemed that up to a certain wave height the forces were of the order of the initial tensions, but if the wave height was increased by a small amount the force jumped to some value very much higher. There was a wave height range in which two consecutive runs with as nearly as possible the same wave conditions produced force records which were very different in magnitude. Observation of the model motion led to the conclusion that if the motion was such that the mooring lines did not become completely taut the forces were comparatively low. However, once the model ship pulled against the mooring lines hard enough to make them taut the motion and the force tended to amplify. Also the lower amplitude motion and mooring line force did not always occur for each wave period, but tended to be random; whereas the records for higher amplitude waves showed peak forces for each wave period. When the forces became relatively high, the mode of oscillation experienced by the ship model changed. For the low amplitude forces there were two general kinds of ship motion. The first can be described as follows: the ship would be displaced in the lee direction and held so that the tension in lines number 1 and 4 was greater than the normal initial tension, and the tension in lines number 2 and 3 was less than normal. While the ship was held displaced, it would experience a small amplitude motion generally a combination of heave and roll which caused small amplitude variations in the force in the seaward mooring lines. The other type of motion which the model ship experienced for short wave periods (less than 1.2 seconds) and low wave heights was when the model ship seemed to be excited into a long period oscillation (5 to 7 seconds) by the first few waves of the train. Superimposed on the long period motion was a small amplitude rolling or heaving motion. The two types of motion described above were generally experienced for the lower wave heights. The critical wave height can be seen on the force as a function of wave height curves (Fig. 4). That is, when the forces began to increase rapidly with increase in wave height, the motion changed. The two types of motion mentioned above were relatively small compared to the motion that occurred for the higher waves.

Above the critical wave height the motion for wave periods less than 1.2

seconds was a combination of pitch and yaw. The natural period of pitching was 1.34 seconds as determined by the bifilar pendulum method of measuring. This method of measurement does not consider the damping due to the water or the effect of the mooring lines. The damping due to the water would tend to increase this value, but the mooring lines acting as springs would tend to decrease the period. Also due to the non-linearities of the system the natural period or resonant period would decrease as the wave amplitude increased. Since the motion was not pure pitch, but rather a combination of pitch and yaw, it may have a resonant period for certain wave heights in the region of the wave periods encountered.

The wave periods between 1.2 and 3.2 seconds and wave heights above the critical caused motion which was a combination of sway and yaw. Below the critical wave height the motion was primarily sway for these conditions. The 4.5 and 6.5 second period waves caused sway at all the wave heights tested. Even the lowest wave at the 6.5 second period caused the mooring lines to become taut.

For some test conditions some of the mooring line forces were noted as negative. This is because the force recorded is the force above the initial tension in the mooring lines. Since the mooring lines cannot support compression these negative forces cannot exceed the initial tension. Negative forces recorded for runs without jet action were usually on lines 2 and 3 and were for the wave periods less than one second. This was caused by the mode of motion where the ship was displaced to the lee. Another cause of negative forces was the jet action under certain conditions. For large flow rates and low wave heights one or two mooring lines would experience forces less than the initial tension, because the difference between the flow rates on the two sides of the ship model was great enough to cause a net force on the ship and hold it displaced.

A resonance curve is shown in Fig. 5. The ordinate is a measure of the rate of change of force with change of wave height. These curves were constructed by taking the slopes of the force vs. wave height curves for a series of wave heights. These data then were plotted for constant wave heights as a function of wave period. The range of resonant forces increases as the wave height increases.

Fig. 8 shows the dependence of the natural period of the initial tension. This plot shows that the natural period of the system decreases with increasing tension. The natural periods plotted here are for relatively small oscillations of the ship model. Any motion which pulled the mooring lines taut was damped out before one complete cycle could be recorded. Because of the damping, it was not possible to check directly the effect of amplitude on the natural period.

## CONCLUSIONS

1. Within the range of wave heights tested and the range of experimental error the wave attenuation for a given jet-flow rate and ratio of wave-length to water-depth was unaffected by wave height (Fig. 6).
2. The jet flow rate to give a certain value of wave attenuation increases as the ratio of wave-length to water-depth increases.
3. In general the motions of the ship model were less violent and consequently the forces were lower when the jets were running than when the jets were not running.

4. The motions of the ship model were relatively complicated. Small differences in wave conditions sometimes caused large differences in the ship model response.
5. There was a critical wave height above which the mooring line forces increased very rapidly with increases in wave height. This wave height decreased with increased wave period.
6. The range of resonant wave periods increased as the wave height increased.
7. The natural period of oscillation varied inversely as the initial tension in the mooring lines.

## ACKNOWLEDGMENTS

The author wishes to express his appreciation to Professors J. W. Johnson and P. L. Chambre and Mr. R. L. Wiegel for their helpful comments concerning this paper. The author wishes to thank Mr. A. L. Arnold for his assistance with the experimental work, Miss M. M. Lincoln for her assistance in preparing the figures and Mrs. V. Bauer for typing the manuscript.

## REFERENCES

1. Wiegel, R. L., Beebe, K. E., and Dilley, R. A., Model Study of the Dynamics of an LSM Moored in Ocean Waves, Sixth Conference on Coastal Engineering, The Engineering Foundation.
2. Snyder, C. M., Model Hydraulic Breakwater Studies: Preliminary Report, University of California, Institute of Engineering Research, Series 104, April 1957 (Unpublished)
3. Straub, L. G., Experimental Studies of Hydraulic Breakwaters, St. Anthony Falls Hydraulic Laboratory, University of Minnesota, Project Report No. 51, June 1956 (Unpublished)
4. Wiegel, R. L., Dilley, R. A., Clough, R. W. and Williams, J. B., Model Study of Floating Drydock Mooring Forces, Proceedings Symposium on Behavior of Ships in a Seaway, Netherlands Ship Model Basin, Wageningen, page 563, 1957.
5. Wiegel, R. L., Parallel Wire Resistance Wave Meter, Proceedings First Conference on Coastal Engineering Instruments, Council on Wave Research, The Engineering Foundation, Berkeley, Calif., pp. 39-43, 1956.
6. Wilson, B. W., Ship Response to Range Action in Harbor Basins, Proc. ASCE Volume 76, Separate No. 41, November 1950.
7. Wilson, B. W., and Abramson, H. N., A Further Analysis of the Longitudinal Response of Moored Vessels to Sea Oscillations, The A & M College of Texas, Texas A & M Research Foundation, A & M Project 24—Reference 55-16 T, April 1955. (Unpublished)

## APPENDIX I

### List of Symbols

$L$ = wave-length

$d$ = water-depth

$H_i$ = incident wave height or seaward wave height

$H_t$ = transmitted wave height or leeward wave height

$T$ = wave period

$Q$ = jet-flow rate

$S$ = mooring line scope

$T_i$ = initial tension in mooring lines

$e$ = wave attenuation

$L_o$ = deep water wave-length

Ave= average

## APPENDIX II

### Prototype Prediction

Assume that an area of ocean is to be protected by a Liberty Ship with a hydraulic breakwater on board. The allowable wave height in the lee area is 3 feet. The waves in the area are 10 feet high and the wave period is 9.3 seconds. The water depth is 50 feet. The length of the Liberty Ship is 454 feet, and the model used was 5.25 feet. This makes the ratio of length in prototype to length in model equal 86.5. From this we get the following scale ratios according to Froude Model Laws:

$$\frac{\text{Length in prototype}}{\text{Length in model}} = \lambda = 86.5$$

$$\frac{\text{Jet-flow rate prototype}}{\text{Jet-flow rate model}} = \lambda^{\frac{5}{2}} = 69500$$

$$\frac{\text{Mooring force prototype}}{\text{Mooring force model}} = \lambda^{3} = 648{,}000$$

$$\frac{\text{Time in prototype}}{\text{Time in model}} = \lambda^{\frac{1}{2}} = 9.3$$

In order to reduce the wave height the necessary amount a wave attenuation of 70 per cent is needed.

The model wave characteristics corresponding to the conditions above are $T = 1.0$, $H_i = 0.115$ ft. and $H_t = 0.035$ ft.

Then the model average mooring line force from Fig. 4c is 2.25 lbs. and the jet-flow rate required is 48 gpm or 0.107 CFS from Fig. 6a. Then scaling up to the prototype we get:

Average mooring line force = 2.5 x 648000 = 1,460,000 lbs.

Jet-flow rate = 0.107 x 69500 = 7380 CFS

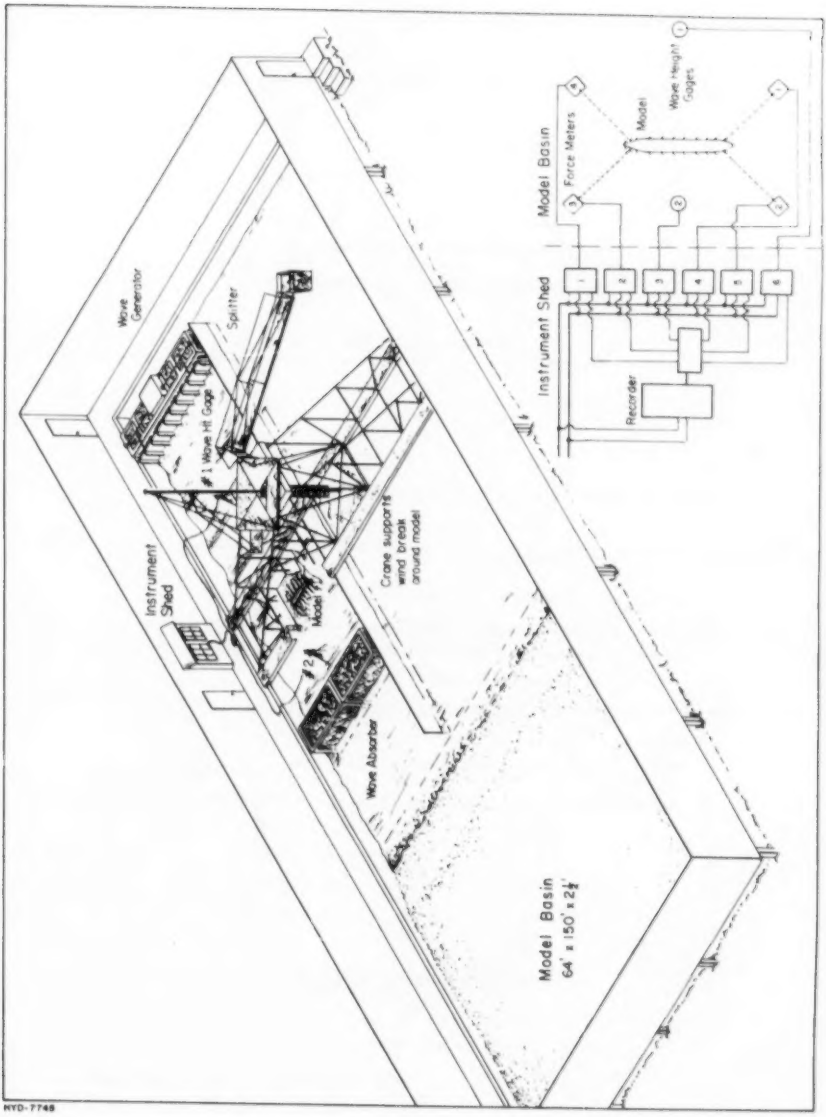
Model Basin
Force Meters
Model
Wave Height Gages
Instrument Shed
Recorder
Wave Generator
Splitter
#1 Wave Ht Gage
Instrument Shed
Model
Crane supports wind break around model
Wave Absorber
Model Basin
64' x 150' x 24'
HYD-7748

FIGURE 1

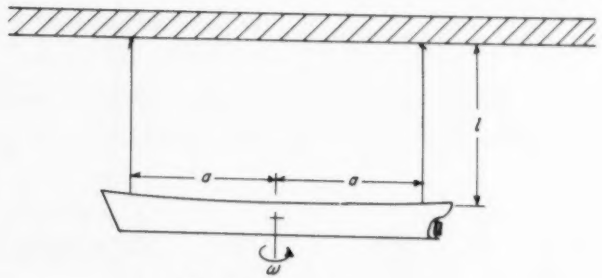


Bifilar pendulum

a.

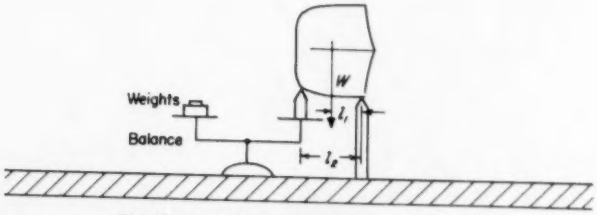


Vertical center of gravity

b.

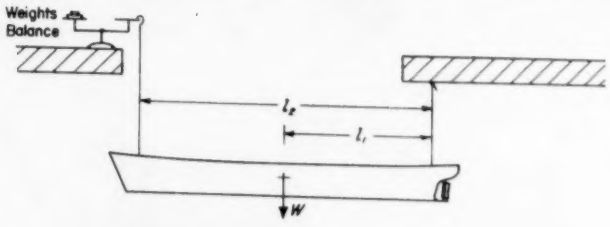


Horizontal center of gravity

c.

HYD-7747

FIGURE 2

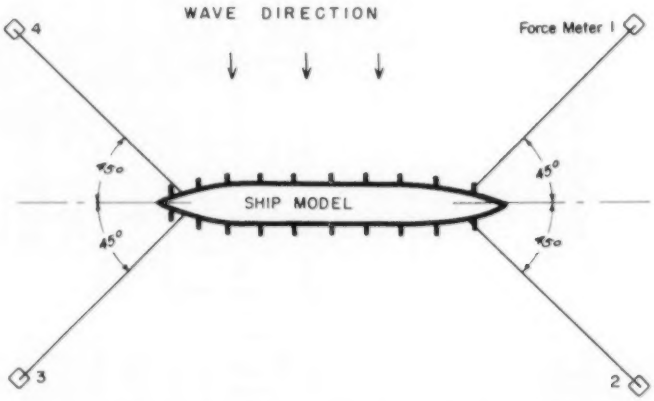


Sketch showing anchoring system and wave direction

a.

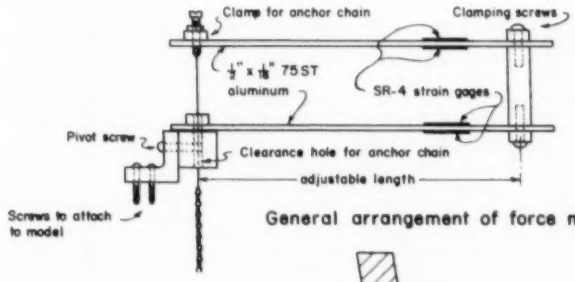


General arrangement of force meter

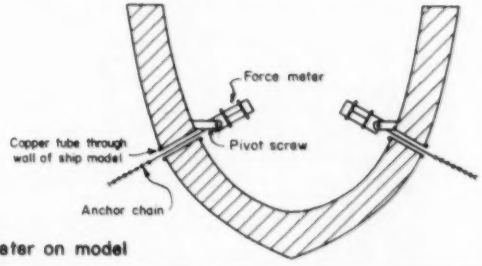


Mounting of force meter on model

b.

HYD-7746

FIGURE 3

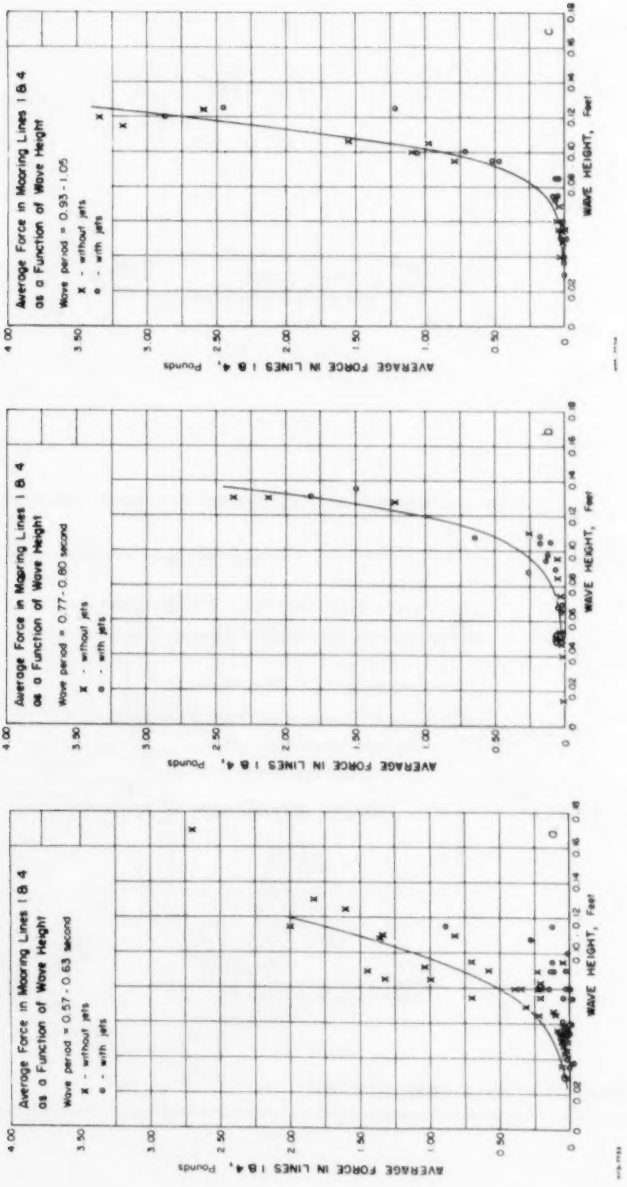
Average Force in Mooring Lines 1 & 4
as a Function of Wave Height
Wave period = 0.93 - 1.05
X - without jets
o - with jets
c
Average Force in Mooring Lines 1 & 4
as a Function of Wave Height
Wave period = 0.77 - 0.80 second
X - without jets
o - with jets
b
Average Force in Mooring Lines 1 & 4
as a Function of Wave Height
Wave period = 0.57 - 0.63 second
X - without jets
o - with jets
a
AVERAGE FORCE IN LINES 1 & 4, Pounds
WAVE HEIGHT, Feet

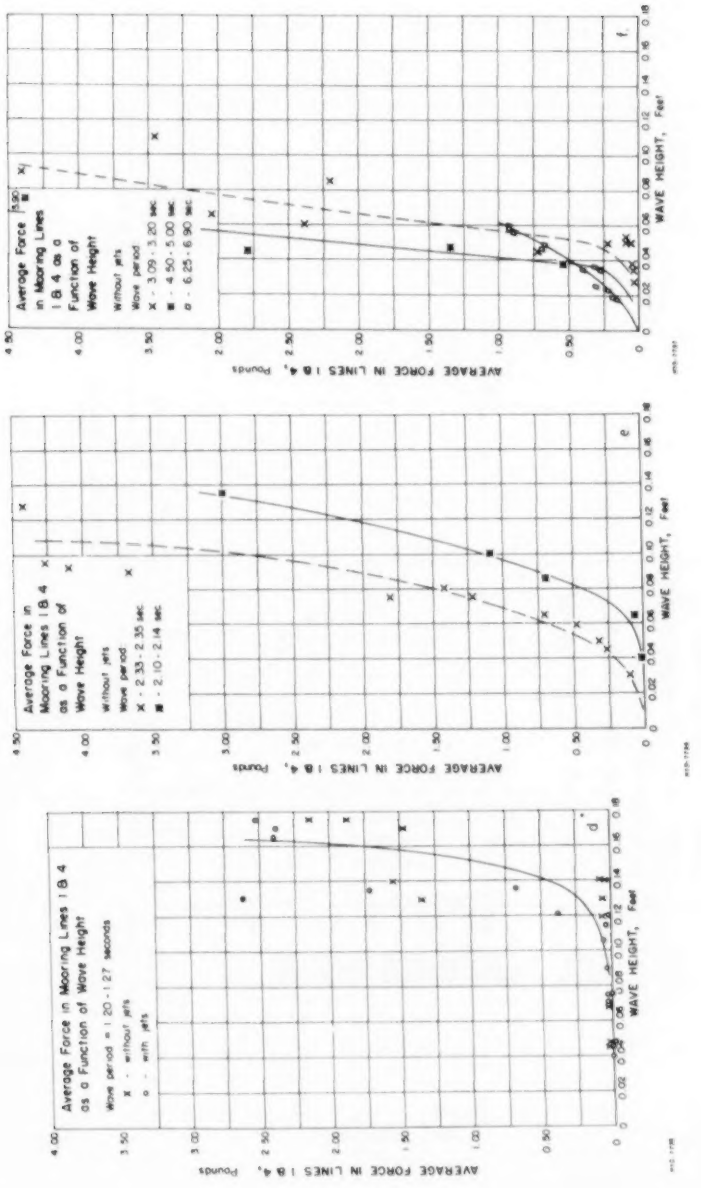
Average Force in Mooring Lines 1 & 4 as a Function of Wave Height
Without jets
Wave period
x - 3.09 - 3.20 sec.
■ - 4.50 - 5.00 sec.
o - 6.25 - 6.90 sec.
f
AVERAGE FORCE IN LINES 1 & 4, Pounds
WAVE HEIGHT, Feet
Average Force in Mooring Lines 1 & 4 as a Function of Wave Height
Without jets
Wave period
x - 2.33 - 2.35 sec.
■ - 2.10 - 2.14 sec.
e
AVERAGE FORCE IN LINES 1 & 4, Pounds
WAVE HEIGHT, Feet
Average Force in Mooring Lines 1 & 4 as a Function of Wave Height
Wave period = 1.20 - 1.27 seconds
x - without jets
o - with jets
d
AVERAGE FORCE IN LINES 1 & 4, Pounds
WAVE HEIGHT, Feet

FIGURE 4

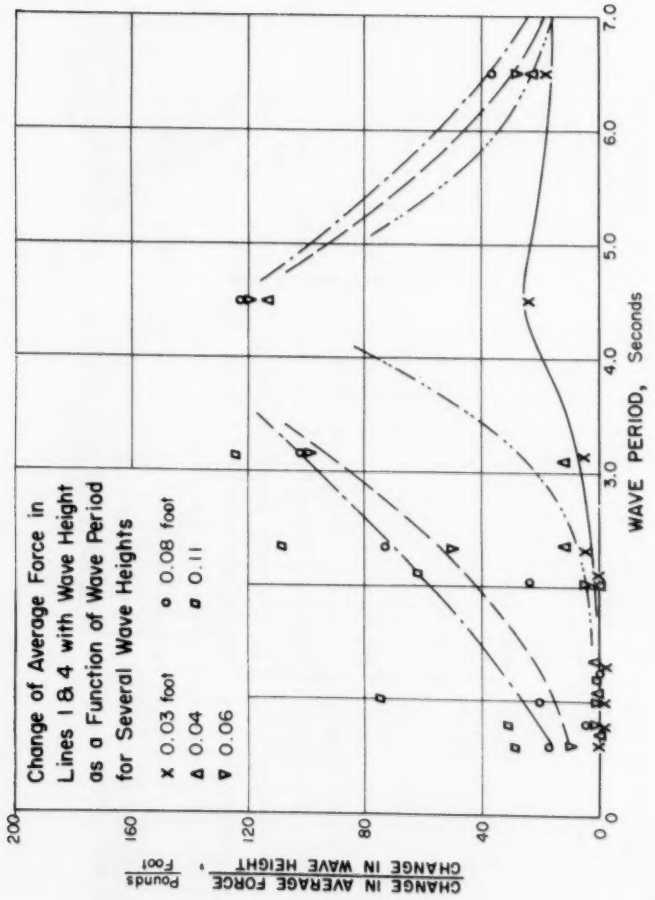


HYD-7738

FIGURE 5

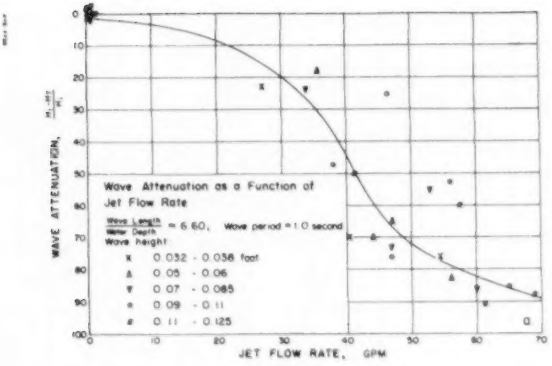
Wave Attenuation as a Function of Jet Flow Rate
Wave Length / Water Depth = 6.60, Wave period = 1.0 second
Wave height:
x 0.032 - 0.038 foot
Δ 0.05 - 0.06
▽ 0.07 - 0.085
○ 0.09 - 0.11
# 0.11 - 0.125
a.
WAVE ATTENUATION, (H - Hr)/Hi
JET FLOW RATE, GPM

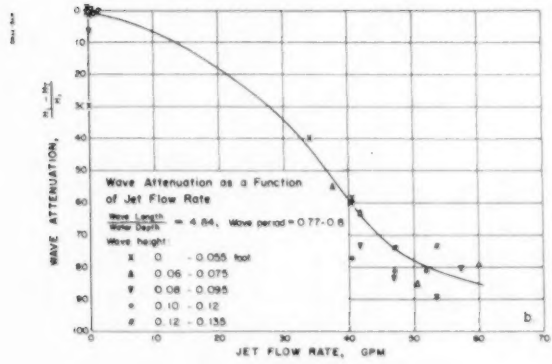
Wave Attenuation as a Function of Jet Flow Rate
Wave Length / Water Depth = 4.84, Wave period = 0.77-0.8
Wave height:
x 0 - 0.055 foot
Δ 0.06 - 0.075
▽ 0.08 - 0.095
○ 0.10 - 0.12
# 0.12 - 0.135
b.
WAVE ATTENUATION, (H - Hr)/Hi
JET FLOW RATE, GPM

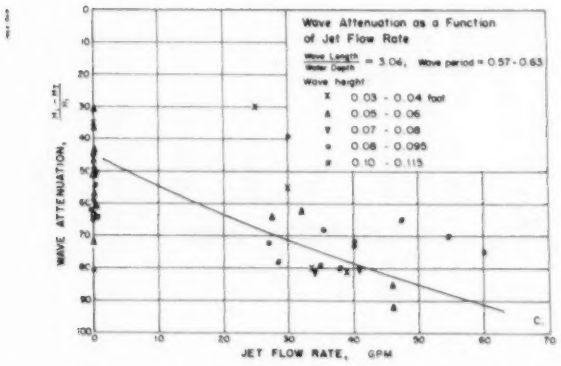
Wave Attenuation as a Function of Jet Flow Rate
Wave Length / Water Depth = 3.04, Wave period = 0.57-0.63
Wave height:
x 0.03 - 0.04 foot
Δ 0.05 - 0.06
▽ 0.07 - 0.08
○ 0.08 - 0.095
# 0.10 - 0.115
c.
WAVE ATTENUATION, (H - Hr)/Hi
JET FLOW RATE, GPM

FIGURE 6

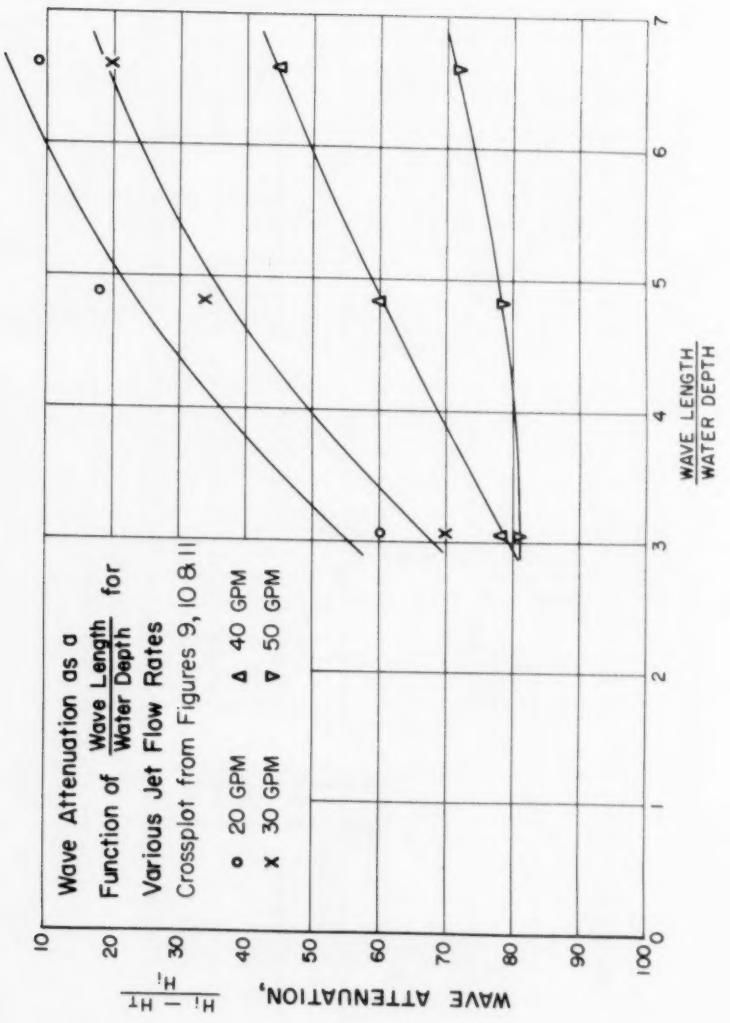


HYD-7742

FIGURE 7

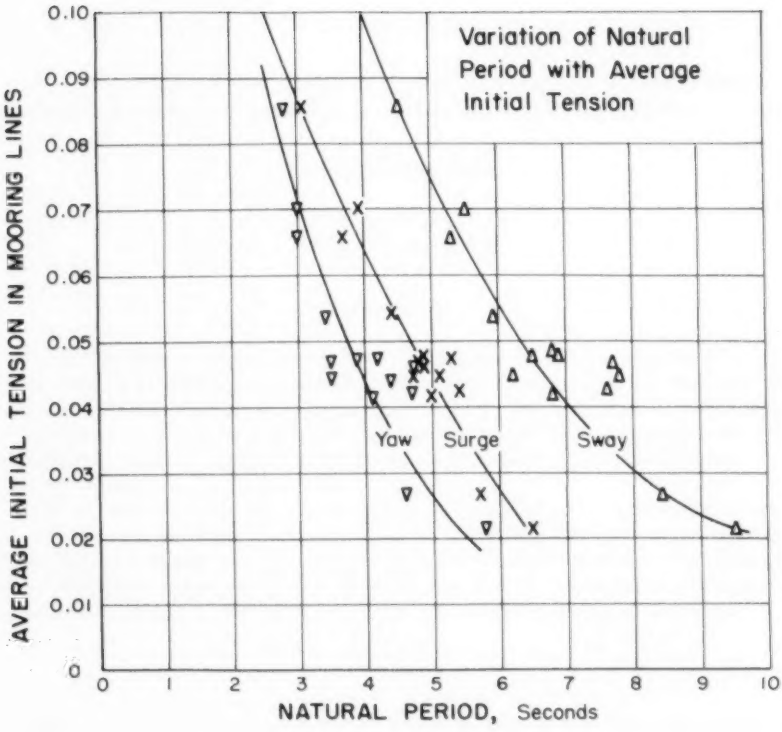


HYD-7744

FIGURE 8

Paper 1570 March, 1958 WW 2

Journal of the
WATERWAYS AND HARBORS DIVISION
Proceedings of the American Society of Civil Engineers

# THE WELLAND CANAL

W. A. O'Neil[1]
(Proc. Paper 1570)

## SYNOPSIS

The first major step towards the construction of a deep waterway from Lake Erie to Montreal, was realized with the completion of the Welland Canal in 1932. This canal connects Lake Erie to Lake Ontario, Fig. 1, a difference in elevation of 326.5 feet, and provides a channel 25 feet deep and locks to accommodate vessels up to 735 feet long, so that navigation may bypass Niagara Falls.

The St. Lawrence Seaway Authority was established by the Government of Canada for the purpose of constructing, maintaining and operating all Canadian works in connection with a deep waterway between Montreal and Lake Erie. The additional deepening on the Welland Ship Canal to the Seaway Standards is therefore being undertaken under the jurisdiction of this Authority.

## History

The present Welland Canal is the latest in a series of four which have been built in the Niagara Peninsula to overcome the obstacle to navigation presented by the Niagara River, its Rapids and Niagara Falls.

### First Welland Canal

The first Welland Canal was built between 1824 and 1829 as a private enterprise by The Welland Canal Company. The builders utilized natural watercourses as much as possible to save expense and labour. The route led up the Twelve Mile Creek from Port Dalhousie on Lake Ontario following its wavering course to the escarpment. Here a deep cut was made across the height of land to Chippawa Creek (also known as the Welland River,) at Port Robinson where boats descended the creek to the Niagara River and thence to Lake Erie. To obtain sufficient water to operate the canal, the summit level was connected by

Note: Discussion open until August 1, 1958. A postponement of this closing date can be obtained by writing to the ASCE Manager of Technical Publications. Paper 1570 is part of the copyrighted Journal of the Waterways and Harbors Division, Proceedings of the American Society of Civil Engineers, Vol. 84, No. WW 2, March 1958.

1. Div. Engr., Welland Div., St. Lawrence Seaway Authority, St. Catherines, Ontario.

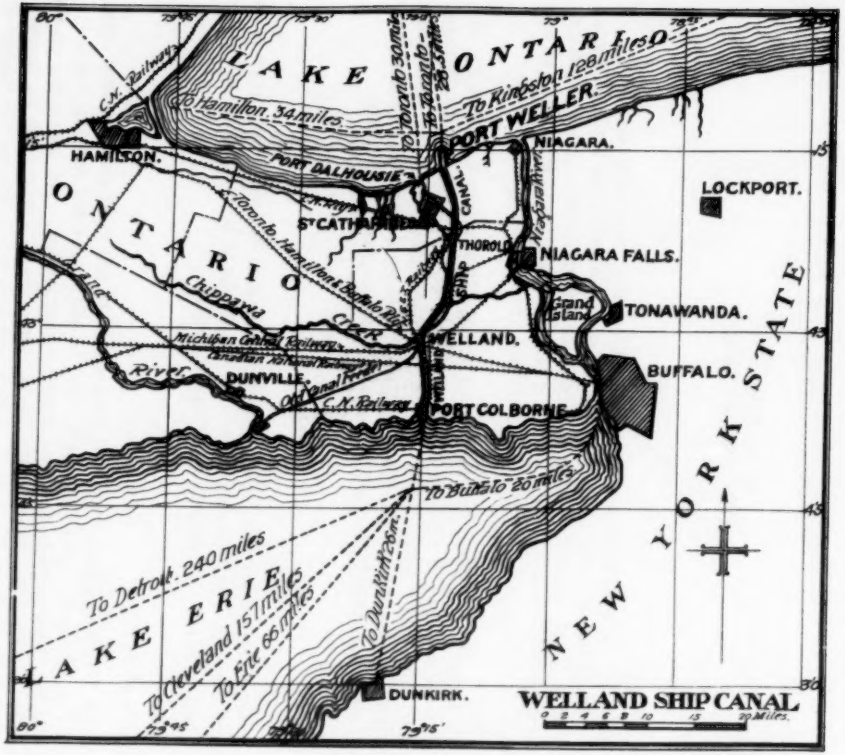


FIGURE Nº 1

28-2.

a feeder canal to the Grand River at Dunnville. To overcome the difference in elevation required 40 wooden locks, each 110 feet long, 22 feet wide with a depth of water of 8 feet on the sills. The sailing vessels usually had to be towed up the Niagara against the strong wind and current. Ice jams in the early spring also held up navigation. An extension of the canal from Port Robinson south to Port Colborne eliminating this bottleneck was constructed and opened to navigation in 1833, however, the canal was still fed from the Grand River.

### Second Welland Canal

In 1841 the legislature of Upper Canada purchased the canal and decided to enlarge it to 9-foot navigation. By increasing the lift, the number of locks was reduced to 27, and they were redesigned and built of cut stone, the dimensions being 150 feet long, 26 1/2 feet wide, and a depth of 9 feet of water on the sills. The Port Maitland, Dunnville Branch on the Grand River was built at this time. By 1853, it had become evident that the Grand River would not suffice as a feeder for a canal with much traffic, and plans were devised for a further reconstruction, so that the canal could be fed directly from Lake Erie. It was not until 1881 that this was finally accomplished, the water coming from the lake at Port Colborne.

### Third Welland Canal

Confederation of the provinces of Upper and Lower Canada in 1867 placed the inland water-ways under Federal jurisdiction. A uniform scale of navigation for the St. Lawrence route and the Welland Canal was recommended, with locks 270 feet long, 45 feet wide, and 12 feet of water on the sills, which was later changed to 14 feet. The work of enlarging the Welland Canal to these dimensions, was started in 1873 and completed 14 years later.

The course of the third canal utilized much of the previous channel, but climbed the escarpment east of the second canal to Allanburg. It then followed the previous route. Its 26 locks were built of cut stone with lifts of 12 to 14 feet. An aqueduct carried the canal over the Chippawa Creek at Welland.

This improved and enlarged waterway, together with a similar canal system along the St. Lawrence River from Lake Ontario to deep water at Montreal, met the immediate demands of inland water commerce until the beginning of the 20th Century, but failed to keep pace with the ever-increasing size of cargo carriers being built on the upper lakes. Transshipments to small ships at the Lake Erie entrance to the Welland Canal was costly, and caused traffic congestion on Lake Erie at the junction of 14-foot navigation with greater draft accommodation of the Upper Lakes. To remedy this situation, the fourth, or Welland Ship Canal was planned.

### Welland Ship Canal

The route of the Ship Canal was radically changed from the previous canals at the Lake Ontario end, so that it runs essentially in a straight line across the Peninsula, a distance of nearly 28 miles, Fig. 2. It leaves Lake Ontario at a point about 4 miles east of Port Dalhousie, the northern terminus of the previous canals, and follows in practically a straight line, due south along the valley of the Ten Mile Creek to the foot of the Niagara Escarpment at Thorold. This alignment is maintained in the ascent of the escarpment itself, although the route of the previous canals is followed from the top of the escarpment to

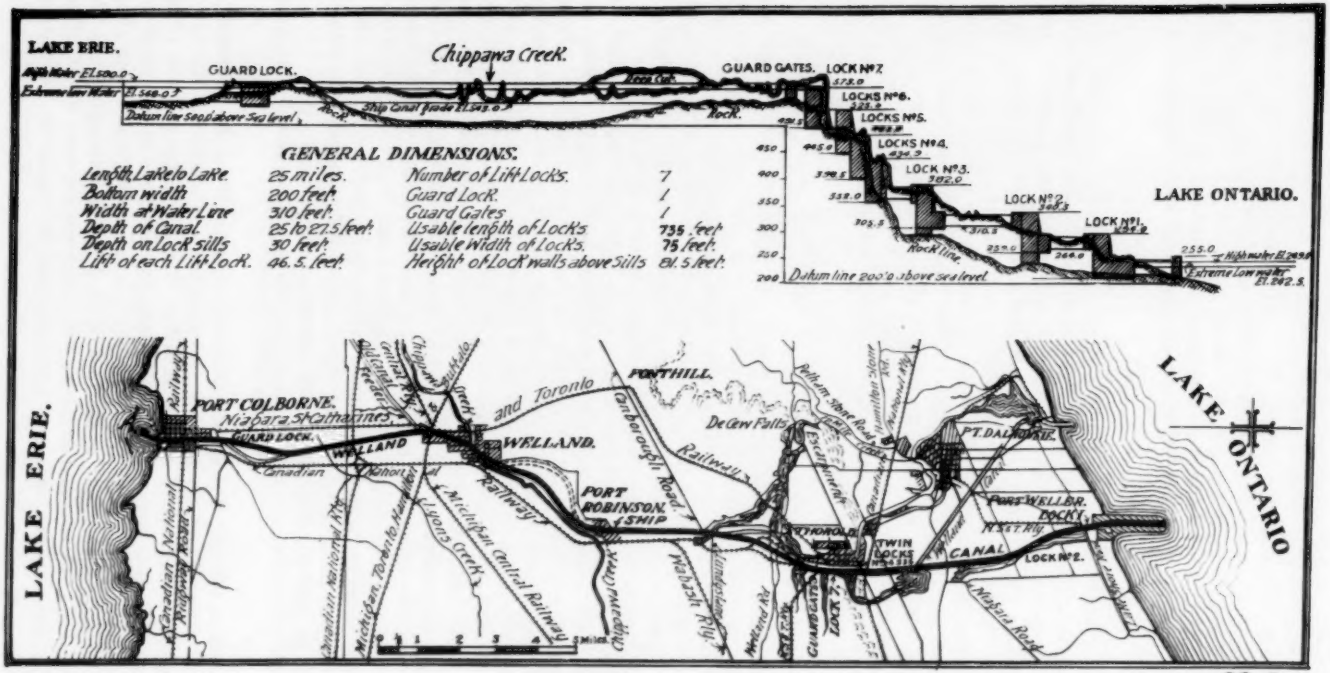
LAKE ERIE.
Chippawa Creek.
GUARD LOCK.
GUARD GATES.
LOCK No 7
LOCKS No 6.
LOCKS No 5.
LOCKS No 4.
LOCK No 3.
LOCK No 2.
LOCK No 1.
LAKE ONTARIO.
Rock line.
Datum line 200'0 above sea level.
GENERAL DIMENSIONS.
Length, Lake to Lake. 25 miles.
Bottom width 200 feet.
Width at Water Line 310 feet.
Depth of Canal 25 to 27.5 feet.
Depth on Lock Sills 30 feet.
Lift of each Lift Lock. 46.5 feet.
Number of Lift Locks. 7
Guard Lock. 1
Guard Gates 1
Usable length of Locks 735 feet.
Usable Width of Locks. 75 feet.
Height of Lock walls above Sills Ft. 5 feet.
LAKE ERIE.
PORT COLBORNE.
Niagara Falls
GUARD LOCK.
WELLAND
WELLAND.
PORTHILL.
Toronto
Canborough Road
Railway
De Cew Falls
PORT ROBINSON SHIP
Welland Canal
Welland River
Michigan, Toronto & Hamilton Railway
Lyons Creek
Canadian National Railways
Canadian Pacific Railway
Thorold
TWIN LOCKS
CANAL
LOCK No 2.
PT. DALHOUSIE.
PORT WELLER DOCKS
LAKE ONTARIO
Niagara River
Welland Ship Canal
0 1/2 1 2 3 4 5 Miles
28-3.

FIGURE Nº 2

Port Colborne in a general way, all of the sharp bends of the previous canals are eliminated.

Port Weller Harbour

As no harbour existed on Lake Ontario at the mouth of the Ten Mile Creek, now the northern terminus of the Welland Ship Canal, as artificial harbour, Port Weller was one of the necessities of construction. By means of a standard double track railway, extending from Lake Ontario south for seven miles or more along the route of the canal, the surplus excavation of this northern division of the work was disposed of in the form of two embankments projecting north from the shoreline 1-1/2 miles into Lake Ontario, to form an artificial harbour. At their outer and inner ends these embankments are outlined by reinforced concrete cribs, those at the inner end of the harbour providing ample dockage space. Rock excavation placed along the exterior of the two embankments protects them against storm erosion.

Locks - General

To overcome the difference in elevation between the two lakes, 7 concrete locks with an average lift of 46.5 feet have been built. The locks are 80 feet wide, 859 feet long between gates and with a depth of water of 30 feet over the sills. The usable length for navigation is 715 feet and the widest ship which has transitted the canal is 75 feet.

The first seven miles of the Welland Ship Canal south from Lake Ontario are banked by the slightly rising lower level of the peninsula, which is deservedly called the Garden of Canada because of its natural rolling beauty and intensively cultivated fruit lands. In this section of the canal are the first three single locks, Nos. 1, 2, and 3 which elevate navigation 139.5 feet above the Lake Ontario level and bring it to the foot of the Niagara Escarpment.

The climb up the face of the escarpment, by means of equal lifts is obtained without any deviation from the direct route. Three locks in flight are superimposed immediately one above the other so that in a distance of slightly over one-half mile, navigation is elevated another 139.5 feet. So that serious delays to navigation do not occur, these locks nos. 4, 5 and 6 are twin locks which provide separate passage for upbound and downbound navigation, Fig. 3.

With a short intervening stretch of canal prism, the last of the seven locks, which brings navigation to Lake Erie level, is reached in the town of Thorold. In this short reach there is sufficient distance for vessels to pass.

As it is essential to control the summit level of the canal from Thorold to Port Colborne at a regulated level of elevation 569.0 there is at Port Colborne a supply weir and a guard lock (Lock No. 8) through which vessels are locked between the summit level and the fluctuating level of Lake Erie at Port Colborne. Lock 8 has a usable length of 1148 feet. A Guard Gate and a safety weir are situated just above Lock 7 to retain the summit level in case of accident to Lock 7.

Locks - Filling and Emptying

The locks in general have been built with concrete entrance walls at both ends. The 46.5 foot lift permits the upper gate to be situated on a high concrete breast wall and thereby prevents this gate from being struck by a ship proceeding up the lock at the lower pool level. The pond for filling the lock is

WELLAND CANALS - WELLAND SHIP CANAL Twin locks Nos 4, 5 & 6.
View looking South from Lower West end of locks No. 4.
64-J-56 Sept/56

FIGURE N° 3

situated on the east side at its upper end and the waste water passes over a weir provided with stoney valves which are opened automatically, should the water in the reach rise too high. The waste water flows down through an open raceway into the canal prism below the lock. Each lock wall has running through it, longitudinally, at floor level, a water culvert 14 feet wide by 16.5 feet high with a semicircular top. Both culverts lead to an intake situated in the east wall, and the inflow of water is controlled by four intake valves of the vertical sector type. Each culvert discharges into the canal prism below the lower gate, and the outflow from each culvert is controlled by two discharge valves also of the vertical sector type. These culverts deliver or take the water to or from a lock chamber through laterals or ports 3 feet wide by 4 feet high situated in the lock walls at floor level and spaced longitudinally at intervals of 30 feet.

Flight locks No. 4, 5 and 6, the first two of which take the water directly from the lock above, are twinned in order that ships may be passed simultaneously in opposite directions through the flight. The flow of the water is controlled in a manner similar to that of the other locks, except that the intakes for the culverts in the centre wall are in its upper end, and take the water direct from the entrances of the lock chambers, whereas the culverts in the east and west walls are fed from an intake in the east wall which takes the water from the pondage.

It requires about 70 acre feet to fill one single lock with a lift of 46.5 feet, so it is essential to provide a large pondage area above each lock to avoid lowering the canal water level too much when filling a lock. In order to form the pondage for Lock No. 6 an earth dam 3300 feet long with a maximum height of 75 feet was built.

## Locks - Gates

The operating gates used at all locks are of the mitering horizontal girder type, sheathed on both sides and built entirely of steel, all leaves being 48 feet long and having girders 5 feet in depth. The lower gates are 82 feet high, each leaf weighs almost 490 tons; the upper gates are 35 feet 6 inches high each leaf weighing about 190 tons and the gates of Lock 8 and the Guard Gate are 44 feet 6 inches high and weigh 235 tons for each leaf.

Spare gates of each size have been provided, a pair of lower gate leaves being stored under water in a special dock below Lock 1. The remainder are stored under water in the pondage area east of the shipping channel above Lock 1.

The leaves swing on a hemispherical nickel steel pintle anchored to the concrete, and are anchored at the top to two structural steel anchorage frames embedded in the concrete.

The gates are opened and closed by 1-1/4" wire ropes operated by double drum winches housed in buildings on the lock wall. Should the gates of Locks 6, 7 and 8 be carried away, serious damage might be caused to the canal and navigation interrupted for considerable time. Double gates have been provided at each end of these locks, thus providing extra protection, however the real protection is provided by the lock gate fenders.

## Locks - Safety Features

Certain safeguards have been provided to reduce the chance of damage to the canal from misadventure with shipping. All service gates on the locks

have rows of mitre safety castings, staggered at their mitre ends, which permit a gate leaf to be opened about 4 feet before the two leaves lose their mitre contact with each other. The essential protection is provided by 3.5-inch-diameter wire rope fenders, situated about 70 feet away and carried across the lock chambers by booms. The fenders are designed so that should they be struck, the boom will be smashed, but the wire rope will be carried along by the vessel, the rope paying out against a friction force on each side computed to be sufficient to bring a 25,000 ton vessel, travelling at the rate of 3.0 m.p.h. to rest in a distance of about 46 feet. Since the canal was put into operation, the fenders have been struck 13 times and have provided the required protection for the gates. No gates have been damaged by ship movements in 25 years of operation.

Long distance electric light signals are situated above and below a lock, and regulations provide that a vessel shall not proceed past the "limit of approach" sign until the signal changes from red to green. The signals, fenders, bridges at locks, gates, valves etc., are all electrically interlocked to give proper sequence of operation. This arrangement not only protects the equipment of the locks, but prevents disaster consequent upon the operation of lock gates or valves in other than the predetermined order. Similarly the introduction of limit switches on all lock and bridge machinery protects the equipment from careless operation.

## Locks - Operation

The gates, valves and fenders of the locks are all operated electrically by remote control from control houses placed one at each end of the lock. The control boards in the two houses are electrically interlocked with one another and the movement of the apparatus is indicated, by signal lights.

Vessels pass through the canal, including the locks, under their own power. To control the lock requires a 7 man crew on duty 24 hours a day, 7 days a week. The lockmaster is responsible for its complete operation and he supervises an operator in each of the control houses and 4 linesmen who moor the vessel.

Electrically operated capstans with local controls have been provided to handle the ships lines up over the lock walls.

## Lock Maintenance

To assure a minimum of delay to navigation, an extensive maintenance program is carried out during the 3-1/2-month winter season. In addition, routine greasing cleaning and inspections are undertaken, while the canal is operating. As with all machinery, proper lubrication is a chief factor in maintaining a long life and a low wear rate. There are a number of widely varying lubrication programs on the canal. The lock gate operating ropes are removed each winter and given a thorough lubrication in a pressure vat system, consisting of treatment in a cleaning oil, a core lubricant, and a cable dressing.

When the canal was built, it was felt that water would provide sufficient lubrication for the gate pintles, however, shortly after operation one of the pintles seized in its bushing, shearing the dowel pins holding the pintle casting. A program was commenced of jacking up the gates, cutting grease grooves in the pintles, and installing grease pipes up to the wall coping to permit regular lubrication during the operating season. Since this system was

provided, there has been no trouble until very recently. One of the gates was seizing, and on being lifted, it was found that the grease grooves were full of bronze filings, which had been gradually scraped off over the years. This was due to the grease pipe becoming plugged and, because of inadequate lubrication, the pintle being scored. A program is now in force whereby one or two gates each year are jacked up, and new pintles and bushings installed.

The tainter valves which control the filling and emptying of the locks provide a difficult problem to lubrication, owing to their position and construction. After the canal had been opened several years, considerable wear was noticed at the yoke pins and main bearings of the valves, and a program was instituted of installing grease fittings and cutting grease grooves in the appropriate locations in the bushings. This has lowered the rate of wear considerably, however, each winter a number of valve bushings, and pins are replaced as found necessary at the winter inspection.

Corrosion protection is a very serious matter on the canal, and a continuous painting program on structures both above and below the water is carried out. A bituminous type paint is used on underwater structures, such as gates and valves, which are painted during the winter months, and structural black and aluminum paints are used on the steel work not subject to immersion in water, such as bridges.

Each year the interiors and exteriors of twelve to 14 lock gates are painted, and 35 tainter valves are painted and reconditioned. This program continues at a rate sufficient to provide a new coat of paint for each structure every five to seven years.

## Locks - Replacement of Worn Elements

A number of programs are in continual effect, replacing various worn or fatigued members.

Shortly after the canal opened, in 1932, the anchorage I-bars holding the tops of the gates were noticed to have fatigue cracks developing at the shear-necks, which had been provided in case a ship should strike a lock gate, so that the I-bars would fail rather than pull and warp the A-frame embedded in the concrete.

These I-bars were removed and new stronger ones installed without a shear-neck. No further trouble has been encountered from this source.

The anchorage jaw plates which carry the load from the I-bars to the embedded A-frame, were noticed to have developed slight cracks. These jaw plate assemblies are being replaced, the thickness of the plates being increased from 1/2" to 1-1/4". Where this has been done, no further cracking has occurred.

The stoney valves which regulate the reach levels through the by-pass weirs, consist of flat gate valves raised and lowered vertically by means of racks and pinions, the thrust against the face being taken by a roller train. The roller trains which consisted of steel rollers 4" in diameter and 8" long, with journals running in steel side plates, were reconditioned, using several methods. One was the installation of cast iron rollers with mild steel journals. Another was steel rollers with stainless steel overlay, and a third was by installing Meehanite rollers, with journals running in Oilite bearings pressed into the steel sideplates. Owing to the difficulty of examining the roller trains, an assessment of these different methods will not be available for several years.

A program was commenced recently of replacing the 3-1/2" wire rope on the wire rope fenders, as it was found to have corroded badly where it passed around a fixed snubbing bollard in a semi-circular groove. The cable is in good condition where it has been allowed to hang free in the air, but where it has been clamped, or otherwise confined, it has rusted.

Cavitation and corrosion have caused some disintegration of concrete in the lock structure. The deteriorated sections are chipped out and the new concrete placed as required during the winter maintenance period.

The white oak timbers which form the mitre sills have been found to deteriorate through time, and replacements are made periodically.

Electrical maintenance is now largely confined to routine matters following corrective measures taken to eliminate severe induction conditions in the original installation.

Interlocking of the various operations was accomplished initially at the main circuit voltage of 550 and gave considerable trouble. The interlocking circuit was changed to 220 volts which eliminated this condition.

Cables in ducts, galleries, and undercrossings have been subjected to surprisingly little corrosion or cold flow of the sheath, but in the case of cables in exposed positions where water was able to accumulate in the conduit and then freeze, replacement has been necessary. The original tile shelves installed through the cable galleries to carry the cables, pulled away from the wall due to the weight of the cables, and have been replaced with steel racks fastened to the wall.

### Lock - Gate Lifter

To handle the gates should any be damaged or need taking out for any purpose, a pontoon gate lifter capable of lifting the large 490-ton gates is kept moored below Lock 1. The gate lifter is a self-contained unit, except that it has to be towed from place to place by tugs. Trimming of the pontoon is accomplished by shifting water ballast by means of pumps.

### Canal Prism

The canal is generally 200 feet wide at the bottom and 310 feet at the water line, with the banks being sloped on two to one. To prevent damage to the banks by wave action, they have been protected by a concrete wash wall 12 inches thick extending from 5 feet below to 5 feet above water line where excavation was done in the dry and by a layer of broken stone protection at all other sections.

The banks have proven unstable at various locations and minor slides have occurred. These have been remedied by flattening the slope by dredging, relieving the top of the bank or placing adequate drains in the banks to reduce moisture content. Bank protection and renovations have proven to be one of the major maintenance items.

### Chippawa Creek

As in the case of the previous canal, it has been necessary to provide a suitable structure to allow Chippawa Creek to cross under the Ship Canal. This has been accomplished by constructing a concrete inverted syphon culvert consisting of six 22 ft. diameter tubes which pass under the canal.

Port Colborne Harbour

The outer harbour is formed by two breakwaters some 7200 feet long placed approximately parallel to the shore with a 500 foot opening through which navigation passes. A 2000 foot spur extends outwards from the westerly breakwater providing protection against south westerly gales.

Bridges

Twenty bridges, 14 highway and 6 railway span the Welland Ship Canal. Eleven of these are of the vertical lift type, giving a clearance of 120' from the surface of the water. They are counter-balanced by means of heavy concrete weights and chains. Other bridges are of the rolling lift type. Large concrete weights counter-balance the weight of the moving span, as the bridge rocks upward to an 80° angle. Only two swing bridges are used on the canal for the railroads, since they limit the width of the shipping lane.

A regular lubrication program is carried out on all bridge machinery and wire ropes.

The ropes which hold the counter-weights on the vertical lift bridges have been in continuous use since the canal opened, and last winter the ropes at the east end of bridge 10, a railroad bridge, were changed as a part of a program of replacement. Under the clamps, which gather the cables together, to line up for passage over the crown sheave, the wire ropes were corroded. The operating ropes which move the bridge up and down are replaced from time to time as wear develops. To replace one of these wire ropes, usually takes four to five hours. On some of the bridges these ropes lasted 20 years, on others they average 8 to 10 years. The difference has been attributed to care taken in keeping the tension adjusted properly and in precautions taken to keep the wind from slapping them against the tower legs.

As originally installed, the counter-weight guides were steel castings which rubbed on angles back to back, keeping the counter-weight in line, as it travelled up and down the tower. Severe wear was noted on both the guide castings and the guide rails, and at each of the vertical lift bridges the guide castings were machined out, and replaceable bronze gibs installed which has reduced the wear considerably.

The main power supply to the vertical lift bridges is at 550 volts and is transmitted to the span via trolley connectors running on three wires up the inner vertical face of one tower. The auxiliary control at 110 volts for the traffic lights and roadway gates and the telephone line are taken from the moving span by two flexible cables attached half way up each tower. The normal life of 10 years is often reduced as this cable catches on tower projections in a high wind, despite protective guide wires.

Electrical System

All valves, gates, fenders, bridges etc., are operated electrically. A transmission line extends from the mouth of Port Weller harbour to Port Colborne harbour. A Power House belonging to the canal is situated at the foot of Lock 4, containing three 5000 H.P. turbine-driven generators, actuated by a nominal head of water of 186 feet, conveyed through an 8'-6" diameter penstock from above lock 7 to below Lock 4, and connected to 200,000 volts with 550-volt 3-phase power being used for all main motors. Electric power at various voltages to suit requirements is used for lighting and heating.

Substations for transforming and switching the 22,000-volt power to the various stages are situated at locations convenient to the various canal locks, bridges etc.

The main problem to uninterrupted power is caused by tree branches being blown into the line during summer storms. In the 25 years of operation only a few transformers have failed, and have had to be rewound or emptied, dried and reinsulated in spite of a regular inspection and oil testing program.

In general, the installed capacity of the power house is more than required, and hence each generator is run only approximately 1/3 of the time. This allows ample opportunity for preventative maintenance.

The turbines are periodically stripped down and the runners built up by stainless steel welding where cavitation has eroded them. In addition, the generators themselves have been torn down, the cooling ducts cleaned and the winding revarnished. The lack of response with the hydraulic governors is causing considerable difficulty in operating and changing machines, and new hydraulic governors are to be provided, having an electrical sensing circuit. This will allow for a more constant speed and steadier 60-cycle frequency than is attained at present.

### Telephone System

A complete self-contained automatic telephone system is in use along the canal, linking the locks, bridges, substations, power house, and executive buildings.

## Navigation

### Canal Traffic

A comparison of the traffic through the past and present canals is interesting. During 1831, the second year of operation of the first Welland Canal, 210,104 bushels of wheat passed through it. It might be noted that there are presently several vessels in the Upper Lake Class capable of carrying in one trip approximately 600,000 bushels or nearly three times the total amount in 1831. In 1901, the total tonnage passing through the third canal was 620,200 tons but by 1914 this had increased to 3,860,000 tons. In 1932 when the Welland Ship Canal was opened, the tonnage was 8,535,000 tons and in 1956 it had increased almost three fold to 23,066,000, Fig. 4. The ship canal was designed to allow vessels to make a complete through passage in 8 hours. With the present tonnage and number of vessel movements in 1956 the average time for an upbound vessel was 8 hours 51 minutes and for a downbound vessel 10 hours 43 minutes. The larger boats over 640 feet in length require an average of 9 hours 14 minutes for an upbound passage and 11 hours 48 minutes downbound. The greater length of time for the passage of the larger ships has been attributed to the difficulty in safely manoeuvering these vessels in the canal, particularly when approaching lift bridges and locks. The larger vessels do not respond as quickly as the smaller ones and consequently the speed of these ships is reduced by the master so that canalling may be safely carried out.

Cargoes are as varied as the vessels which can be seen in the canal. The main items, however, are grain, ore, coal, and petroleum products. Pulp, sulphur, limestone and "package freight" are large secondary cargoes.

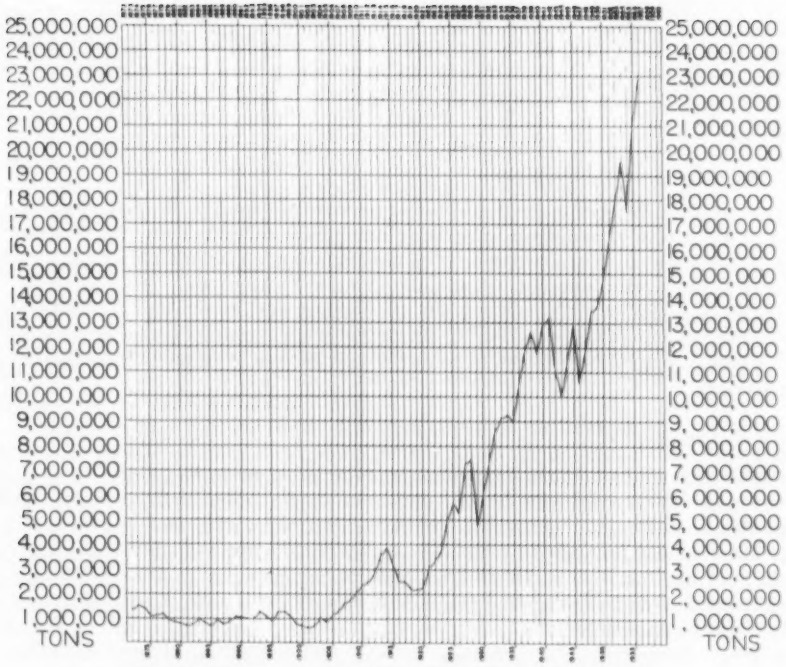


THE WELLAND SHIP CANAL

GRAPH SHOWING TONNAGE OF FREIGHT PASSED THROUGH ANNUALLY SINCE 1872

FIGURE Nº 4

Tolls

No ship, whatever her home port, pays any toll for the privilege of using the canal; but captains must have a "let pass," obtained either by agreement before the navigation season, or at the canal office, to facilitate passage.

Though tolls were abolished in 1905, a linesmans service fee is charged. Ships up to 262 feet in length pay $25.00 while larger vessels pay double that. In the old days prior to construction of the Ship Canal, casual labour was employed to moor and cast off the lines, the men following along the tow paths. Since this system was impossible in the Ship Canal, men were engaged by the canal to do this work and the linesman's fee was established to pay for this service.

Deepening to Seaway Standards

The present deepening program being undertaken by The St. Lawrence Seaway Authority is required to provide navigation facilities on The Welland Ship Canal equal to those which will be available upon completion of the present construction project, from Lake Ontario to Montreal. This necessitates the removal of 1,324,000 cu. yd. of common excavation and 1,100,000 cu. yd. of rock in the canal reaches, by dredging or dry excavation to provide 27 feet of water where the bottom is in earth and 30 feet of water where the bottom is rock.

Dry Excavation

Excavation using normal heavy construction equipment is possible for three canal reaches between Lock 1 and Lock 4. In these sections where the canal can be unwatered during the non-navigation or winter season, three separate contracts bounded by the lock structures, were awarded in the fall of 1955 for the removal of 735,000 cu. yds. of common excavation. Two of these contracts were completed in 1956 and the third is scheduled for completion by the spring of 1958.

In the vicinity of Bridge 4 between Lock 2 and 3 slides in the canal bank have developed after deepening. When the canal was originally excavated in this area, prior to 1932, severe slides occurred and the top of the bank was cut back to relieve the unstable sections. Since that time additional slumping of the banks to a minor degree has been observed, however, no interference was caused to navigation and the remedial measures consisted of placing stone protection to prevent erosion. When deepening was carried out under the present program the weight was removed from the toe of the slope and shallow slides developed. To prevent further action of this nature, the top of the bank is being excavated, thus reducing the surcharge and returning the bank to a stable condition.

Dredging - General

Deepening of Port Weller harbour north of Lock 1 will be accomplished in two stages. The first consists of the removal of silt and loose material by suction dredging, disposal being made on the outer face of the harbour breakwaters. The contract for dredging 340,000 cu. yd. of this material was completed in May of this year.

Dredging of rock shoals which are uncovered after suction dredging will comprise the second stage. It is expected that this contract will be awarded during the summer of 1957.

Another dredging contract was awarded late in 1956 for the deepening of 3.9 miles of canal southerly from the Guard Gate at Thorold. In this contract, which is for the removal of 250,000 cu. yd. of common material and 400,000 cu. yd. of rock, it is extremely important that the turbidity of the water in the canal be kept to a minimum. This is a critical matter for the paper companies in the immediate vicinity who use unfiltered canal water in their process. It could also present a problem for municipalities in the area should the turbidity content reach proportions beyond the capacity of their filters. To alleviate the condition all common material, including the silt overlying rock, will be removed by a suction dredge. An area must be cleared in this manner before drilling and blasting can begin.

The largest dredging contract which is for 672,000 cu. yd. of shallow rock will provide a deepened channel for 4.2 miles of the canal from north of Lock 8 to Lake Erie. This contract was awarded to two companies in a joint venture in the late summer of 1956.

## Underwater Drilling and Blasting

The rock is being broken by conventional methods using drill boats and regular underwater explosives or blasting agents. Each drill boat has four spuds and two pneumatic drills mounted on towers which travel on rails along the same side of the boat (Fig. 5) thus permitting several holes in a row to be drilled before moving the boat.

An interesting feature is the different methods of blasting used by the contractors. While similar drill equipment is used, two contractors employ the hole-at-a-time method of firing and two use millisecond delays. With the first method, individual holes are drilled, loaded with from 8 to 14 lbs. of gelatin dynamite and fired. The drill boat remains in place when the charge is exploded. When millisecond delays are used, several holes in a row are drilled, loaded with a blasting agent "Nitrox," which consists largely of ammonium nitrate, and fired without fear of propagation. Because of the load it is necessary to move the drill boat at each time of firing. Each of the contractors is convinced that his method is equal to or better than that used by the other.

Some difficulty with the delay method has been experienced in that misfires have occurred. These have been attributed to current leakage in the leg wires and extra precautions have been taken to make sure that a ground is not made from the wires to the steel scow. In addition the charges are being fired using a generator rather than condenser discharge blasting machine so that 120 volts may be applied to the circuit for the required length of time rather than 480 volts for an extremely short duration. This will assure that sufficient heat will be available to fire the caps.

## Precautions to Prevent Blasting Damage

Special precautions are required when blasting in the immediate vicinity of the lock structures or when near certain sections of the old third canal wall which form the present canal wall. Here, close drilling is used to reduce the possibility of rock breaking back under the wall thereby undermining it and causing a failure. To assure a proper line of breakage one contractor is installing in the close drilled holes, sealed metal tubes three inches in diameter to provide an intermittent air space in the rock through which the shock cannot travel.

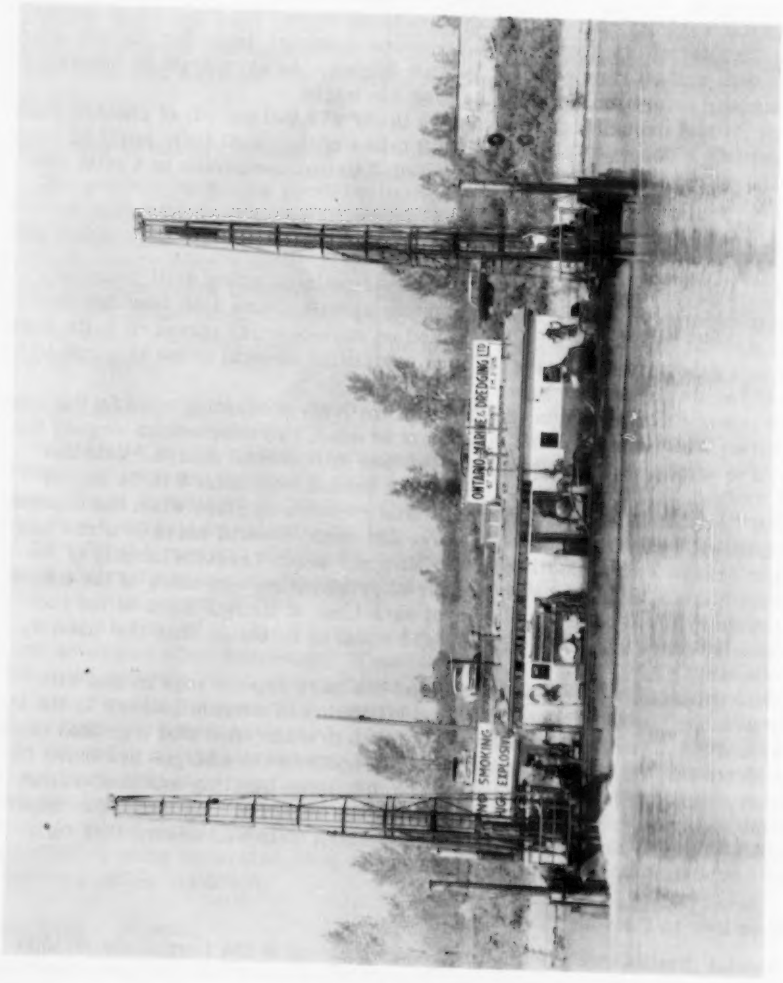


FIGURE Nº 5

When blasting rock in water shock pressure waves are set up in the water and can damage nearby structures in contact with it. To obviate such damage a method is being employed which was developed by the Hydro-Electric Power Commission of Ontario and suggested by Mr. A. Laprairie of Canadian Industries Limited who have patented the process. A screen of air bubbles is placed between the blast and the structure to be protected by placing a three inch diameter perforated pipe horizontally along the bottom of the canal and then pumping 15 c.f.m. of air per lineal foot of pipe into the pipe while blasting. The air bubbles in rising to the surface form the curtain which absorbs a portion of the energy of the blast transmitted through the water. Tests undertaken by The Hydro-Electric Power Commission in connection with a blast set off in the vicinity of one of their power stations at Niagara Falls suggest a pressure reduction of at least 70 to 1.

To establish the maximum amount of explosive which may be fired at any specific distance from the canal wall, seismic monitoring of the blasts is being carried out. Information obtained when blasting at 25 feet from the wall in a depth of 30 feet of water indicates that the charge at 50 feet should be 20 lbs. per delay and at 25 feet 10 lbs. per delay. It is known that existing criteria for establishing a safe powder load is not reliable within 50 feet of a structure and therefore trial blasts with small charges at 5 foot intervals will be monitored. From the data thus obtained a drill pattern and maximum load per delay will be established.

## Underwater Television

Before commencing work in the vicinity of the old third Canal walls at Port Colborne, it was deemed advisable to make an underwater inspection of the timber cribs, forming the wall, to ascertain their present condition. The survey was planned for a diver, however an underwater television camera owned by The National Research Council of Canada was available and it was decided to use it to make the survey and at the same time make an appraisal of the television system for future work of this nature. The camera in its water tight container presented too much resistance to the current to be satisfactorily handled by lines from the surface and it was necessary to utilize a diver to manoeuver the camera into the proper position. A satisfactory picture was obtained which was viewed by several engineers and simultaneously photographed using a camera focussed on the picture tube. The major disadvantage with the equipment was the extremely small field of view possible with the camera. To obtain a comprehensive picture of a hole undermining the wall of say 4' x 6' it was necessary to prepare a mosaic of some 12 photographs. A diver could see the hole and its relation to the remainder of the structure from one position. To be used extensively for this type of work it will be necessary to develop a camera which can provide a clear picture of 6' x 6'.

## Underwater Excavation

Standard mucking methods using dipper and clam dredges with dump scows are being employed, Fig. 6. In addition one contractor is removing the rock to shore in a unique way. Two flat scows 32' x 170' lashed together side by side have standard land cranes mounted on one end, Fig. 7. The cranes are equipped with rock grabs which are a special type of clam shell bucket designed in Germany and operated in the conventional manner. On the land side

FIGURE Nº 6

FIGURE Nº7

of these scows, which are placed parallel to the canal bank, is placed a third flat scow equipped with a Bailey bridge which acts as a gang plank. The bridge can be raised and lowered from the scow. Trucks then travel from shore over the bridge and onto the flat scows where they are loaded directly by the cranes. The round trip tow to Lake Erie of 38 miles which would be required using standard methods is thereby eliminated.

During the winter, dredging is completed at locations where interference would result with navigation during the shipping season. The standard method employed is to dredge the rock after blasting with a dipper dredge and scow it to a site for rehandling to shore disposal. The scows are dumped and the material then picked up from the water by clams and loaded into trucks. Ice causes a great deal of trouble while carrying out this operation. In addition to tripping the buckets on the dipper dredges it fills the tunnels in one type of dump scow making it impossible to open the doors and dump the rock. As a result the scows must be clammed out with a resulting loss in time. The winter dredging is carried out at a greatly reduced efficiency.

### Navigation During Dredging

Navigation must continue in the canal while dredging is in progress and co-ordination between the contractors operations and the requirements of vessels is continually considered. Accurate scheduling of the work along the face of docks is of the utmost importance so that the normal operation of these facilities will be interfered with as little as possible. As mentioned previously, winter dredging is required where interference with navigation could be hazardous. This is particularly true at lock entrances where there would not be room for a vessel to navigate past the dredging equipment.

## CONCLUSION

This paper has been presented as a non-technical description and report on the main features of the Welland Canal and the work required to deepen it to Seaway Standards.

Paper 1571 March, 1958 WW 2

Journal of the
WATERWAYS AND HARBORS DIVISION
Proceedings of the American Society of Civil Engineers

# FORCES INDUCED ON A LARGE VESSEL BY SURGE[a]

John T. O'Brien,[1] A.M. ASCE and D. I. Kuchenreuther,[1] J.M. ASCE
(Proc. Paper 1571)

## ABSTRACT

Field measurements are presented of forces of up to 40,000 pounds as induced by two predominant standing waves—those with 1 and 2 1/2 minute period which produced water surface slopes of up to 0.0015—in the lines of a Ship (USS NORTON SOUND (AVM-1)) of 12,000 long tons as moored alongside by unusually taut lines at Port Hueneme, California and near to a node of the shorter wave. The two waves acted simultaneously to produce only significant surge. It is stated that tight lines tend to reduce the inertial force and that the excitation in surge is defined sensibly by the product of the slope of the water surface and the weight of the Ship where restoring forces of up to 30,000 pounds in surge as calculated on this basis are about 1/3 greater than those measured. In no case was it considered that resonance was encountered.

## INTRODUCTION

The reaction of a moored ship subjected in surge to the excitation produced by standing waves has been considered systematically at least since Knapp and Vanoni (1945) and Carr (1947). The latter likened the moored ship oscillating against the restoring force of its lines to that of a mass oscillating with an initial velocity against the restoring action of two linear springs with a clearance or gap, where the period of oscillation depends not only on the spring factor but also on the magnitude of the gap and the initial conditions. It is postulated that when the calculated value of this period tends to coincide with that of the exciting wave then a condition of resonance is produced with relatively high mooring forces.

Wilson (1951) in a remarkable paper derives an expression for the periodicity, $T_n$, of the longitudinal oscillation of a moored ship of mass m at resonance with the exciting standing wave in water of depth d. As rearranged by

Note: Discussion open until August 1, 1958. A postponement of this closing date can be obtained by writing to the ASCE Manager of Technical Publications. Paper 1571 is part of the copyrighted Journal of the Waterways and Harbors Division, Proceedings of the American Society of Civil Engineers, Vol. 84, No. WW 2, March, 1958.

a. Presented, Oct., 1957, ASCE Convention.

1. Engrs., U. S. Naval Civ. Eng. Research and Evaluation Lab., Bureau of Yards and Docks, Dept. of the Navy, Port Hueneme, Calif.

the writers, his expression appears to be that for the natural period of oscillation of a non-linear spring-suspended mass [ $T_n = 2\pi (m/k)^{1/2}$ where the spring factor k for the lines collectively is equal to D N/4 where D is the spring factor for a representative line and N is the total number of lines. The k has the unusual dimensions of: force per movement$^n$. ] multiplied by a factor that expresses the non-linearity of the system and the amplitude, A, of the standing wave in the ship's basin [ $(mgA^2/kd)^c$ where $c = (1-n)/2\ (1+n)$.] When the lines become significantly taut (n = 1 and k has usual dimensions), the second factor becomes equal to unity, the spring factor becomes linear, and the general expression of Wilson becomes that for a simple system. He showed also the $T_n$ was related to the initial tension in the lines and demonstrated that the maximum force in surge to be expected in the moorings as a whole was related inversely to this period and directly to the weight of the ship and the characteristics of the standing wave, $2\pi WA/T_n\ (gd)^{1/2}$, which expression Deacon, Russel & Palmer (1957) state can be shown to be that for the maximum force on the ship if the cables are all tight, the ship is held stationary, and the virtual mass of the ship is neglected.

Wiegel et al (1956) measured the mooring forces induced by short laboratory type "wind" waves on five moored ship models; no particular analytical treatment was made of the results. Among other things, they concluded that: the importance of initial tension as a factor in the explanation of maximum forces had been demonstrated; all of the systems were found to have non-linear load-movement characteristics; that in most cases mooring forces reach their maximum during the passage of only the second or third wave; and that any satisfactory analytical treatment of the problem must include coupled motions.

On the basis that the theory advanced by Wilson (1951) ". . . is so unamemable to analysis that approximations have to be made which spoil its many virtues. . ." Deacon et al (1957) present simpler methods for estimating the line tensions for the case of a ship with lines that periodically go slack. When such a ship is released from rest at an instant when the standing-wave-excited water particles are also at rest they indicate by use of simple mechanics that the maximum force required to hold the ship stationary is that given by Wilson (1951), and presented herein, multiplied by the factor 1.5. Like Wilson, they cite the desirability of tight cables as a means of reducing the mooring forces. Joosting (1957) states that while the forces which excite a moored ship can be considered sinusoidal, the mooring system generally does not have linear extension characteristics, so that no actual resonance can be expected, and the general behavior should be examined on the basis of forced oscillations. He states further that he has found some anomalies in Wilson's theory when applying it to an important case. On the basis of the familiar equation for the forced vibration of a damped spring-suspended mass he evolves an expression for the longitudinal movement of a moored ship in which the inertia force on the ship is taken to be the product of the mass of the ship and the difference between the acceleration of the water and the acceleration of the ship. Deacon, et al (1957) have objected to the use of the same reasoning by Wilson (1951).

An exceptional analytical study of the forces and movements induced by ocean waves on a large floating platform moored in about 1200 feet of water in the ocean about 300 miles off-shore was made by Continental Copper and Steel Industries, Inc. (1956) in which use was made of basic hydrodynamic theory to calculate the forces and movement induced by the deep water waves. It

appears that a significant restraining force was considered to be present at all times so that, as in this study, it was not necessary to cope with the problem posed by periodically slack moorings.

## Analytical Considerations

The condition of force equilibrium on a moored ship in surge, based on the damped motion of a simple spring-suspended mass under the action of a periodic disturbing force is considered to be:

$$\text{inertial} - \text{damping} - \text{restoring} + \text{excitation} = 0 \tag{1}$$

From a consideration of basic hydrodynamic theory the inertial reaction is considered to be made up of two parts: that of the ship and that of the hydrodynamic mass of the ship. This can be expressed as follows:

$$\text{inertia force} = m\,(1 + C_m)\,d^2x/dt^2$$

where:

$m$ = static mass of the ship
$C_m$ = inertial coefficient (ratio of hydrodynamic mass to displaced mass)
$d^2x/dt^2$ = acceleration of the ship in the surge direction = $\ddot{x}$

In most cases, $(1 + C_m)$ is written as $C_M$ so that:

$$\text{inertia force} = C_M\, m\ddot{x} \tag{2}$$

where $C_M$ is termed a mass factor.

The damping reaction is based on the well known expression:

$$\text{damping force} = C_d\, A\, \rho\, (dx/dt)^2\, /2 \tag{3}$$

where:

$C_d$ = is a drag coefficient, experimentally derived where form is considered.
$A$ = the project underwater area of the Ship for form drag
= wetted area of Ship for frictional drag
$dx/dt$ = speed of the ship in the surge direction = $\dot{x}$

With cables which are always significantly taut, the restoring reaction consists significantly of that due to the elasticity of the cables where by the application of Hooke's Law: (total elongation = $P\ell/AE$)

$$\text{restoring force} = \sum \left[\text{total elong.}\ (\cos\alpha_i \cos\beta_i)\right]\ A_i\, E_i/\ell_i \tag{4}$$

where i represents an item number.

When there is significant slack in the moorings, as is the usual case, then the restoring force is no longer given completely by eq. (4) but rather by one of the type given by Wilson (1951):

$$\text{restoring force} = \sum k_i \ (\text{surge movement})^{n_i} \tag{5}$$

where:

k is the spring factor for a single mooring line and n is a numerical exponent

This function must be obtained through a consideration of eq. (4) and the characteristics of the moorings in the case of resiliant but significantly weightless lines such as ropes. The catenary equation should be used in the case of very heavy but significantly non-resiliant moorings such as chains.

The excitation force from a consideration of basic hydrodynamics is that obtained by integrating the proper components of the wave-induced pressure over the wetted surface of the ship. It is beyond the scope of this paper to attempt to accomplish this analytically; however, as an approximation for waves much longer than the ship the David Taylor Model Basin (1954) and Joosting (1957) consider the excitation to be that due to a ship sliding up and down a sloping water surface such that:

$$\text{excitation force} = m\,g\,dz/dx \tag{6a}$$

$$= m\,g\,(2\pi A/L)\,(\sin 2\pi t/T) \tag{6b}$$

where dz/dx represents the slope of the water surface in the surge direction and A the amplitude of the exciting wave. The above assumes that there is no appreciable trim of the ship as it oscillates in surge which assumption seems adequate for many cases because the standing waves and combinations thereof ordinarily active in harbors are of low amplitude even though very long.

If the relationships: $L = T\,(g\,d)^{1/2}$ and $m\,g = W$ are used in equation (6b) it becomes:

$$\text{excitation force} = (2\pi WA/T\,(g\,d)^{1/2})\,(\sin 2\pi t/T) \tag{6c}$$

When t = T/4 or 3T/4—extremes of the oscillations—the sine term becomes unity and eq. (6c) reduces to that given by Wilson for the maximum tension in the lines as referred to in the Introduction.

In an environment of standing waves—it is well to consider that moored ships will be subject to a maximum variation in water level which is that produced by the sum of the various standing waves. Thus, a computation of the slope of the water surface by an expression such as that contained in eq. (6b) is not likely to give accurate results, because this equation considers only one wave (and that of strictly sinusoidal form) while it is probable that in most cases two or more waves will be active.

## Test Facilities and Procedures

The investigation was conducted in a virtually closed Basin, (Figure 1) about 1900 feet long, 280 feet wide and 32 feet deep at MLLW where the tidal variation was about four feet.

The missile launching ship used in the study—the USS NORTON SOUND (AVM-1)—is one of about 12,000 long tons (Table I) which has Port Hueneme, California as its home port. It was selected for the study because it is

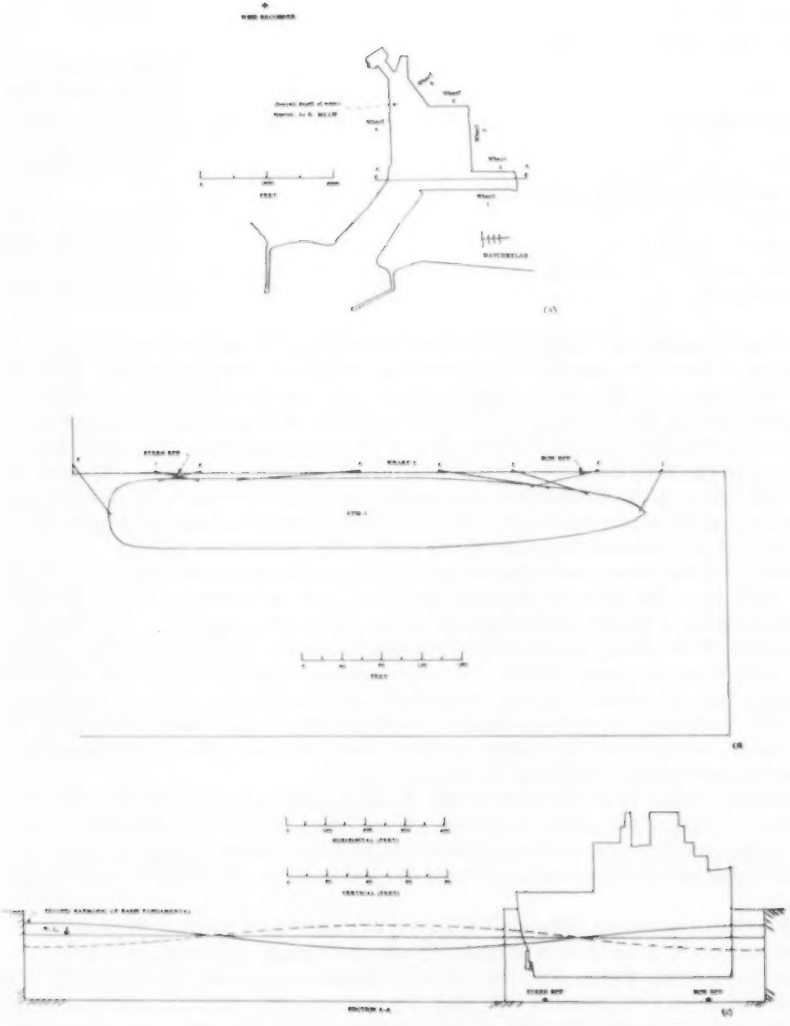

Figure 1 The Harbor and Basin with Ship as moored during the study.

Table I Characteristics of the Ship

| | |
|---|---|
| Length, overall | 540 feet |
| Beam, extreme | 72 feet |
| Projected area above water line | |
| side | 31,000 square feet |
| end | 5,100 square feet |
| Displacement | 12,000 long tons |
| | 26,880 kip pounds |
| Mass | 835 kip slugs |
| Projected area below water line | |
| side | 10,800 square feet |
| end | 1,150 square feet |
| Draft | 20 feet |
| Wetted area | 40,000 square feet |

berthed conveniently close to NAVCERELAB; further, it was known that the Harbor of the Port contains an interesting system of standing waves which it was considered would induce interesting if not high-level mooring forces.

Because the Basin is part of the Harbor as a whole, where the water in both is excited by waves from the Ocean, it is apparent that more than one wave system is likely to be active in the Basin at any given time. This is in fact the case, because standing waves with periods of about 1, 2 1/2 and 12 1/2 minutes are known to be active. The Ship was moored alongside Wharf No. 2 (Figure 1) and near to the node of the wave with one minute period.

Water-level variations were measured at two points—one near the bow and the other near the stern of the Ship (Figure 1)--by means of pressure pickups as described by Knapp (1952) placed on the bottom of the Basin. The variations due to the long-period waves encountered were reflected directly by the output of these pickups, where as it is recognized that this is not the case with those of shorter period usually referred to as "wind waves." The variations induced by these long-period waves are important, because as determinats of the significant slope of the water surface, they evaluate the major parameter in the expression for the Ship excitation (eq. 6a).

In some cases only the stern water-level pickup was available because of malfunctioning of the other; however, on the basis of trends established with data from two pickups, it was possible to obtain a reasonable approximation to the slope of the water surface from the water-level variation at the single location.

The Ship restraints consisted of seven manila ropes varying in circumference from 8 to 12 inches (Figure 2) and one spring-lay cable of 1 1/2 inches diameter. The lines were in various states of condition (Table II). The two surge lines always were kept taut, an unusual circumstance and one which served to make easier the task of reducing the force data, because it assured that a significant restoring force—later shown to vary almost linearly with movement—would be present at all times. This eliminated consideration of an unrestrained "run" of the Ship as would have been the case if all the lines periodically went slack.

Mooring forces were measured on a continuous basis by means of dynamometers of the tube-strain-gage type incorporated directly into the lines (Figure 3). Because the incorporation procedure involved a line handling effort slightly over and above that required normally, it was generally only on

Table II Characteristics of the Ships Moorings

Note: Date presented is the result in part of measurements made in the field at various tide levels. The results presented herein have been reduced to a common tide level of 4.8 feet MLLW. on 18 Nov 1954. Initial tension is a variable depending upon wishes of Ships crew and tide level. See Figure 1 and 2 for explanation of symbols.

| Line | Pt. attchd to ship (meas. along ℄) | Initial Tension | Length $l$ | $\alpha$ | $\beta$ | x | y | z | r | $r_1$ | $z_1$ |
|---|---|---|---|---|---|---|---|---|---|---|---|
| | ft. | kips | ft. | d-m | d-m | ft. | ft. | ft. | ft. | ft. | ft. |
| 1 bow | 536.0 | 0 | 51.5 | 32-00 | 59-20 | 21.5 | 36.2 | 26.4 | 42.1 | 49.6 | 35.2 |
| 2 aft bow spr. | 428.0 | 2.0 | 72.0 | 17-00 | 12-26 | 67.0 | 14.5 | 20.8 | 68.6 | 71.8 | 29.6 |
| 3 fwd bow spr. | 482.0 | 3.0 | 79.3 | 16-50 | 13-05 | 73.8 | 17.0 | 22.8 | 75.7 | 79.1 | 31.6 |
| 4 fwd surge | 444.0 | 15.0 | 117.0 | 10-53 | 5-04 | 114.5 | 9.6 | 24.0 | 114.9 | 117.0 | 32.8 |
| 5 aft surge | 130.0 | 16.0 | 124.0 | 5-03 | 0-20 | 124.0 | 6.5 | 13.2 | 123.0 | 124.0 | 22.0 |
| 6 aft stern spr. | 50.0 | 0 | 47.4 | 14-32 | 11-45 | 42.1 | 8.9 | 10.9 | 43.0 | 44.4 | 19.7 |
| 7 fwd stern spr. | 90.0 | 0 | 44.0 | 14-18 | 9-56 | 40.3 | 7.0 | 10.2 | 40.9 | 42.2 | 19.0 |
| 8 Stern | 0 | 0 | 63.0 | 12-30 | 55-10 | 34.5 | 49.6 | 14.2 | 60.4 | 61.9 | 23.0 |

Lines 1, 2, 3, 6, & 7 are three parts 8" manila & line 8 is three parts $1\frac{1}{2}$" spring lay (steel & manila)

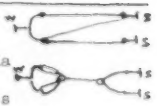

Line 4 is two parts 12" manila for 20' frm Ship; one part 12" manila for next 77'; two parts 1" dia steel cable for remaining 20'

Line 5 is two parts 12" manila for 49' frm Ship; one part double 12" manila for next 65'; two parts 1" steel cable for remaining 10"

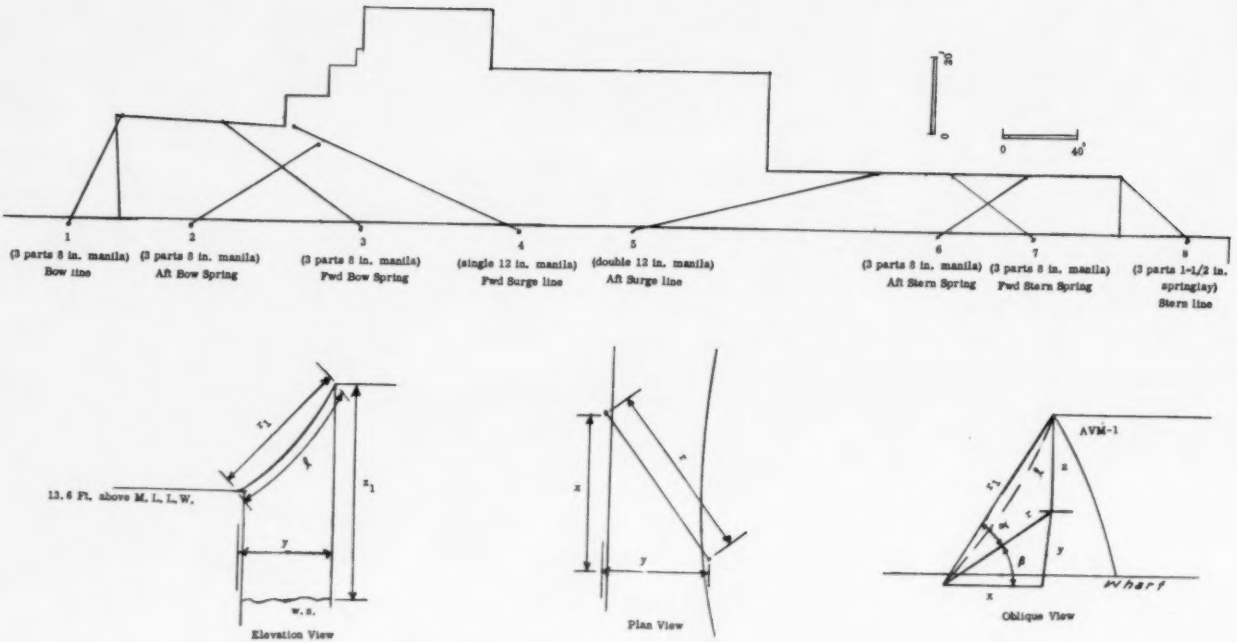


Figure 2 Portside profile of the Ship showing the mooring lines.

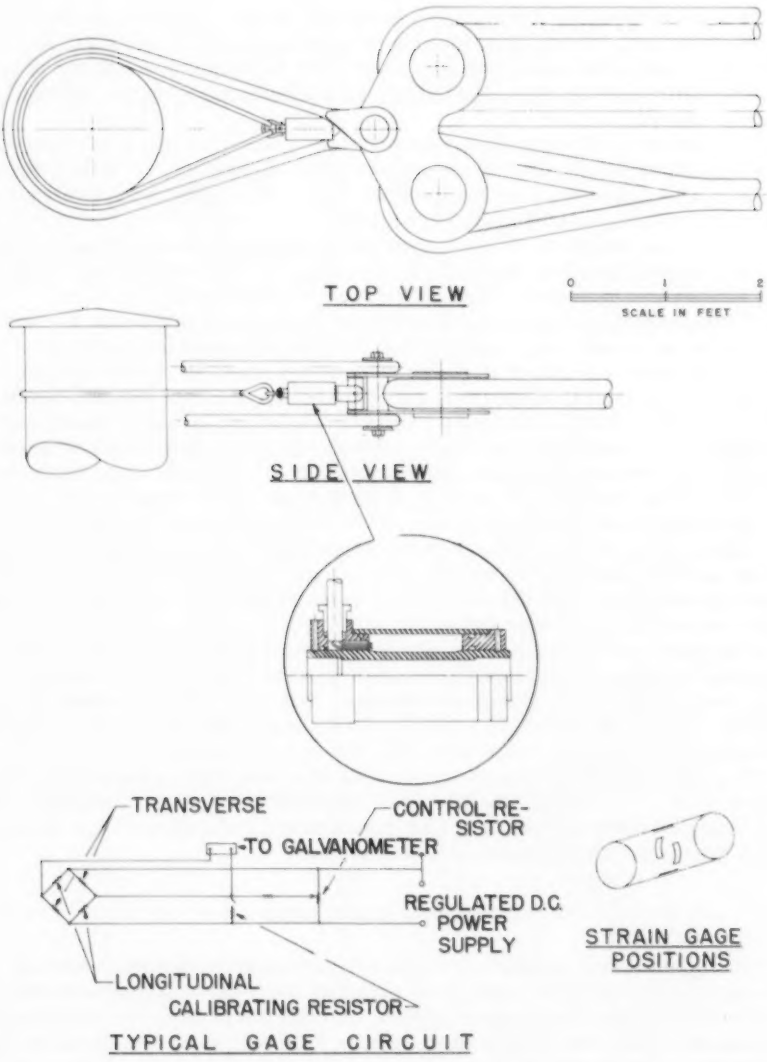


Figure 3. Tension force pickup as used in the Ships lines.

weekends, when the Ship did not take to sea, or at other infrequent periods of inactivity, that it was possible to activate the dynamometers and collect force data.

Data on the relationship between loads in the mooring lines and their elongation were obtained by special measurements, some of which were made in place (Figure 4). It will be noted that in most cases the relationship is sensibly linear where the data presented represents the mean of a number of data points which in many cases showed significant scatter due in part to hysteresis effects.

The outputs of the dynamometers and water-level pickups were transmitted through cables to a photographic-type oscillograph (Miller, Model H) operating at a slow paper speed—12 inches per hour—where they were recorded in terms of force and water level versus time.

During one portion of the investigation, measurements were made of the on-off forces induced on the Wharf by the Ship, but these proved to be slight and further measurements of these forces were abandoned.

If ship movements were to be measured, it was considered that it would have to be on a continuous basis in order to permit selection for analysis of only those intervals that proved amenable to analysis. Because a proper pick-up of this type for the relatively small movements involved was not available—that outlined by Knapp (1952) was found too insensitive—, and ordinary survey methods were considered too laborious and expensive, direct measurement of ship motion was not attempted. Rather, such a determination was made analytically on the basis of the calculated elongations of the surge lines.

No attempt was made to measure mechanically the water currents, because no proper meter of the continuous type considered necessary was available. Those utilizing propellers and drag spheres proved inadequate. Data from floats placed in the area indicated that unidirectional-type currents, including those caused by tides, were insignificant.

Windspeed and direction were obtained by means of a recording selsyn-type annemograph which, although located about one-half mile northwest of the Ship, was considered to give pertinent data. Wind data was important in the negative sense because those intervals during which the wind was at a significant level were eliminated as unsuitable for use in this study.

The study procedure was to collect data on a continuous basis, then, after a review of the records, to select certain significant periods for analysis. There were many periods of relatively high disturbance levels when it was not possible to collect data because the Ship was at sea.

## Experimental Results

The experimental results are characterized by an unsteadiness and are considered very different from those obtained using uniform, periodic waves normal to laboratory-type investigation. Facsimiles of certain oscillograms considered typical are presented in Figures 5 through 9. It will be noted that the pattern produced by the water-level variations, wherein the major and minor peaks shift constantly in a somewhat orderly if not systematic manner, seems to indicate the presence of two or more wave trains. The prominent long period surge—that of about 12 1/2 minutes—shows considerable variation in height but less so in period. Note also that by far the greatest line tensions were excited by the shortest of the significant waves—those of about 1 minute

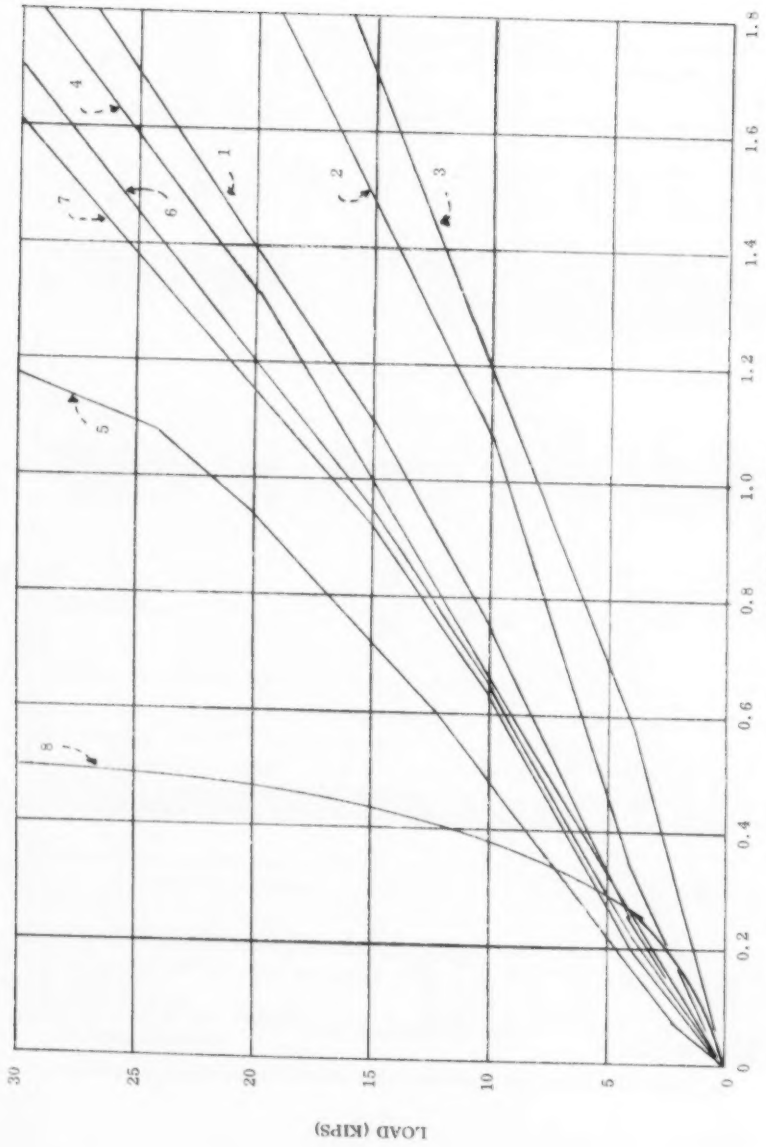


Figure 4 Variation of elongation with load for all ships lines.

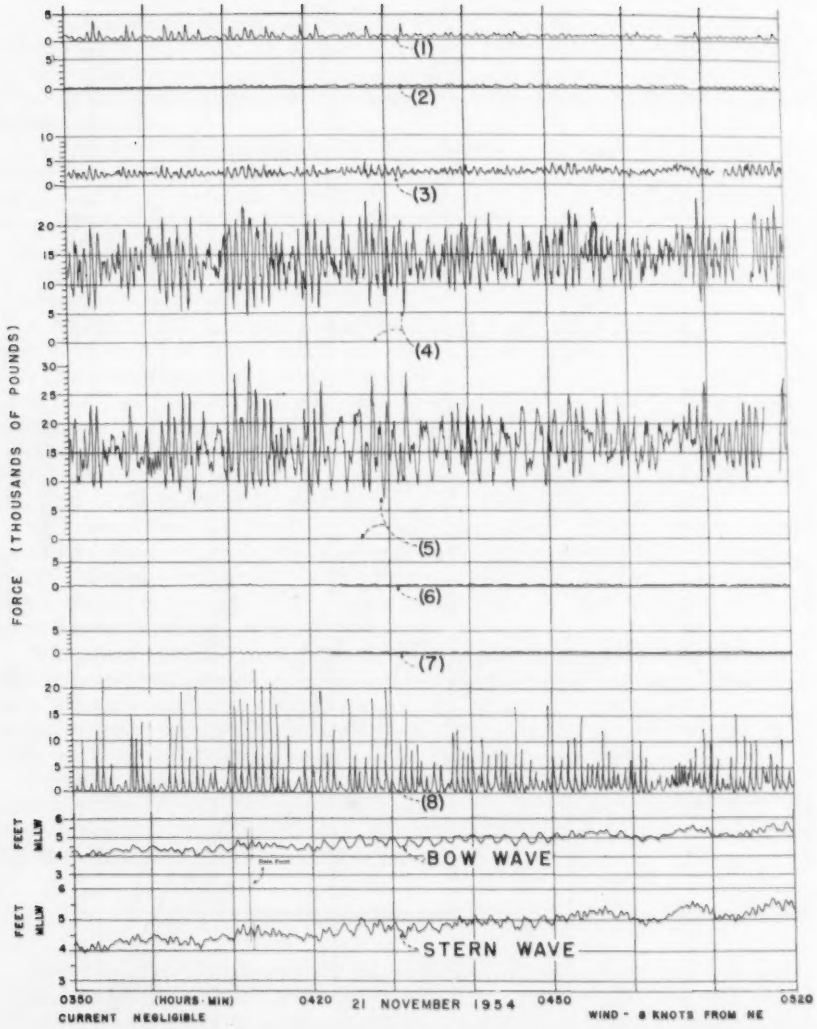


Figure 5 Facsimile of oscillogram with noticeable waves of 0.98, 2.50 and 12.5 minute period and high initial tension.

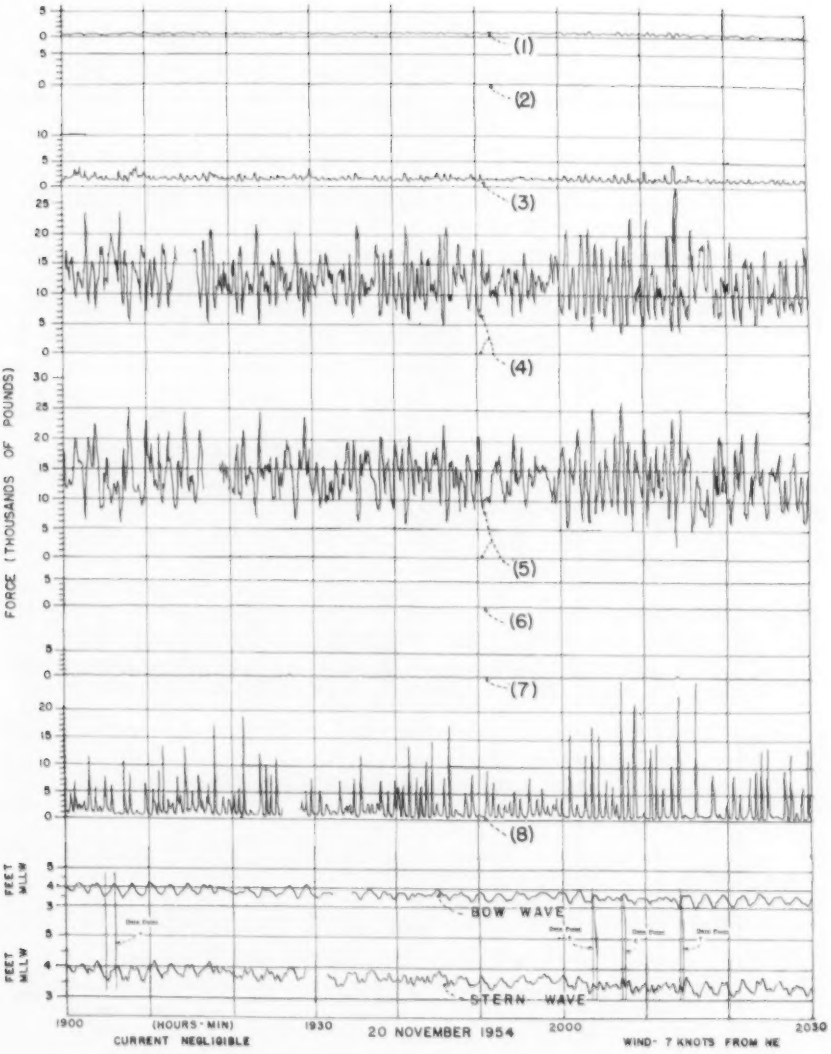


Figure 6 Facsimile of oscillogram with waves of 2.50 minute period predominant and a high initial tension.

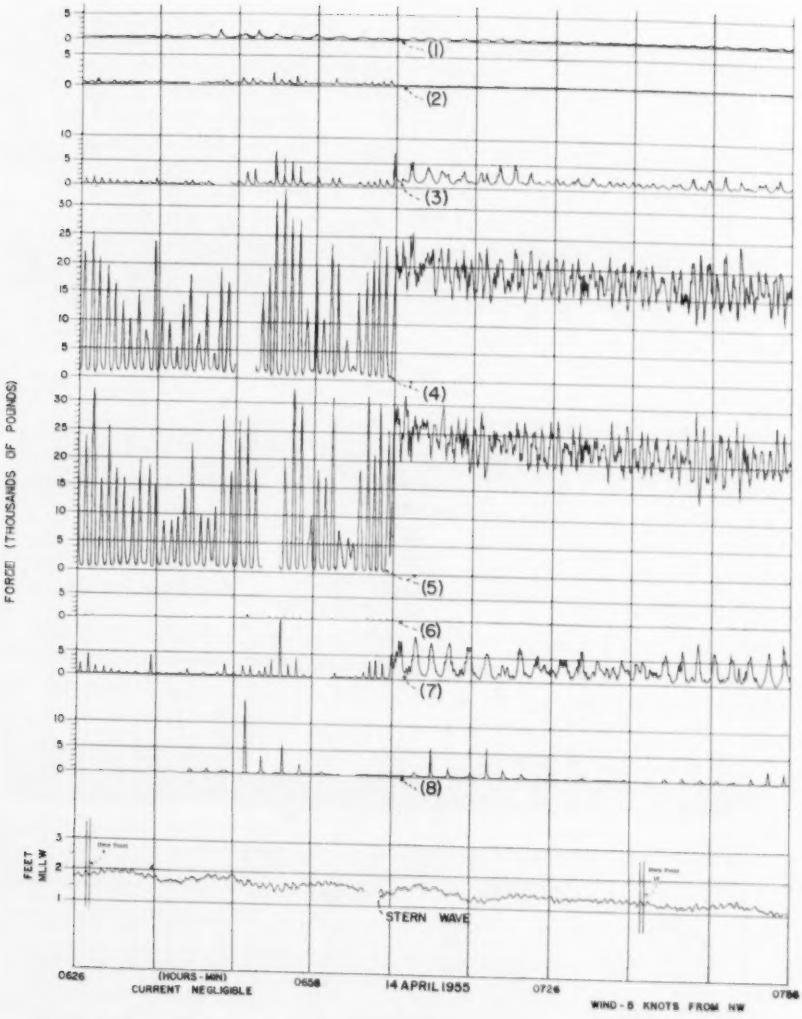


Figure 7 Facsimile of oscillogram with waves of 0.98 minute period predominant and an extra high and extra low initial tension.

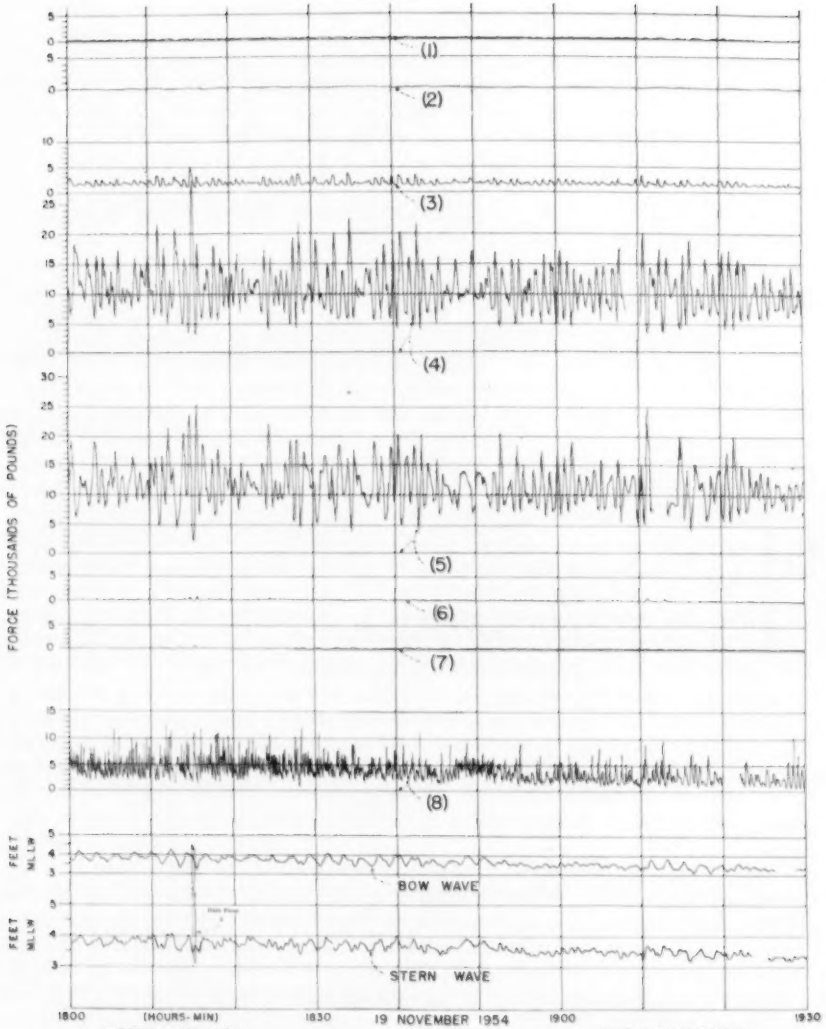


Figure 8 Facsimile of oscillogram with waves of 2.50 minute period predominant and a medium initial tension.

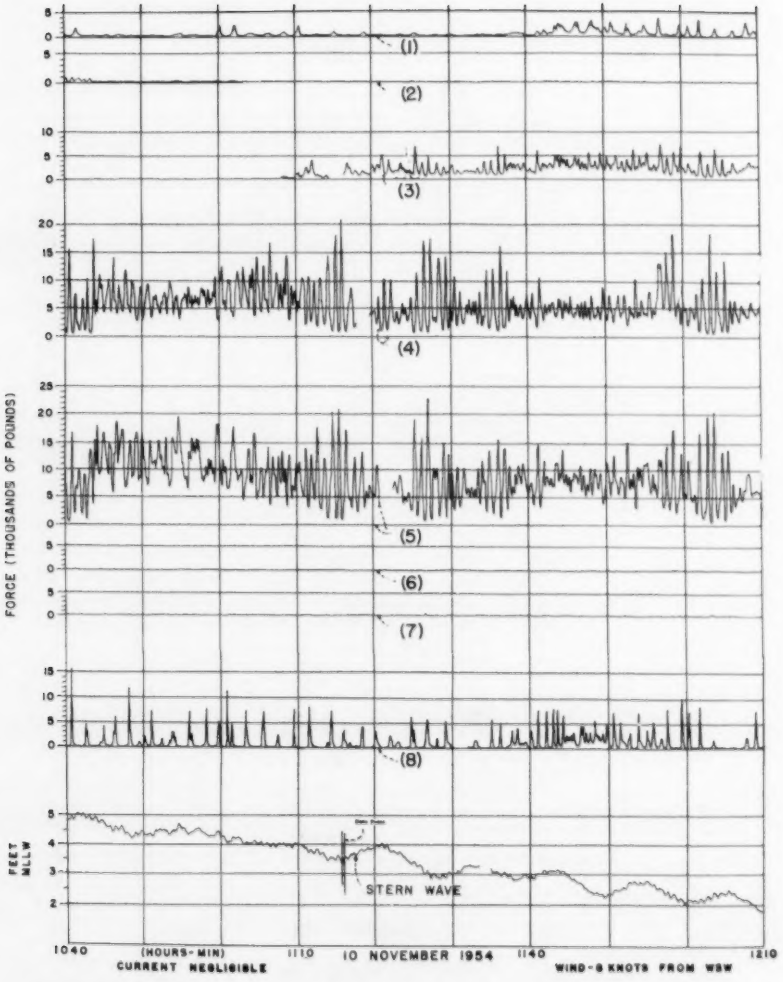


Figure 9 Facsimile of oscillogram with waves of 12.50 minute period predominant and low initial tension. Note the effect of heave on line tensions.

period—because with them the attendent slope of the water surface was greatest. Indeed, the two other conspicuous waves—those of about 2 and 12 1/2 minute period—excited the Ship only a negligible amount in surge, although the 2-minute waves induced considerable yaw, as witnessed by the high forces present in the stern line (#8). The longer wave induced a heave which at times noticeably affected all of the lines. The effect of the initial tension is apparent particularly in the Figure 7 data where a quick shift from about 3 to 22 kips in initial tension in the forward and aft surge lines produced a significant reduction in the restoring force for about the same excitation.

It is apparent also (Figures 5, 6, 8) that the variations in water level near the bow and stern of the Ship due to the standing wave with about 1 minute period are 90 degrees out of phase with each other, which is indicative of the fact that the center of the Ship is located near to a node of this standing wave. (Figure 1-c). This is considered to be a very fortunate circumstance from a research viewpoint and influenced to a considerable extent the decision to use this Ship for this study.

The wave spectrum in the Basin was dominated (Figures 5 - 9) by waves with periods of approximately 1, 2 1/2 and 12 1/2 minutes. It is not known reliably whether or not such long-period waves, assumed to be of the standing type, are periodic. It is considered that the various basins in any harbor can respond naturally only in a periodic manner depending upon their geometrical characteristics; however, it is thought that their excitation is not periodic, because it is produced by ocean-type waves.

In an attempt to bring some order to the results, the period, $T_n$, of the free oscillation of the water in pertinent basins of length $\ell$ was calculated using the expression: $T = B\ell/n\,(gd)^{1/2}$, where n has a value of 1, 2, 3 etc. for a closed basin and 1, 3, 5 etc. for an open basin and B has a value of 2 and 4 for respectively closed and open basins. These calculations indicate that the fundamental and second harmonic for the Basin oscillation are respectively 1.96 and 0.98 minutes while the fundamental and third harmonic for the Harbor as a whole are respectively 7.50 and 2.50 minutes, the second harmonic being supressed entirely. Such calculations do not seem to explain the source of the prominent wave with period of about 12 1/2 minutes in Norton Sound slip. As speculated by O'Brien (1957), it may be the result of the oscillation of water over the very deep submarine canyon which fronts the Harbor.

No investigation specifically intended to determine the origin of this wave is known to have been made.

In a modest study of the wave environment, a portion of the water-level oscillogram obtained from the bottom pressure pickup located near the Stern of the Ship was reduced to eliminate the effects of tide and the 12 1/2-minute wave. It was then analyzed using the method of residuation as originated by Chrystal (1904) and replotted (Figure 10). This procedure involves the offsetting of the traces by a certain increment of time to induce cancellation of certain components. The original record was residuated first with respect to the 2.50 minute wave to expose the 0.98 minute wave and then vice versa, so that the result is two separate traces of water level versus time in which the waves of 0.98 and 2.50 minute period are respectively predominant. It will be noted (Figure 10) that the maximum amplitude of the 2.50 minute wave—0.10 feet—is about double that of the 0.98 minute wave. From the geometry of the Harbor it is apparent that the crest of the 2.50 minute wave as the third harmonic of the fundamental oscillation of the water in the Harbor as a whole likely is somewhat oblique to the long axis of the Basin; the noticeable

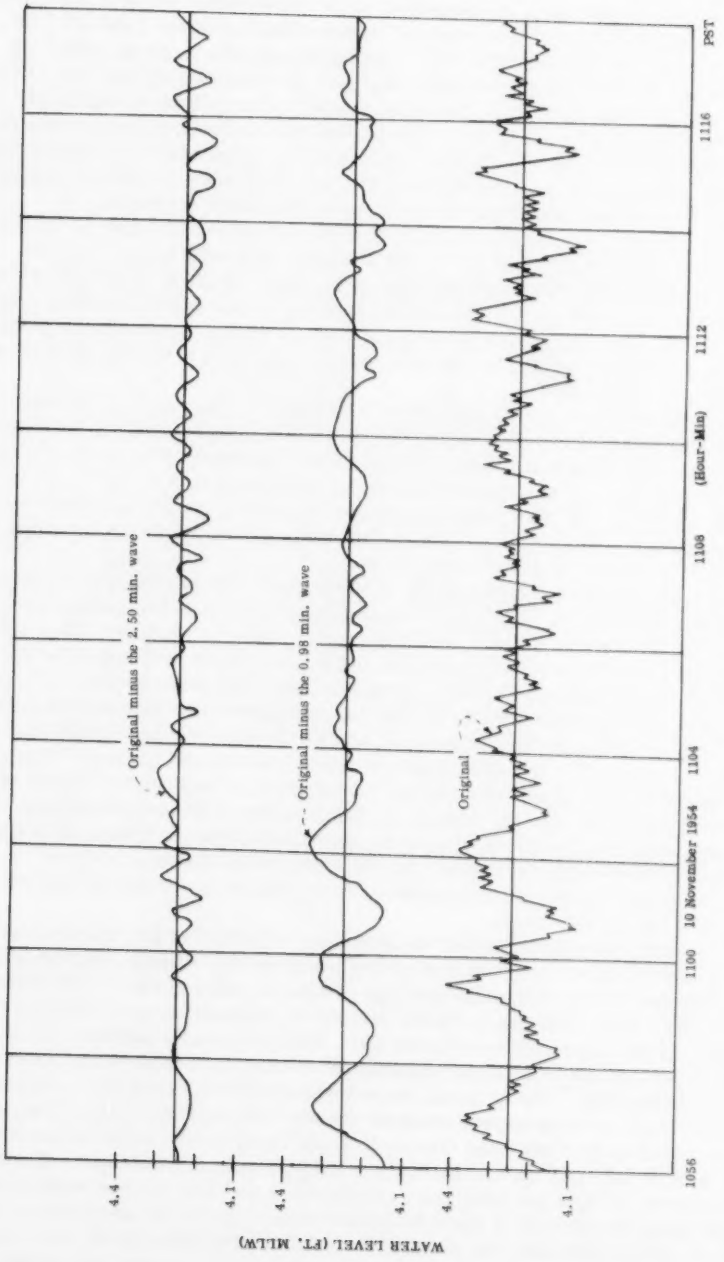


Figure 10 Results of applying the residuation technique.

tendency of the Ship to yaw when such a wave is predominent may be explained on this basis. It is probable that a wave with the fundamental period of the Basin—about 1.96 minutes—is also present, but to a minor extent for it was not exposed by the residuation technique. This may have been due to the tendency toward accumulated errors inherent in the technique.

The Ship movement was resisted at all times by at least the two surge lines—No. 4 and No. 5—which were kept taut such that their tension never became less than about one kip. This is indicated in Figure 11 which presents restoring force—the surge component of the individual line tensions—as a function of surge and indicates that movements of about one-half foot result in restoring forces of about 20 kips.

As a standard operation, the tension in the lines for any given tide level was varied as desired by the Ship's crew operating to change the length of the aft surge line (No. 5), which operation caused the Ship to move and thus altered the tension in all the lines. This is illustrated in Figure 11-C where a tension of 15 kips in the aft surge line caused the forward bow spring line (No. 3) to become active and to operate with the forward surge line (No. 4) which was always active. In the case cited there was a decrease in the slackness of the remaining lines but not enough to induce significant tensions. Only in rare cases—as for example during the visit of a personable young lady selected by the crew and others as Miss Guided Missile when a sense of gallantry prompted action to attain maximum ship stability—was the length of any line, other than the aft surge, altered.

When the Ship yawed considerably—as it did frequently when 2 1/2 minute waves were predominant—then the stern line (No. 8) was loaded in the order of 20 kips. Such intervals were not analyzed because enough difficulty was encountered in dealing with significant surge movements without attempting to cope with those involving obvious coupling.

Analysis of the experimental data (Figure 11) shows that the relationship between restoring force and Ship movement was continuous and sensibly linear in all significant cases. The factor expressing this relationship—designated k—was found to vary from 34 to 48 kips per foot as a function of the initial tension where a value of about 40 kips per foot seems to cover all cases adequately. Substitution of this value of k in the familiar expression for the natural period $T_n$ of the undamped oscillation of a simple spring-suspended mass ($T_n = 2\pi(m/k)1/2$) gives a value for $T_n$ of about 30 seconds. It is obvious that this is considerably less than the period of the significant standing waves encountered in the Basin during the study, and thus in no instance was the condition of resonance encountered.

An interesting example of the Ship's behavior is presented in Figure 12, an enlargement and elaboration of the basic data presented in facsimile form in Figure 5 (point 8). The restoring-force data is the result of summing in the surge direction the pertinent components of the measured line tensions. The ship movement was deduced from the calculated elongation of the forward surge line (No. 5). By graphical differentiation of the ship-movement curve, the velocity curve was developed, and from it the acceleration curve was developed by the same process. The accelerations were multiplied by the mass of the Ship to obtain data for the inertia-force curve; the measured slope of the water surface was used in equation (6a) to obtain the data for the excitation-force curve. Thus, a sensible approximation of the Ship's behavior in this typical instance is displayed in terms of the equilibrium components as given in equation (1).

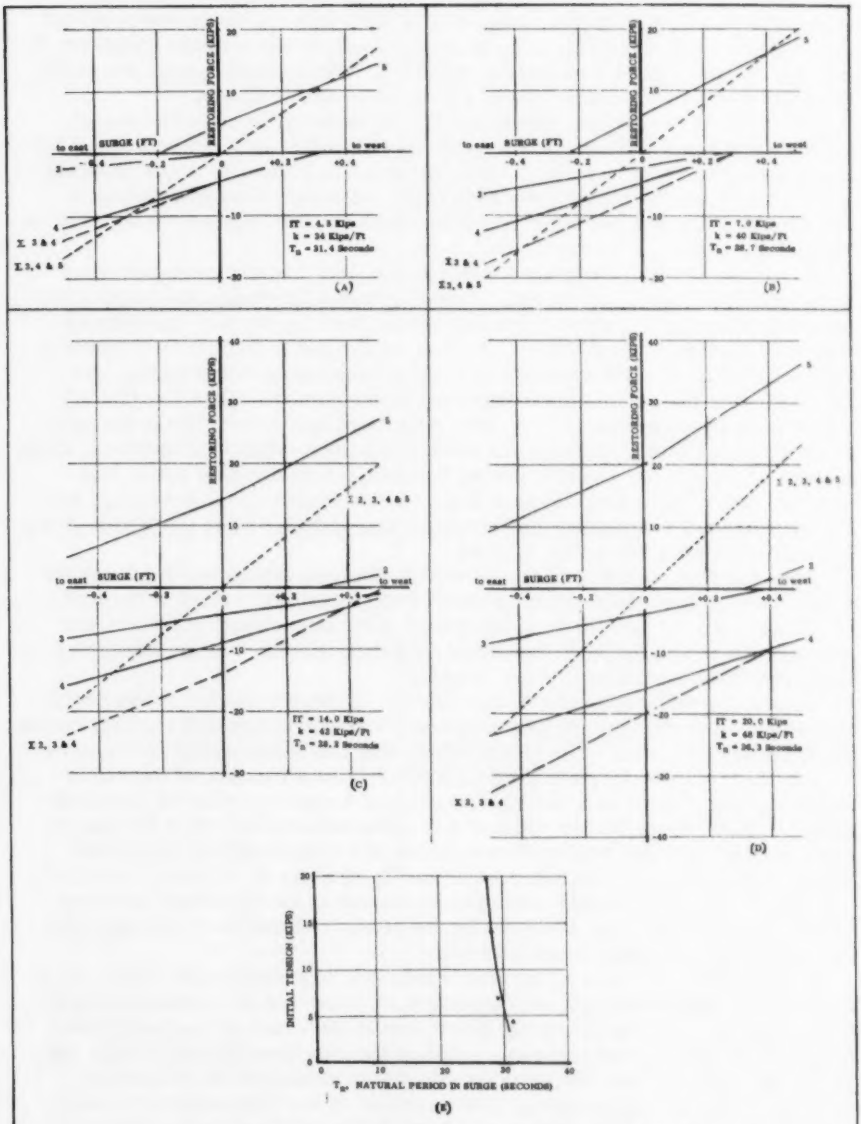


Figure 11 Variation of calculated restoring force with ship movement in surge

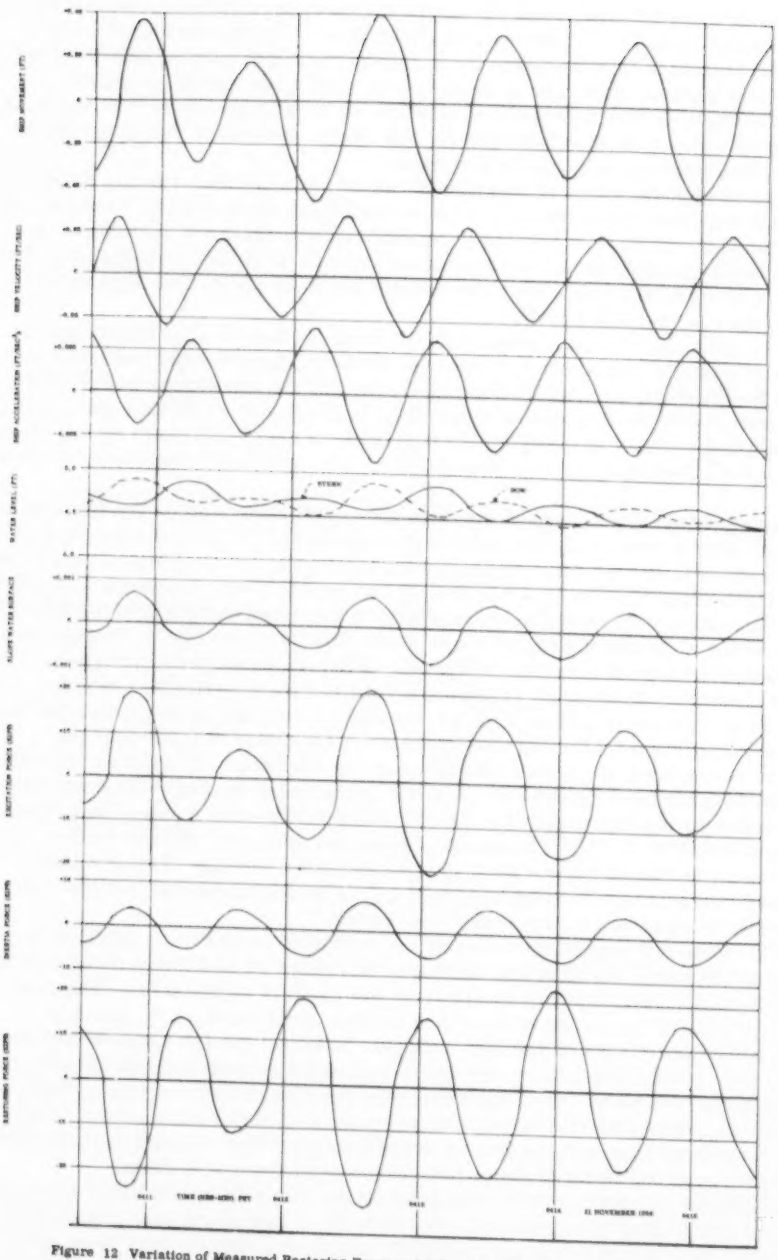


Figure 12 Variation of Measured Restoring Force and Calculated Inertia and Excitation Forces with time.

Note (Figure 12) that, while the restoring force is always opposite to the displacement, the inertial force is in phase as well as the excitation. The last circumstance is substantiated not only by the experimental data but also by a consideration of the performance of the analogous spring-suspended mass when subjected to periodic excitation. It is indicated that, if damping is negligible, as can be demonstrated for this study, then there can be no lag between the excitation and the displacement.

In reviewing the effect of damping it will be assumed that viscous damping is dominant—that due to wave generation by the Ship is negligible—and that of this, the part due to skin friction is negligible since forces of less than one-pound are calculated from the expression given by Schlichting (1949) for a flat plate in longitudinal flow. This leaves only the drag due to flow separation—form drag—to be considered.

In equation (3) it would appear that the drag coefficient ($C_d$) should not be taken as greater than about 1.0, because for a circular cylinder with axis in the flow direction, Rouse (1946) gives a value for the coefficient of 0.90 for a condition where the Reynolds Number ($N_r$) is greater than $10^3$ and the length-to-diameter ratio is 20. The $N_r$ for this study is about $10^6$ based on the maximum particle velocity and the Ship's beam. The length-to-beam ratio is about 7.

The value of $\dot{x}$ to be used in equation (3) can be estimated on the assumption that the Ship is stationary and subject to a standing wave of one-quarter foot amplitude (A). In this case the maximum particle speed ($V_m$) calculated from the relationship $V_m = A\,(g/d)^{1/2}$ is 0.25 feet per second. From equation (3), with the values of $C_d$ and $V_m$ as calculated substituted along with 1150 square feet for the underwater projected end area of the Ship, a value is obtained for the damping force of less than 100 pounds which is considered negligible.

At a number of points of maximum acceleration—the extremes of ship movement—the mass factor, $C_M$, was evaluated using equation (1) and the data presented in Figure 12. For accelerations of the order of 0.007 feet per second per second, the factor was found to vary between 1.0 and 1.2. The definition from the oscillograms of the slope of the water surface—the controlling parameter in the expression for the excitation force—was found to be critical in the evaluation of $C_M$. Treatment of a second situation, similar to that illustrated in Figure 12, resulted in similar values for $C_M$. These values seemed close enough to unity to permit $C_M$ to be so considered and thus effectively to eliminate it as a significant factor.

The measured maximum values of the restoring forces (as a function of the slope of the water surface) are compared in Figure 13 and Table III with maximum values of such forces calculated on the basis of equation (1). The measured values of the slopes of the water surface were used on the basis of readings from both Stern and Bow pickups. In two of the ten cases where the Stern pickup only was active, this slope was deduced from the relationship between maximum water-level variation near the Stern and the slope as determined from data collected when both water level-pickups were active. The Ship movement was deduced from a consideration of the elongation of the two surge lines on the basis of the particular loads measured in them.

Values for the maximum acceleration in the Table III calculations were obtained by assuming the Ship to be oscillating in simple harmonic motion at a constant circular frequency, $\omega$, and amplitude, A, such that the maximum acceleration was equal to $A\omega^2$. That this method of obtaining the acceleration is not entirely accurate is indicated by considering the situation which existed at

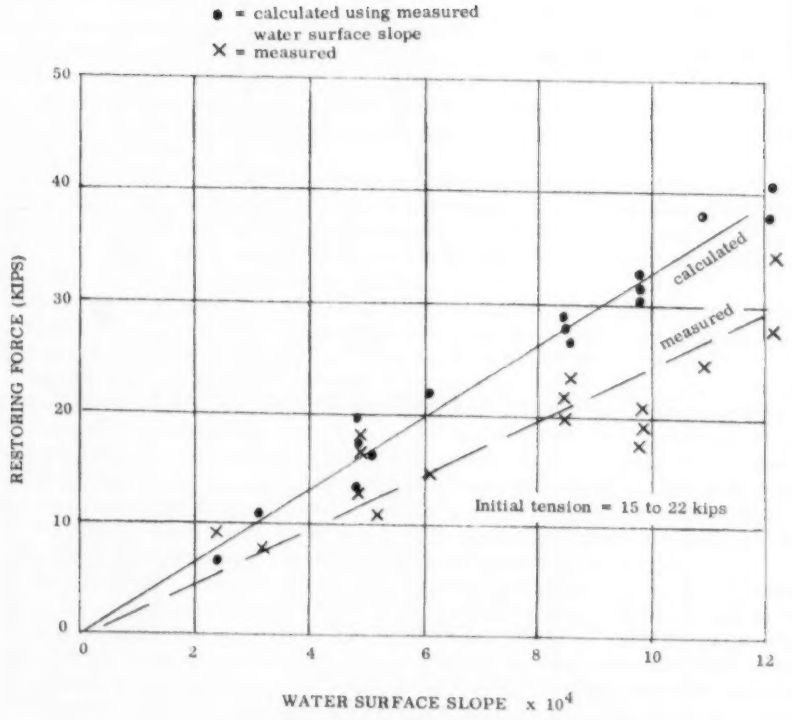


Figure 13 Variation of restoring force with slope of water surface for initial tensions of from 15 to 22 kips.

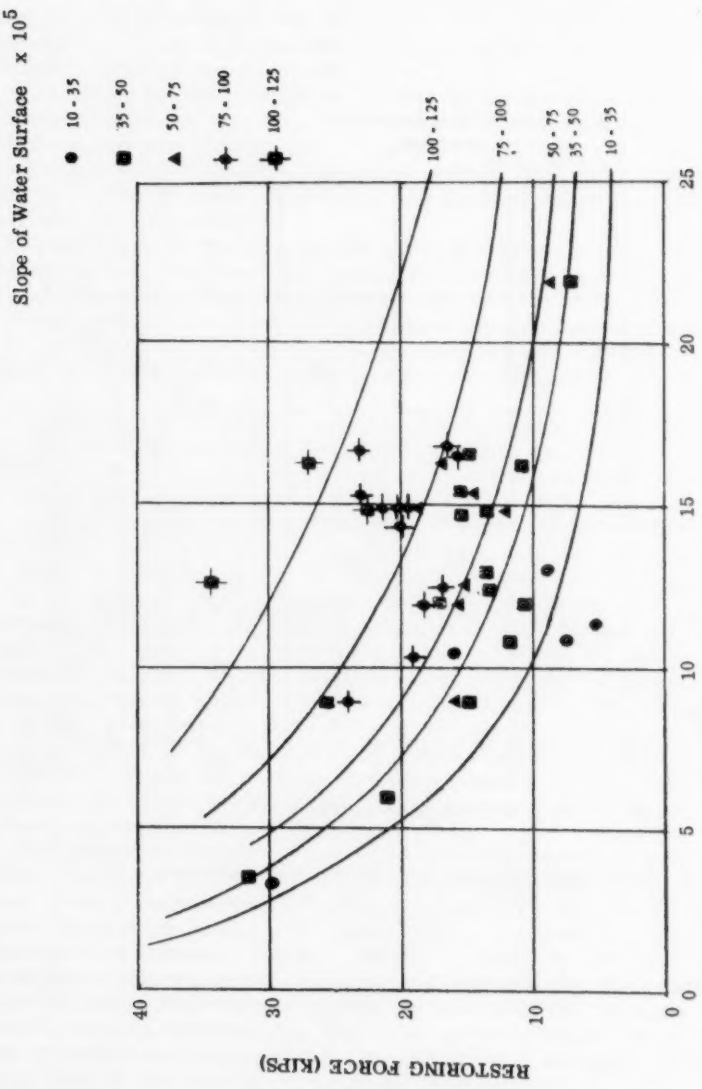


Figure 14 Variation of restoring force with initial tension for various water surface slopes.

21-04:12:36 Nov. 1954 (point number 8 in Table III and Figure 12) where the acceleration as calculated is 0.0057 fpsps, while that obtained by graphical differentiation of the ship-movement curve is 0.0075 fpsps. While the difference of 30% based on the calculated value of the acceleration is considerable, the effect on the restoring force will not be nearly as great—a change of 1.5 kips in a total of 38.0 kips—because in this case inertia is not predominant. It is considered that, notwithstanding the differences cited, the approach presented in Table III should be viewed with interest in an engineering field where, at present, estimates, especially of the forces induced by waves, to within one-hundred per cent or so of the true value frequently are welcomed.

It will be noted (Figure 13) that the measured values of the restoring forces are about three-quarters of those calculated. This circumstance may be due in a large part to the liberties taken with the actual mechanics in the calculation of the acceleration and the equally approximate measures taken to obtain the Ship movement.

When the Ship was tied relatively loosely, as it was in the situations designated numbers 1 and 9 in Table III, it was apparent from the analysis of the data, if not from intuition, that the ship tended to possess a considerable inertia force which, when added to that of the excitation, required restoring forces that were relatively large—20 to 30 kips.

It is apparent from a review of Figure 13 data that for any given mooring condition the slope of the oscillating water surface is the dominant parameter and one with which the restoring force seems to vary almost linearly.

On the basis of limited data with considerable scatter, an attempt was made to demonstrate this further by presenting (Figure 14) restoring force as a function of initial tension with the various slopes of the water surface encountered drawn as contours in the body of the data. It is apparent that an inverse relationship exists for any particular water-surface slope so that it is possible to substantiate a conclusion arrived at by Wilson (1951) and Deacon et al (1957) among others, and one which may be intuitavely obvious, namely: that tight lines tend to reduce the restoring force required.

As a designer, concerned with the indirect determination of the restoring force for non-resonant cases for a ship moored with taut lines in long waves, it is speculated that one could cope with the deduction of sensible values for the inertial term in equation (1) on the basis of a reasonable estimate of the elongation of the ships lines and the amplitude of the water particle movement, but that he would be bothered considerably in obtaining, with the same degree of confidence, a valve for the excitation. The reason for this lies in the difficulties inherent in the calculations of the slope of a water surface which likely is disturbed by two or more waves.

## CONCLUSIONS

The following conclusions are drawn from this study of the 12,000 ton Ship as berthed with unusually taut lines in a standing wave environment at a location in the Harbor sensibly near to the node of one of two significant standing waves, such that the significant movements—those of up to 1 foot induced by water surface oscillations at periods of about 1 and 2 1/2 minutes with slopes up to 0.0015—were only in surge.

1. The restoring force for initial line tensions of about 20 kips varied directly with the slope of the water surface, being about 10 and 30 kips at slopes of respectively .0004 and .0012.

**Table III** Calculation of restoring force on basis of measured slope of water surface and ship movements inferred from changes in tension in aft barge line.

| Data Point | | 1 | 2 | 3 | 4 | 5 | 6 | 7 | 8 | 9 | 10 |
|---|---|---|---|---|---|---|---|---|---|---|---|
| Date | year | 1954 | 1954 | 1954 | 1954 | 1954 | 1954 | 1954 | 1954 | 1955 | 1955 |
| | d and n | 10 Nov | 19 Nov | 20 Nov | 20 Nov | 20 Nov | 20 Nov | 20 Nov | 21 Nov | 14 Apr | 14 Apr |
| | hour | 11 | 18 | 17 | 19 | 20 | 20 | 20 | 04 | 06 | 07 |
| water level | | | | | | | | | | | |
| trough at Bow | ft. | not meas | 3.90 | 4.05 | 3.90 | 3.80 | 3.80 | 3.65 | 4.90 | not meas | not meas |
| trough at Stern | ft. | 3.35 | 3.50 | 3.70 | 3.60 | 3.40 | 3.45 | 3.30 | 4.40 | 1.70 | 1.80 |
| diff : B - S | ft. | --- | 0.40 | 0.35 | 0.10 | 0.40 | 0.35 | 0.35 | 0.50 | --- | --- |
| slope: B-S/ℓ10 | -- | *0.00063 | 0.00098 | 0.00086 | 0.00024 | 0.00098 | 0.00085 | 0.00085 | 0.00122 | *0.00050 | *0.00052 |
| crest at Bow | ft. | not meas | 3.20 | 3.65 | 4.10 | 3.35 | 3.50 | 3.10 | 4.40 | not meas | not meas |
| crest at Stern | ft. | 3.35 | 3.70 | 3.85 | 3.95 | 3.55 | 3.75 | 3.55 | 4.80 | 1.85 | 1.36 |
| diff : B - S | ft. | --- | 0.50 | 0.20 | 0.20 | 0.20 | 0.25 | 0.45 | 0.40 | --- | --- |
| slope: B-S/ℓ10 | -- | *0.00040 | 0.00122 | 0.00049 | 0.00048 | 0.00049 | 0.00061 | 0.00110 | 0.00098 | *0.00030 | *0.00032 |
| height of oscill. | | | | | | | | | | | |
| Bow : tr.-cr. | ft. | not meas | 0.70 | 0.40 | 0.60 | 0.45 | 0.30 | 0.55 | 0.50 | not meas | not meas |
| Stern: tr.-cr. | ft. | 0.20 | 0.20 | 0.15 | 0.35 | 0.15 | 0.30 | 0.25 | 0.40 | 0.15 | 0.16 |
| time of oscill. | | | | | | | | | | | |
| trough: B and S | m and s | 15:33 | 15:00 | 48:47 | 04:45 | 03:54 | 07:24 | 14:25 | 18:36 | 28:00 | 37:30 |
| crest : B and S | m and s | 15:57 | 15:24 | 48:18 | 05:00 | 03:30 | 07:00 | 14:00 | 12:09 | 27:36 | 37:54 |
| diff: T/2 | sec. | :24 | :24 | :29 | 1:15 | :24 | :24 | :25 | :27 | :24 | :24 |
| inertial force | | | | | | | | | | | |
| T | sec/cyc | :48 | :48 | :58 | :150 | :48 | :48 | :50 | :54 | :48 | :48 |
| $\sigma_n = 2\pi/T$ | cyc/sec | 0.131 | 0.131 | 0.108 | 0.042 | 0.131 | 0.131 | 0.126 | 0.116 | 0.131 | 0.131 |
| $\sigma^2$ | $(c/s)^2$ | 0.0172 | 0.0172 | 0.0117 | 0.0018 | 0.0172 | 0.0172 | 0.0158 | 0.0135 | 0.0172 | 0.0172 |
| at trough | | | | | | | | | | | |
| $\ddot{x} = a\sigma^2$ | $ft/sec^2$ | 0.0124 | 0.0075 | 0.0046 | 0.0004 | 0.0066 | 0.0069 | 0.0063 | 0.0057 | 0.0183 | 0.0019 |
| force = m $\ddot{x}$ | kips | 10.4 | 6.3 | 3.9 | 0.34 | 5.5 | 5.8 | 5.3 | 4.8 | 15.4 | 1.6 |
| at crest | | | | | | | | | | | |
| $\ddot{x} = a\sigma^2$ | $ft/sec^2$ | 0.0172 | .0097 | 0.0047 | 0.0004 | 0.0077 | 0.00064 | 0.0104 | 0.0056 | 0.0217 | 0.0024 |
| force = m $\ddot{x}$ | kips | 14.5 | 8.1 | 3.9 | 0.34 | 6.5 | 5.4 | 8.7 | 4.7 | 18.7 | 2.0 |
| movement of ship | | | | | | | | | | | |
| initial cond. | | | | | | | | | | | |
| tension | kips | 6.0 6.0 | 12.7 | 15.5 | 13.0 | 15.0 | 15.0 | 15.0 | 16.5 | 3.5 ,3.5 | 22.0 |
| elongation | ft. | 0.28 0.40 | 0.62 | 0.75 | 0.63 | 0.72 | 0.72 | 0.72 | 0.78 | 0.14,0.24 | 1.00 |
| at trough | | | | | | | | | | | |
| tension | kips | 21.5 0.5 | 23.5 | 28.3 | 8.0 | 25.2 | 26.5 | 25.1 | 32.0 | 32.0,0.5 | 26.0 |
| elongation | ft. | 1.00 --- | 1.06 | 1.14 | 0.38 | 1.10 | 1.12 | 1.10 | 1.20 | 1.80,--- | 1.11 |
| at crest | | | | | | | | | | | |
| tension | kips | 0.5 21.5 | 2.0 | 7.5 | 21.0 | 6.0 | 7.5 | 2.0 | 7.8 | 8.4 ,25.0 | 18.5 |
| elongation | ft. | --- 1.40 | 0.06 | 0.35 | 0.97 | 0.27 | 0.35 | 0.06 | 0.37 | --- ,1.50 | 0.86 |
| movement ( a ) | | | | | | | | | | | |
| L.e.diff.in elng | ft. | | | | | | | | | | |
| tr. - initial | ft. | 0.72 | 0.44 | 0.39 | 0.25 | 0.38 | 0.40 | 0.40 | 0.42 | 1.06 | 0.11 |
| cr. - initial | ft. | 1.00 | 0.57 | 0.40 | 0.24 | 0.45 | 0.37 | 0.66 | 0.41 | 1.26 | 0.14 |
| excitation force | | | | | | | | | | | |
| tr.: slope w.s. x W | kips | 17.0 | 26.4 | 23.1 | 6.5 | 26.4 | 22.9 | 22.8 | 32.8 | 13.5 | 14.0 |
| cr.: slope w.s. x W | kips | 10.8 | 32.8 | 13.2 | 12.9 | 13.2 | 16.5 | 29.4 | 26.4 | 0.1 | 8.6 |
| restoring force (calc) | | | | | | | | | | | |
| tr.: -Exc. - m $\ddot{x}$ | kips | 27.4 | 32.7 | 27.0 | 6.8 | 31.9 | 28.7 | 28.1 | 37.6 | 28.9 | 15.6 |
| cr.: -Exc. - m $\ddot{x}$ | kips | 25.3 | 40.9 | 17.1 | 13.3 | 19.7 | 21.9 | 38.1 | 31.1 | 26.8 | 10.6 |
| restoring force (meas) | | | | | | | | | | | |
| trough | kips | 21.0 | 17.8 | 23.4 | 9.0 | 20.8 | 21.8 | 19.8 | 27.6 | 32.0 | 11.0 |
| crest | kips | 21.0 | 34.3 | 16.4 | 13.0 | 17.4 | 18.2 | 25.0 | 19.3 | 30.7 | 7.5 |

* Obtained from plot of measured slope versus height of water level oscillation at the stern.

Note: ℓ10 ft = distance between Bottom Pressure Pickups at Bow and Stern of Ship.

2. Restoring force varied inversely with initial tension for any particular water surface slope such that with a slope of about .0007 this force was about 20 and 10 kips for initial tensions of respectively 10 and 25 kips.

3. Tight lines tended to reduce the restoring force required to resist any particular excitation force since the inertia force was reduced thereby.

4. Measured values of the restoring force were found to be about three-quarters of those calculated on the basis of the slope of the water surface and simple harmonic motion.

5. The excitation can be considered to be represented significantly as the product of the slope of the water surface and the weight of the Ship.

6. The maximum inertial force—the product of mass and acceleration—can be calculated to a sensible degree of accuracy by considering the Ship to be oscillating in simple harmonic motion. The value of the maximum acceleration is equal to the product of the amplitude of the Ship motion—deduced from the elongation of the lines as calculated on the basis of the forces measured in them—and the square of the frequency of the oscillation deduced from that of the water surface.

7. The restoring force can be considered as the sum of the inertia and excitation forces where damping and the added mass effect are neglected.

8. A satisfactory estimate for the natural period of oscillation of the moored Ship can be obtained by considering this to be analogous to the natural period of the undamped oscillation of a spring-suspended mass. A sensible value for the spring factor required can be obtained by linearizing the relationship between restoring force and Ship movement.

## ACKNOWLEDGMENTS

Appreciation is expressed to the U. S. Naval Civil Engineering Research and Evaluation Laboratory of the Bureau of Yards and Docks of the Department of the Navy for permission to publish this paper and to the officers and men of the USS NORTON SOUND for cooperation and assistance.

## SYMBOLS

| | |
|---|---|
| A | = amplitude of wave; one-half vertical distance crest to trough |
| | = amplitude of ship movement |
| | = projected area of ship |
| | = cross-sectional area of a mooring line |
| B | = constant in the expression for natural period of oscillation of basins; 2 for closed and 4 for those with one end open |
| $C_d$ | = coefficient of drag |
| $C_m$ | = coefficient of mass |
| $C_M$ | = mass factor |
| c | = (1-n)/2(1+n) where n is a numerical exponent used with mooring ropes |
| D | = spring factor for representative mooring line |
| d | = depth of water |

| | |
|---|---|
| $E$ | = Young's modulus of elasticity |
| $g$ | = acceleration due to gravity |
| $i$ | = item number |
| $k$ | = spring factor |
| $\ell$ | = length of a mooring line |
| $\ell$ | = length of a basin |
| $L$ | = length of a wave |
| $m$ | = static mass of a ship |
| $N$ | = total number of mooring lines |
| $n$ | = numerical exponent used with mooring ropes |
| | = integer (1,2,3 etc) defining harmonic order and nodality of an oscillation in a closed basin |
| | = integer (1,3.5, etc) defining harmonic order of an oscillation in an open basin |
| $P$ | = total force in a mooring line |
| $t$ | = time |
| $T$ | = period of oscillation |
| $T_n$ | = natural period of oscillation of a system |
| $V_m$ | = maximum speed of water-wave-excited particles |
| $W$ | = weight of a ship |
| $x$ | = horizontal distance along axis parallel to wharf (surge) |
| $y$ | = horizontal distance along axis normal to wharf (sway) |
| $z$ | = vertical distance along axis normal to water surface (heave) |
| $\alpha$ | = angle between mooring line and horizontal |
| $\beta$ | = angle between horizontal projection of the mooring line and the face of the wharf (the x axis) |
| $\omega$ | = circular frequency = $2\pi/T$ |
| $\pi$ | = 3.1416 etc. |
| $\rho$ | = density of sea water |
| $dx/dt$ | = speed of ship in surge = $\dot{x}$ |
| $d^2x/dt^2$ | = acceleration of ship in surge = $\ddot{x}$ |
| $N_r$ | = Reynolds Number |
| | = (fluid speed) (representative dimension)/kinematic viscosity of the fluid |
| $\Sigma$ | = sum |

## REFERENCES


1. Knapp, R. T. and Vanoni, V. A. Wave and Surge study for Navy Operating Base, Terminal Island, California, Calif. Inst. of Techn. report under contract $No_y$-8522 w/Bur. of Yds. and Docks, Jan. 1945.

2. Carr, R. E. Memo on waves in Los Angeles Harbor associated with the Alaskan Earthquake of April 1, 1946, report under contract $No_y$-13116 w/Bur. of Yds. & Docks, April 1947.

3. Wilson, B. W. Ship response to ranging in harbor basins, Trans. Am. Soc. of Civil Engineers 1951.

4. Deacon, G. W. R., Russel R. C. H. and Palmer, J. E. G. Origin and effect of long period waves in ports, Communication 1 Sect. 2 of Proc. 19th International Cong. of Perm. Intern. Assc. of Navigational Congresses, London 1957.

5. Wiegel, R. L., Dilley, R. A., Clough, R. W. & Williams, J. B. Model Study of ship mooring forces: final report, Wave Research Lab., U. of Calif. (B) series 92, issue 8 (part of contract $No_y$-73264 w/Bur. of Yds. and Docks) August 1956.

6. Joosting, W. C. Q. Investigation into long period waves in ports, Communication 1 Sect. 2 of Proc. of 19th International Cong. of Perm. Intern. Assc. of Navigational Congresses, London 1957.

7. Continental Copper & Steel Industries, Inc. Feasibility report on Continental Defense Stations, Cont. Copper & Steel Industries, Inc. 345 Madison Ave., New York, N. Y. (rept prepared for MIT, Lincoln Lab) copyright 1956.

8. David Taylor Model Basin Estimation of forces action on a floating vessel in a channel of finite depth due to traveling waves, Memo from C. O. & Director DTMB to Chief, Bur. of Ships U. S. Navy A-11/Hydro (596:EYH:1f) dated 1954.

9. Knapp, R. T. Wave produced motion of moored ships, Proc. of 2nd Conference on coastal Engineering, Council on Wave Research, U. of Calif. (B) 1952.

10. O'Brien, J. T. Waves in and around Port Hueneme, California associated with the tsunami of 9 March 1957, report LR-R-015 of U. S. Naval Civil Engineering Research and Evaluation Laboratory, 9 April 1957.

11. Chrystal, G. On the hydrodynamic theory of seiches, Trans, Royal Society of Edinburgh, vol. 41, 1904-05 Pt. III.

12. Schlighting, H. Boundary layer theory, NACA TM 1217, pp 51, 1949.

13. Rouse, H. Elementary mechanics of fluids, J. Wiley and Sons, NYC, 1946.

Paper 1572 WW 2 March, 1958

Journal of the
WATERWAYS AND HARBORS DIVISION
Proceedings of the American Society of Civil Engineers

# CONTRACTOR'S PLANNING FOR NAVIGATION LOCKS[a]

F. J. Larkin,[1] M. ASCE
(Proc. Paper 1572)

## SYNOPSIS

A contractor's planning for all jobs starts in the estimating stage. Some feature of the work becomes the key to the solution and dictates methods and equipment. This paper deals with job planning for navigation locks and is principally concerned with the selection of construction plant The construction of the Markland Locks Project on the Ohio River for the Corps of Engineers serves as an interesting illustration.

## INTRODUCTION

Markland Locks consists of twin lock chambers, one 110' wide by 600' long and the other 110' wide by 1200' long, and is located on the left bank of the Ohio River approximately half way between Louisville and Cincinnati. In addition to the lock chambers proper, more than 3000 feet of guide and guard walls for the approaches are included in this contract. The lift of these locks will be 35 feet.

### Planning the Job

The contractor, on receiving the invitation to bid, is first concerned with the location and physical characteristics of the job. He wants to know something of the amount of work to be done, which is revealed by an inspection of the bid quantities. These quantities will have a definite bearing on the selection of method, and, therefore, the plant. For example, Markland Locks

Note: Discussion open until August 1, 1958. A postponement of this closing date can be obtained by writing to the ASCE Manager of Technical Publications. Paper 1572 is part of the copyrighted Journal of the Waterways and Harbors Division, Proceedings of the American Society of Civil Engineers, Vol. 84, No. WW 2, March, 1958.

a. Presented at the American Society of Civil Engineers Annual Meeting, October 14-18, 1957, New York, N. Y.

1. Plant Engr., Contracting Div., Dravo Corp., Pittsburgh, Pa.

involves some 450,000 cubic yards of concrete, 350,000 cubic yards of rock excavation, 670,000 cubic yards of common excavation, almost 5 million pounds of reinforcing steel, almost 4 million pounds of structural steel and castings, a half-million yards of dredging and over 3/4 million yards of fill. These quantities, as well as the location of the work tell the planner whether or not it is the type of job suited to his organization, and, if he is still interested, he starts looking for the key to the method. In planning a job of this nature, the engineer makes his plant layout early. (Fig. 1) Excavating equipment, of course, has to go to the excavation site, and hauling equipment has to be able to transport from that site to the dump. This phase is a study in itself, but, at least, its location is set. Not so with the concrete mixing plant, which is involved in what is generally the largest single item, dollar-wise, on the job. It may be located close to or somewhat remote from the job. It involves primarily the transportation of materials both before and after mixing process itself. Transportation then may become that key which will dictate a major portion of the plant layout.

In the case of Markland Locks, no rail transportation existed closer than 12 miles from the job site. A good highway system existed, but the closest approved source of crushed stone was over 30 miles away. A contemplated pouring rate as high as 1800 cubic yards of concrete per day would have required a considerable fleet of trucks to operate and maintain. An alternate scheme was the trucking of the aggregates from the nearest rail head. The location of the job on the Ohio River, however, suggested moving the materials by relatively inexpensive water transportation methods. This scheme is most attractive if materials suppliers are conveniently located with respect to the river and have barge loading facilities. In this particular case, one supplier of sand and small aggregates was located almost on the river bank but had no dock. The supplier of large crushed aggregates was located a few miles inland and also had no dock. One cement company who could furnish about half of the 400,000 barrels of cement involved was located on the river and had a fleet of towboats and barges. The other cement producer was located about 4 miles inland. In all cases the contractor, being especially equipped for river construction, was able to overcome these difficulties, and aggregate movement to the job by water was accomplished. Involved were the construction of an aggregate loading dock near Carrollton, Kentucky, and a similar one at Madison, Indiana, as well as a cement loading facility on an existing dock at Jeffersonville, Indiana.

Delivery of materials at the site is only part of the battle. The next steps are unloading, storing, processing the aggregate, mixing the concrete and its transportation to the forms. With the lock located in the river within a cofferdam, it seemed an unwarranted expense to transport the cement and aggregates up the hill to the top of the bank and bring them back down again in the form of concrete, but such a solution was possible and was considered. The primary disadvantage was, of course, the cost of handling materials the extra distance. The advantage was relative freedom from high water, which in the Ohio Valley can be substantial and of long duration. Of course, if the job is flooded out, concrete cannot be placed anyway, so the consideration is simply one of keeping dry. Contour maps revealed general top-of-bank elevations about Elevation 460, with certain permanent fills going up to Elevation 470 and 485. A study of hydrographs for the locality revealed one record flood as high as Elevation 484, while the duration curve for a 15-year period showed the river exceeding Elevation 455, the minimum specified top of the cofferdam,

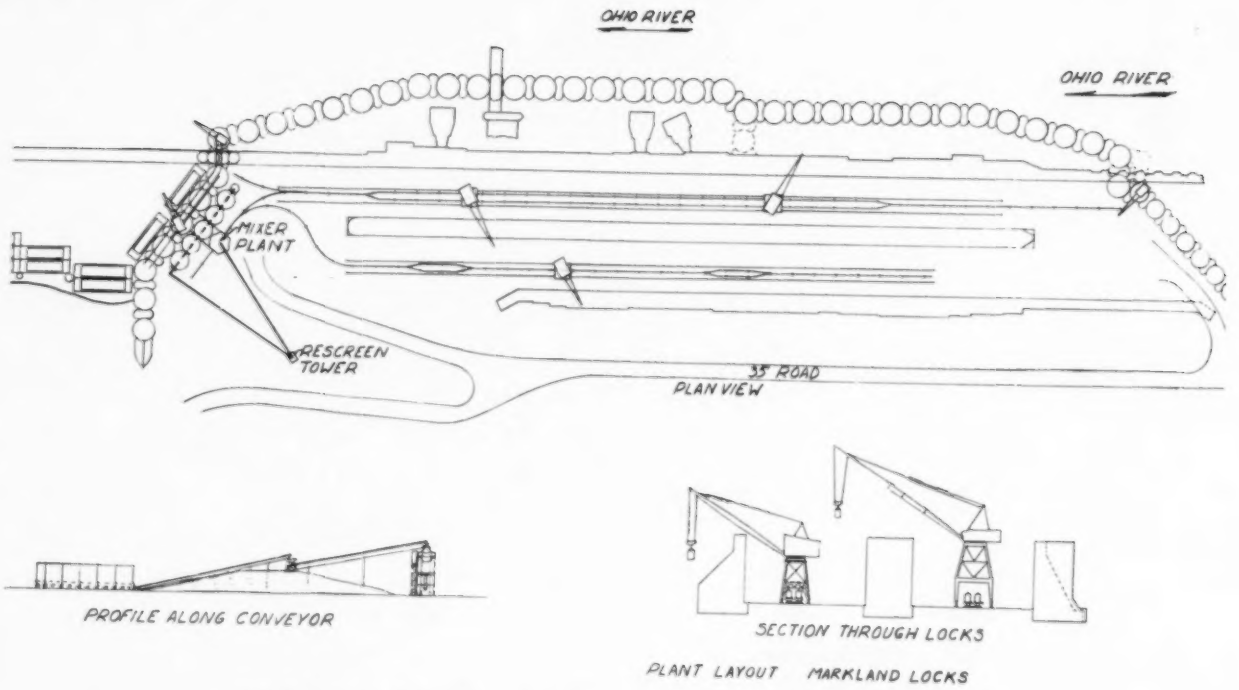


Fig. 1. General plant layout for Markland Locks, showing steel sheet pile cell cofferdam.

for only 2-1/2% of the time. Storage on top of the bank did not preclude flooding but protected most of the plant involved.

A plant located near the material harbor was a logical idea, (Fig. 2) but several things had to be resolved before this decision was reached. Usually at this point the planner is aware of, or is looking at the plant he has available or can buy. In this case, the contractor's floating plants were of such size as to require two of them to suit the capacity required. They were not adapted to washing and rescreening the aggregates as required for the crushed rock; neither were they capable of passing all the specifications concerning control and combined autographic recording of the batched materials, a refinement which was specified by the Corps of Engineers. To render them capable of passing these specifications required a considerable expenditure of money and was particularly difficult to include in the existing plants.

At this point it is well to consider another element that leads the contractor to make certain decisions. On this project four concrete mix alternates were offered:

1. 3" Maximum size stone with all Portland Cement.
2. 3" Maximum size stone with Portland Cement and one-fourth natural cement.
3. 6" Maximum size stone with all Portland Cement.
4. 6" Maximum size stone with Portland Cement and one-fourth natural cement.

The difference between 3" and 6" stone represented over 40,000 barrels of cement in favor of the 6" stone, or about $140,000 saving in cement costs. The difference between natural and Portland cement represented $1 per barrel for 100,000 barrels or $100,000. The floating plants were practically limited to a 3" size stone and one cement by reason of their hull sizes which are governed by lock and bridge clearances. These were, therefore, abandoned by the planner in favor of an owned land plant of considerable size which needed only modernization of its batching apparatus and control to meet the specifications.

The apparent solution was to erect the land plant in the cofferdam with the shortest aggregate conveyor system possible. One prime advantage realized was that short, level concrete haulage was then possible, giving the planner a choice between dinkey locomotives and trucks. Storage of aggregate was arranged in cells built just inside the cofferdam into which the aggregates could be unloaded directly by a whirler crane. (Fig. 3) Draw down of these cells in a reclaiming tunnel onto a belt conveyor would bring the aggregates up the bank through a rescreening plant and on up to the mixer bins ready for batching. Cement could be blown directly from barges to bins located in or alongside the batch plant.

The flood threat was met by placing the batching floor of the plant at Elevation 471, above any likely high water. This placed the mixing floor at Elevation 455 or cofferdam elevation. (Fig. 4) The contractor considered the possibility and decided to take the risk of having to remove such things as mixer motors and control and also the motors and control apparatus in the reclaiming tunnel in the event of a flood. From a study of the hydrographs and duration curves, this risk was not deemed to be of an excessive nature and permitted him to take advantage of the cofferdam location for his plant close to the material coming in by water. An 11-foot extension to the bin structure was necessary in order to get the plant down to the rock elevation found inside

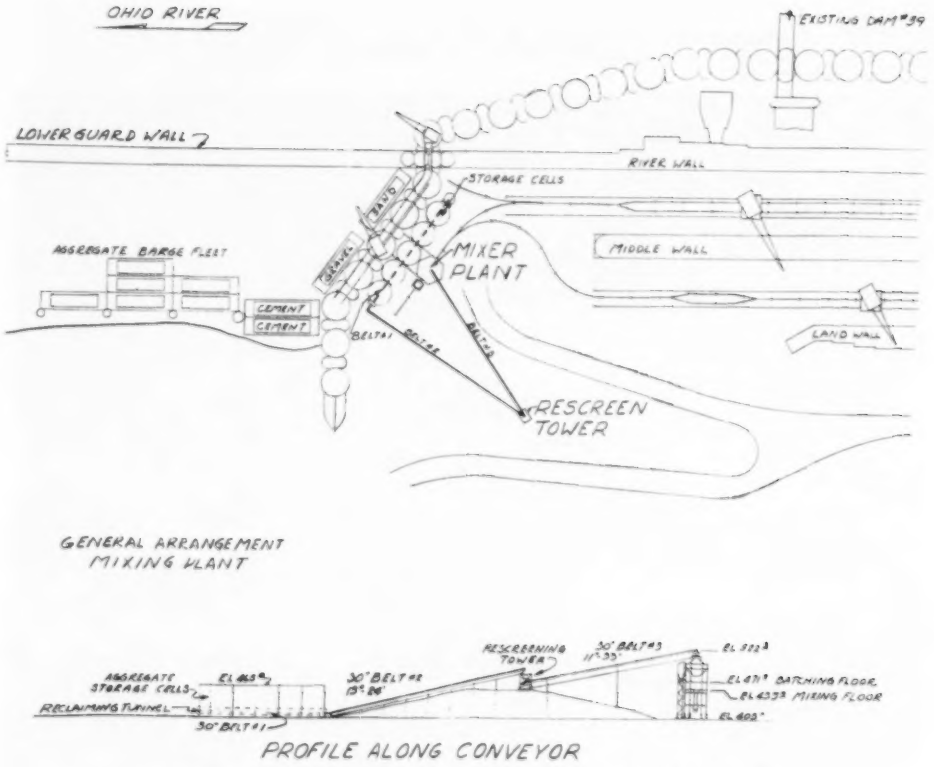


Fig. 2. General arrangement of the mixing Plant, with profile along the conveyor.

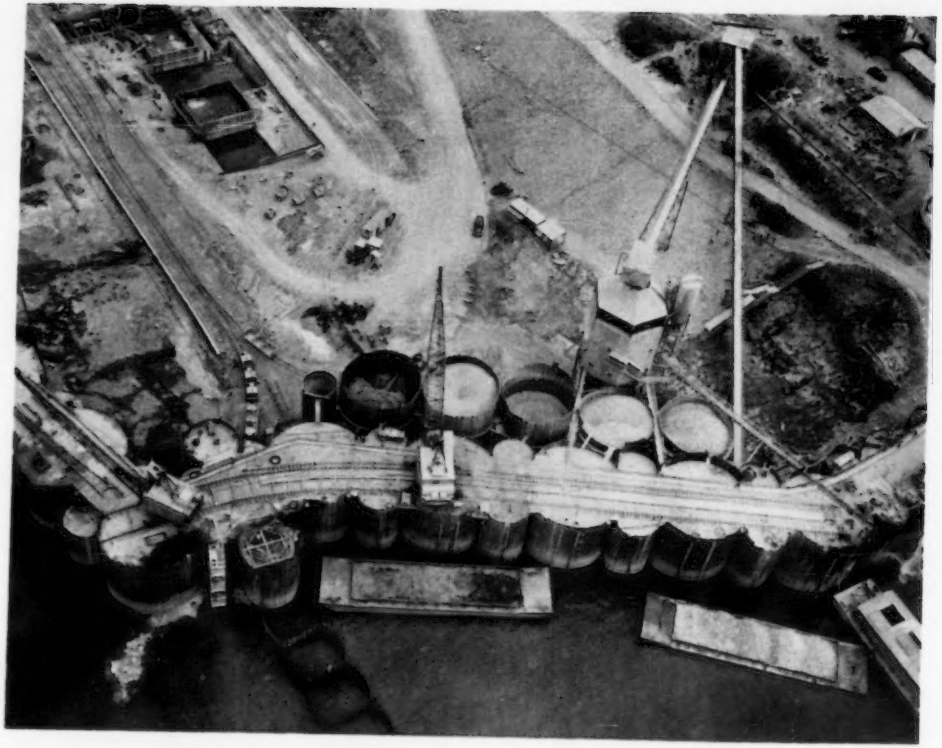

Fig. 3. Aerial view of storage cells for aggregates. Whirler crane was used to unload from barges directly into cells at downstream end of cofferdam.

Fig. 4. This view of the mixing plant shows elevation above the floor of the cofferdam. The mixing floor was at the level of the top of the cofferdam, thus reducing the flood threat.

the cofferdam, but with the plant inside the cofferdam and well braced to it, this did not prove to be an excessive height of plant. A means had to be provided to bring the mixed concrete down to the cofferdam floor, and in this fashion the planner arrived at his method.

The general plan as far as the concrete mixing phase having been decided, the remainder of the planning work was considerably simpler. Bank excavation and the diversion of Stevens Creek (Fig. 5), a stream that ran almost at right angles into the cofferdam area, was obviously one of the first items of work. Stevens Creek had to be turned downstream to come into the river well below the cofferdam. The material, loam, clay and silt, was well suited for loading with motorized scrapers and the dump was on the various fills in the vicinity. One motorized scraper was available in the contractor's plant and two more had to be purchased. A push dozer in the cut and another on the dump, along with a road patrol for the haul road maintenance completed the excavation team except for a tractor drawn sheepsfoot roller which would be necessary wherever the fills were to be compacted.

Borings indicated that the lower portions of the cut for Stevens Creek would be wet and would not provide good footing for the tractor or rubber-tired equipment. For this portion of the work, crawler cranes (Fig. 6) equipped with 2-1/2 C.Y. dragline buckets were available to load this material to 22-ton end dump trucks for hauling to the fills. At the same time that the bank excavation could get underway, work in the river could also start, river stages permitting. A considerable portion of the half million cubic yards of dredging was located (Fig. 7) in the cofferdam area. Much of the excavation material was suitable for coffer fill, so it was essential that the planner figure on the dredging proceeding with the cofferdam construction.

A cellular steel sheet pile cofferdam was judged to be the most adequate and economical type cofferdam for this type of job. Here the planner had to consider the availability of sheeting. He found nearly enough on one of his company's jobs on Lake Superior. It happened to be in the coffer removal stage and so the sheeting could be loaded to barge and towed through the Soo down Lake Michigan to the Chicago Canal, down the Illinois River to the Mississippi with a left turn at Cairo into the Ohio River and up to the job site. (Fig. 8) This situation, of course, was particularly fortunate as it was practically impossible to book mill orders for sheet piling at the time, let alone get delivery on them. In the bidding for the job it was probable that some contractors would be forced to consider expedient cofferdams. Quotations, for instance, were proffered on a cofferdam constructed from interlocking prestressed concrete cylinders. This idea was most ingenious but required heavy lifting equipment for installation and very considerable cost for removal.

With these considerations established, the planner figured on using two small derrick boats for setting and driving sheetpile. A larger dragline derrick boat could dredge the cell sites to scows which in turn would be dumped alongside the driven cells, if acceptable for fill, or towed to disposal if not. Another large clamshell derrick boat was necessary to fill cells from the material dumped from the scows. Enough additional dredging capacity would be necessary to remove overburden above the rock inside the cofferdam. This material, or the excess over that needed for coffer fill, was slated to be scowed away and would have to come out before the coffer was closed. All this work, including the building of the coffer, would have to go at a good rate from the end of the Spring rises in the river through the Summer in order to be able to pump out the cofferdam in the early Fall. The scheme for placing

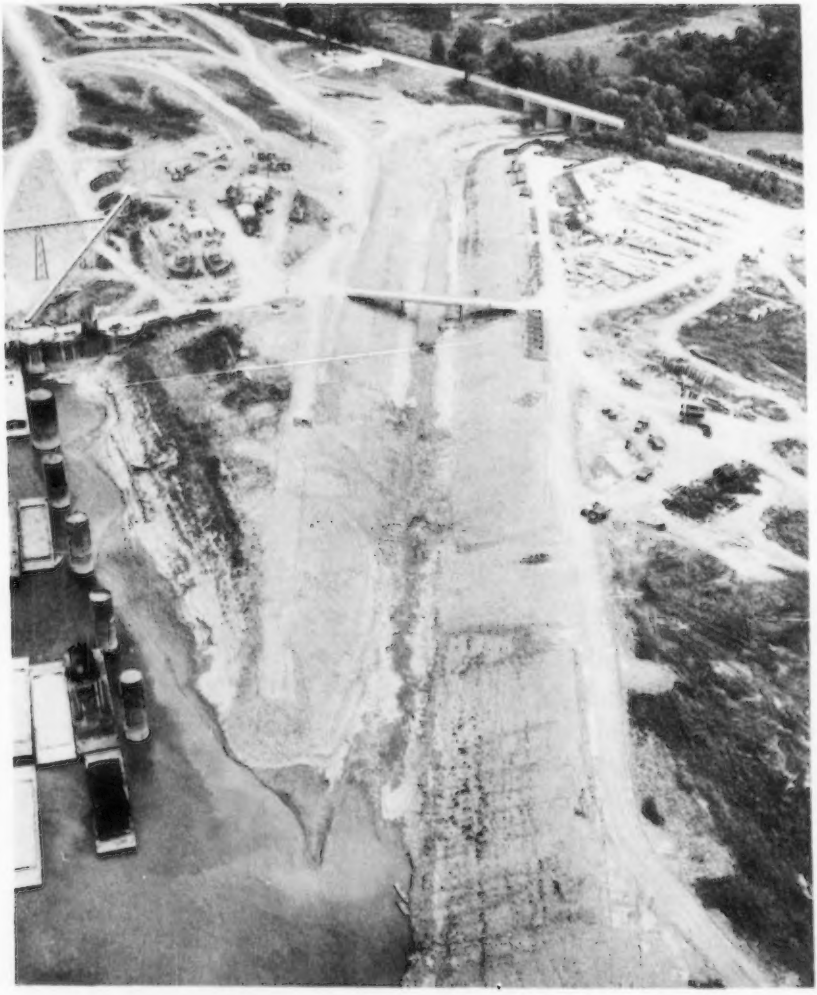

Fig. 5. Aerial view shows excavation and diversion of Stevens Creek to a point downstream of the cofferdam. The stream originally emptied in almost the center of the cofferdam area.

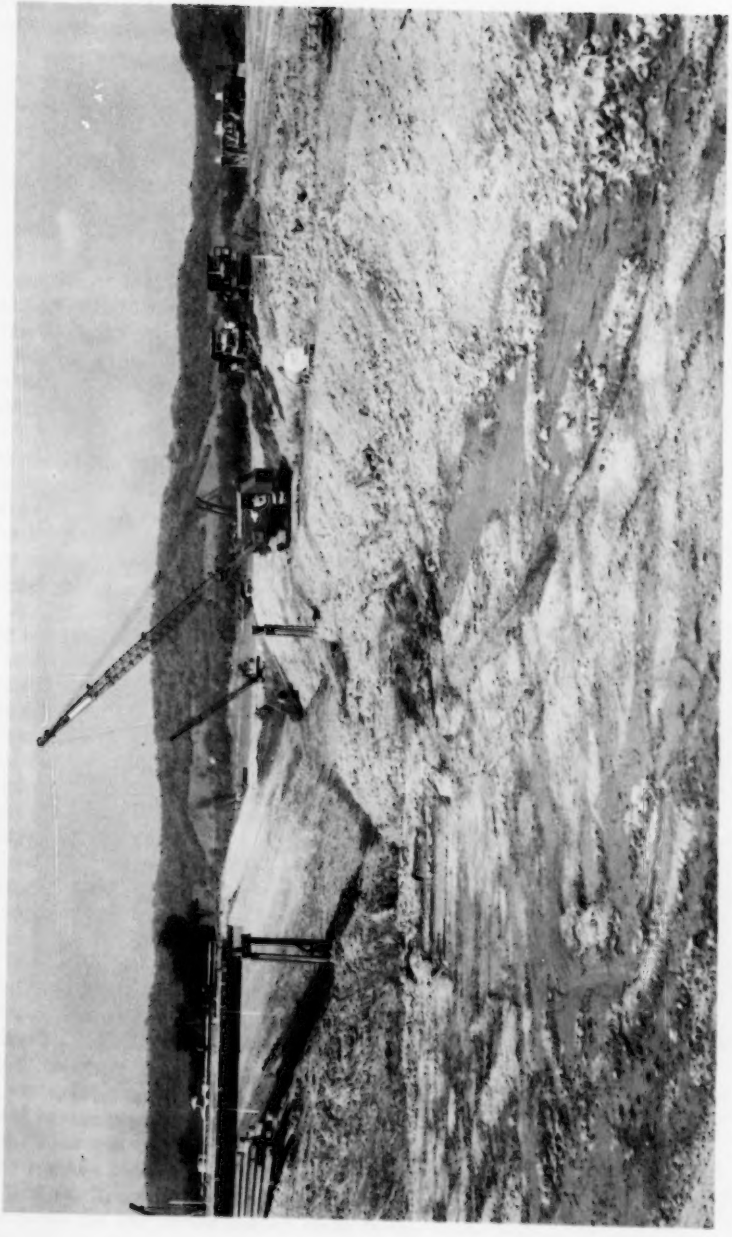

Fig. 6. Crawler cranes equipped with 2-1/2 C. Y. dragline buckets were used in the lower portions of the Stevens Creek cut, which were too wet for rubber-tired equipment.

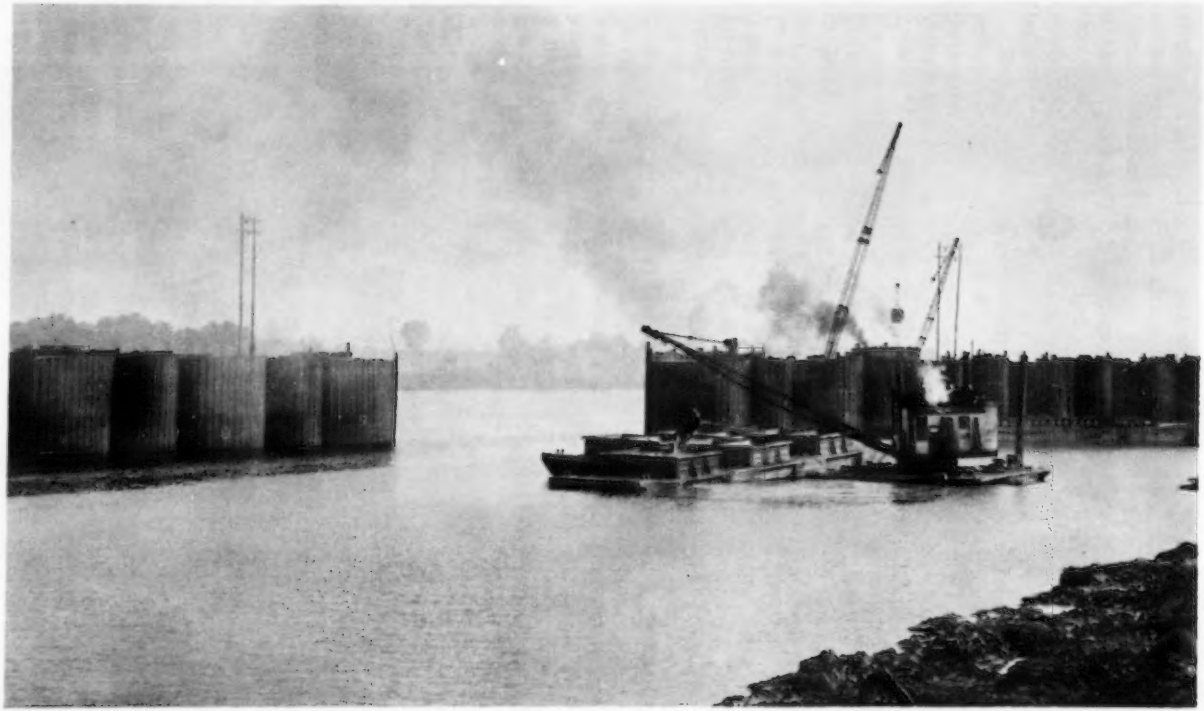

Fig. 7. Much of the half-million cubic yards of dredging required on the Markland project was taken from the cofferdam area before the cofferdam was closed and dewatered.

Fig. 8. Driving one of the steel sheet pile cells used in the cofferdam.
Note the wooden template in the center of the picture.

the mixing plant in the cofferdam meant that erection of it could not start until the coffer was pumped out. Therefore, the plant would have to be gotten ready during the summer and additional items for modernization procured and all assembled on the job site ready for a quick start when the cofferdam was finally unwatered. Before the coffer could be pumped, it would be necessary to cap the cells with concrete to prevent scour in case of over-topping. There was enough concrete required for this to justify moving in a mixer boat, and, since this concrete was not specification concrete, river-dug material could be used.

This, then, was the contractor's plan up through the construction of the cofferdam, and the erection of the mixing plant. As soon as the coffer could be pumped out, (Fig. 9) clean-up of the bottom would be started, followed closely by foundation rock excavation. The planner had noted an area of high rock at the lower approach and so planned his cofferdam to extend downstream far enough to enclose the bulk of this area. This rock then could come out in the dry rather than by submarine methods.

For the rock excavation the same end dump 22-ton trucks could be used for haulage. Loading was to be done by two rock shovels. Line drilling was suited to track-mounted drills owned by the contractor, and for shot hole drilling, a number of wagon drills were available from the job on Lake Superior that furnished the sheetpile. A permanent air plant of 2400 cubic feet per minute capacity would be needed, supplemented by 1800 CFM of portable air during the drilling period.

For concrete placing, (Fig. 10) the planner having all his haulage on one level, thanks to the plant-in-the-hole idea, selected dinkey locomotives of which he owned three at 42-inch gage. Two additional were planned for purchase. For placing concrete he planned to use one of his 35-ton gantry traveler whirler cranes in the shorter land lock. For the river lock two 50-ton similar cranes would be needed which would have to come either from the second-hand market or be built new for the job.

For concreting the upper and lower guard wall extensions which were not enclosed in the cofferdam area, the planner figured to set up two small whirlers, one each on the upper and lower corners of the cofferdam, to rehandle concrete in 2 C. Y. buckets hauled from the mixing plant. These buckets (Fig. 11) would be placed on small barges which could ferry the buckets to the placing site. All material handling on these wall extensions would be by the same small derrick boats which would assist in the building of the cofferdam.

This paper has covered the highlights of the preliminary planning that started with the estimate for Markland Locks. Once the contractor became the successful bidder, planning, especially on details, intensified as dates for putting the general plan in effect approached. Of course, the word "planner" refers to more than one person. Also it must be stated, as Robert Burns once wrote, "The best laid plans of mice and men gang aft a-gley." A little extra high water in the Summer held up coffer work slightly while one mill rolling of a barge of heavy section sheet pile was required for the last two cells. Also a labor tie-up with the electricians slowed down the plant erection so that Spring arrived this year before the plant was ready to run. However, the contractor got ahead on rock excavation and form building and by May 15, 1957 he was ready to roll. (Fig. 12)

Fig. 9. Clean-up of the bottom of the cofferdam after dewatering. Rock drilling began as soon as muck and loose stone were removed.

Fig. 10. Placing concrete in a foundation pour with a 3 C. Y. bucket swung into position by a 50-ton gantry crane. Buckets were hauled from the mixing plant by dinkey locomotives like that at the upper left of the picture.

Fig. 11. Concreting the upper guard wall extension. Concrete, in 2 C. Y. buckets, was ferried from the mixing plant by small barges and placed by whirler derrick boats.

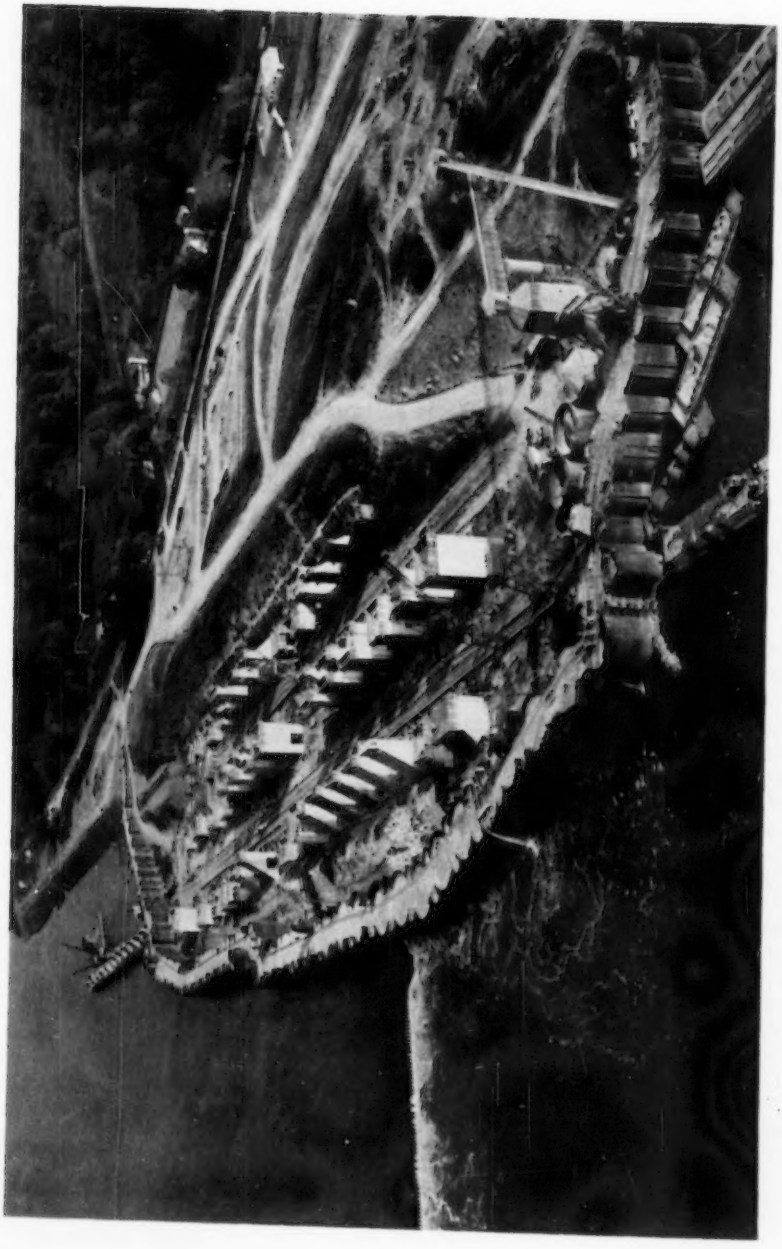

Fig. 12. Aerial view of Markland Locks in late Fall, 1957.

## CONCLUSIONS

Plant layout and construction methods must be simple, fool-proof and flexible. They must also result in economical over-all costs. Simple plant with expensive delivered prices on material or complicated and expensive plant with cheap materials will not ordinarily result in a successful bid. The trick is in selecting the most advantageous method before making a detailed estimate. Since there usually is not enough time to estimate all possibilities before bidding, this phase of a contractor's planning activities is one of the most important to a successful business.

Paper 1573 March, 1958 WW 2

Journal of the
WATERWAYS AND HARBORS DIVISION
Proceedings of the American Society of Civil Engineers

# BREAKING WAVE FORCE PREDICTION

R. L. Wiegel[1] and R. E. Skjei
(Proc. Paper 1573)

## ABSTRACT

Laboratory data of the kinematics of waves breaking on a model beach are analyzed and the resulting water particle velocities and accelerations are used in the Morison-O'Brien-Johnson-Schaaf wave force theory to predict the force field for piles of three different diameters. Comparisons of results with predictions from a modified solitary wave theory are given.

## INTRODUCTION

In a previous paper (Wiegel and Beebe[5])* the problem of the design wave in shallow water was discussed. A modified solitary wave theory was presented and it was shown to predict the velocity profile of the water particles under the crest of a breaking wave (in the laboratory) with an average deviation of zero and a standard deviation of twenty-seven percent provided the actual wave crest velocities be known. In addition, it was found that using the average ratio of the measured wave crest velocity to the theoretical velocity, the velocity profile could be predicted with an average deviation of thirteen percent.

Accelerations were not considered in the previous paper, so a comparison was made of the accelerations computed from the "forced fit" solitary wave theory and those obtained by the velocity vector-subtraction method explained in a subsequent section of this chapter. These comparisons are shown in Table I, and show generally poor correlation.

It appeared that the modified solitary wave theory should be useful to the design engineer, provided the maximum total moment on a pile occurred when a breaker crest passed the pile, because of the good correlation between

Note: Discussion open until August 1, 1958. A postponement of this closing date can be obtained by writing to the ASCE Manager of Technical Publications. Paper 1573 is part of the copyrighted Journal of the Waterways and Harbors Division, Proceedings of the American Society of Civil Engineers, Vol. 84, No. WW 2, March, 1958.

*See Bibliography at end of paper.

1. Associate Research Engr., Inst. of Eng. Research, Univ. of Calif., Berkeley, Calif.

TABLE I. COMPARISON OF THEORETICAL AND MEASURED HORIZONTAL WATER PARTICLE ACCELERATIONS IN A BREAKER.

| Run No. | $x/h^* = 0.2$ | | | $x/h^* = 0.6$ | | | $x/h^* = 1.0$ | | |
|---|---|---|---|---|---|---|---|---|---|
| | Dist. above bottom | Meas. accel. | Theory accel. | Dist. above bottom | Meas. accel. | Theory accel. | Dist. above bottom | Meas. accel. | Theory accel. |
| | ft. | ft./sec.$^2$ | ft./sec.$^2$ | ft. | ft./sec.$^2$ | ft./sec.$^2$ | ft. | ft./sec.$^2$ | ft./sec.$^2$ |
| 22 | 0.55 | -4.4 | 5.50 | 0.55 | — | 7.98 | — | — | — |
| | 0.45 | -1.1 | 3.25 | 0.45 | 2.6 | 7.98 | 0.45 | — | 8.94 |
| | 0.35 | 6.2 | 2.19 | 0.35 | 13.9 | 5.50 | 0.35 | 15.8 | 6.92 |
| | 0.25 | 3.9 | 1.54 | 0.25 | 10.8 | 4.18 | 0.25 | 12.7 | 5.57 |
| | 0.15 | 6.7 | 1.16 | 0.15 | 8.3 | 3.25 | 0.15 | 19.2 | 4.57 |
| | 0.05 | — | 1.03 | 0.05 | 8.6 | 2.86 | 0.05 | 13.6 | 4.18 |
| 23 | 0.35 | — | 3.25 | 0.35 | — | 7.98 | 0.35 | — | 8.94 |
| | 0.25 | 8.5 | 1.90 | 0.25 | 15.7 | 4.99 | 0.25 | — | 6.34 |
| | 0.15 | 11.0 | 1.28 | 0.15 | 15.2 | 3.47 | 0.15 | 21.8 | 4.83 |
| | 0.05 | 8.6 | 1.06 | 0.05 | 11.7 | 2.93 | 0.05 | 16.2 | 4.25 |
| 24 | 0.35 | — | 5.18 | 0.35 | — | — | — | — | — |
| | 0.25 | 5.3 | 2.57 | 0.25 | 19.8 | 6.50 | 0.25 | — | 7.69 |
| | 0.15 | 11.2 | 1.48 | 0.15 | 15.3 | 3.99 | 0.15 | 22.6 | 4.92 |
| | 0.05 | 10.1 | 1.06 | 0.05 | 16.6 | 3.02 | 0.05 | 22.0 | 4.31 |
| 25 | 0.65 | - 2.3 | 6.18 | 0.65 | — | — | — | — | — |
| | 0.55 | 0 | 3.86 | 0.55 | — | 9.30 | — | — | — |
| | 0.45 | — | 2.57 | 0.45 | 12.2 | 6.40 | 0.45 | 20.2 | 7.63 |
| | 0.35 | — | 1.87 | 0.35 | 12.8 | 4.76 | 0.35 | — | 6.31 |
| | 0.25 | 4.3 | 1.42 | 0.25 | 9.8 | 3.80 | 0.25 | 14.8 | 5.15 |
| | 0.15 | 6.7 | 1.13 | 0.15 | 12.3 | 3.12 | 0.15 | 11.1 | 4.44 |
| | 0.05 | — | 1.03 | 0.05 | 7.0 | 2.86 | 0.05 | — | 4.18 |
| 26 | 0.85 | — | 5.57 | 0.85 | — | — | — | — | — |
| | 0.75 | — | 4.18 | 0.75 | — | 9.97 | — | — | — |
| | 0.65 | 3.0 | 3.06 | 0.65 | — | 7.40 | 0.65 | — | 8.46 |
| | 0.55 | 2.8 | 2.19 | 0.55 | 15.0 | 5.41 | 0.55 | — | 6.92 |
| | 0.45 | 10.3 | 1.74 | 0.45 | 13.8 | 4.63 | 0.45 | 9.6 | 6.01 |
| | 0.35 | — | 1.48 | 0.35 | — | 3.96 | 0.35 | 9.8 | 5.34 |
| | 0.25 | 12.7 | 1.22 | 0.25 | 8.3 | 3.35 | 0.25 | 13.4 | 4.67 |
| | 0.15 | 8.9 | 1.09 | 0.15 | 8.2 | 2.96 | 0.15 | 17.0 | 4.28 |
| | 0.05 | — | 1.00 | 0.05 | 10.2 | 2.83 | 0.05 | 15.8 | 4.12 |

* Note:

x = horizontal distance in direction of wave advance as measured from the wave crest

h = water depth below wave trough

the modified solitary wave theory and measurements for water particle velocities, together with the small effect of water particle accelerations under the crest. The only paper which to the authors' knowledge deals with the forces of prototype breaking waves (Morison, Johnson and O'Brien(1)) and which might indicate the degree to which the above condition would be fulfilled makes the statement that the time correlation was not precise enough to determine the time comparison between the water surface profile and the moment history on the pile. Because of the lack of field data it was decided to utilize Iversen's(2) data to plot water particle velocity and acceleration fields for breakers, and from these data to compute force fields and ultimately the total moments about the bottoms for a series of circular cylindrical piles. Since the data presented herein were analyzed, a laboratory study has been made by Hall(1). Hall found that the maximum total moment of a breaking wave on a pile occurred nearly at the wave crest, at least within the accuracy of one frame of a 16 millimeter movie taken at 32 frames per second.

## Procedure

The original data consisted of full-size-scale charts of particle velocities, plotted as vectors in the breaker region of a series of laboratory waves (Figure 1). From all of Iversen's data only five runs, at varying wave heights, had sufficient data for use in this problem. The vertical distance from the bottom to the crest of the breaker, $Y_b$, ranged from about 0.4 foot to 1.0 foot. The method by which the original data were compiled has been described by Iversen(2). From these charts of velocity vectors, acceleration vector charts were derived by the following procedure. Two successive charts were superimposed and vector-subtraction triangles drawn (Figure 2). From the change of velocity in a particular small area, the acceleration was computed by dividing the change of velocity by the time interval between the charts. The accelerations thus computed were assigned to the intermediate stage between the two charts from which the change of velocity was derived. These accelerations were plotted separately on the intermediate wave profile and analyzed into horizontal and vertical components. The original velocity charts were also reproduced, and the velocity vectors also analyzed into horizontal and vertical components. Lines of constant horizontal velocity distribution. Also, constant horizontal acceleration contours were plotted on a separate series of selected profiles to determine the horizontal acceleration distribution for this particular stage of the breaker.

The velocities obtained in this manner are probably satisfactory. However, the interpretation of the "accelerations" is not quite clear. It is believed that they correspond most closely to the total acceleration; that is, they include both convective and local accelerations.

Force charts were obtained for an incipient breaker by the following method. An acceleration chart was selected for the desired stage, and the velocity charts from which this acceleration chart was derived were again superimposed. The horizontal components of velocities over a small area were averaged to obtain an average horizontal velocity. This process, repeated over the area of the chart, resulted in an average horizontal velocity chart for the same intermediate profile for which accelerations were previously computed. This intermediate profile was divided into a one-inch grid

and horizontal velocities and horizontal accelerations averaged over the one-inch squares. The average values obtained were assigned to the centers of the squares.

The following formulas were used to compute the forces on the pile from the above data.

$$F_D = \tfrac{1}{2} C_D \rho A |u| u = \tfrac{1}{2} C_D \rho D |u| u$$

and

$$F_I = C_M \rho V \, du/dt = C_M \rho \pi(D^2/4) \, du/dt$$

where $F_D$ = drag force per unit length of pile (lbs./ft.), $C_D = 1.6$, $\rho$ = the mass density of the water (2.0 slugs/ft.$^3$), A = projected area of the pile per unit length (ft.$^2$/ft.), D = pile diameter (ft.), u = horizontal component of water particle velocity (ft./sec.), $F_I$ = is the inertial force per unit length of pile (lbs/ft.), $C_M$ = is the coefficient of mass (2.0), V = the pile volume per unit length (ft.$^3$/ft.) and du/dt = the horizontal component of total water particle acceleration (ft./sec.$^2$).

Force-per-unit-length values for the same one-inch squares were averaged and added algebraically over the grid and the lines of constant force per unit length were drawn on separate charts for pile diameters of 0.05 foot, 0.1 foot and 0.2 foot (Figures 3, 4 and 5). Moments were computed for three vertical positions in the breaker: the crest, the maximum-force position, and the still water level. These moments were obtained by the equation

$$M = F \cdot l \cdot S$$

where M = total moment about the bottom, F = horizontal component of force, l = length of vertical section for which F was averaged, and S = height of midpoint of the section above bottom (lever arm). Moments were summed for the length of the pile to give total moment about the bottom. Moments at the crests of solitary waves of the same heights were also calculated, using the modified solitary wave formula

$$C = 0.81 \sqrt{g \, Y_b}$$

and Table I of Reference (5) for the horizontal component of water particle velocities, where $Y_b$ is the breaker crest elevation above the bottom. The formula

$$F = \tfrac{1}{2} C_D \rho D |u| u$$

was used to obtain the force diagram from which the total forces were computed. The total force has no acceleration component at the crest since the solitary wave theory shows zero accelerations along the vertical line through the crest.

For comparison, an alternate procedure was used in addition for one run. An original velocity chart was selected, one which had been previously used on the second of two charts superimposed for acceleration computations and for the average horizontal velocity derivation. The profile was divided into a one-inch grid and velocities averaged over the one-inch squares and assigned

to the centers of the squares. The advantage here was that original velocities were used directly without any averaging inaccuracies being introduced. Next, accelerations were computed for the profile by using the change of velocities from the selected chart's preceding chart to the selected chart's succeeding chart. The accelerations were averaged and assigned to the centers of the one-inch grid squares as before. Forces were computed, averaged and added algebraically, and the total force contours drawn. This chart, when compared with the chart drawn by the original method, showed very little difference and had an almost identical force contour pattern.

## Results and Discussion

It is recognized that because the original velocities were derived from photographs taken from the side (profile view), the treatment is two-dimensional and ignores components of velocity which might exist at right angles to the plane of the chart. The effect of this particular limitation is to reduce the true length of the velocity vectors and to deal only with the chart-plane projection of the vector. This two-dimensional treatment will result in smaller velocity, or drag-force components of the total force. However, the components of acceleration in the planes parallel to the still water surface (SWL) are also ignored. The acceleration contour charts show, as a general pattern, the zero acceleration line intersecting the wave profile at a point slightly above (toward the crest) the intersection of the wave profile and the still water level, with negative acceleration (considering direction of wave advance as positive) in the area behind on the wave-crest side of this line (Figure 6).

Ignoring this component of acceleration in the negative area results in smaller negative calculated acceleration forces and thus result in increased total force. As the total force is the algebraic sum of the velocity and acceleration forces, these two effects tend to balance each other in the critical area near the crest of the wave.

The plotted contours of horizontal components of velocity show an approximately vertical zero line near the intersection of the SWL and the wave profile, with increasing contour lines of positive and negative velocity diverging radially from a center near the intersection mentioned. This pattern does not change extensively throughout the wave breaking except that an increasing positive area develops at the crest of the wave. In these runs a +1.5-ft./sec. contour generally extended horizontally from the intersection along the still water level, except for Run 26, the largest wave, in which a 2.0-ft./sec. velocity contour occupied this position (Figure 7).

As a wave breaks further, the outer ends of the positive contour curl upwards and a negative area follows. Generally, the maximum positive velocities observed were 2 to 4 ft./sec., except in the case of Run 26, the largest wave, which had values of from 5 to almost 8 ft./sec., the maximum negative velocities observed ranged from 1.0 to $<2.0$ ft./sec.

The acceleration contours, as previously mentioned, have a general pattern in which the zero value contour interesects the wave profile at a point slightly above the intersection of the SWL and the wave profile. This zero value contour slopes back toward the rear of the wave at varying angles to the vertical, ranging from an estimated $40^{\circ}$ to about $70^{\circ}$; the lower ends of the zero contour generally curved back toward the vertical or past the

vertical in some cases (Figure 8).

Small well-defined areas of maximum positive acceleration occurred slightly forward of the intersection of the still water level and the wave profile in all cases. The maximum positive accelerations observed were values of about 20 to 25 ft./sec.$^2$. There did not appear to be any well-defined corresponding small negative acceleration areas. Maximum negative accelerations observed were generally slightly smaller than the maximum positive, but they extended over broader areas.

Total forces per unit pile length were calculated for these runs using the formulas

$$F_I = C_M \rho (\pi D^2/4) du/dt$$

and

$$F_D = \tfrac{1}{2} C_D \rho D u^2$$

and using three pile diameters, 0.05 foot, 0.1 foot and 0.2 foot. The values of force per unit length, drawn as contours on the wave profile for selected profile are included as Figures 3, 4 and 5 (in the manner of Schurman[4]). Generally, the same sort of pattern exists for all runs with a maximum occurring forward of, or at the crest of, the wave. For Run 26, a large maximum area occurs at the crest. The original data, in the case of this wave, began with the wave well along in the process of breaking. The contours drawn for the 0.05-foot pile diameter, and with the same 0.5-lb./ft. interval, showed wider spacing than for the 0.1-foot diameter pile, of course, and also showed a shift of the center of the maximum force back toward the crest and the maximum velocity center, which is to be expected since the drag force becomes relatively more important as diameter decreases. The opposite effects are seen in the same contour maps, plotted for a 0.2-foot diameter pile. The center of maximum force shifts forward toward the maximum-acceleration center. Also, the contours are more closely spaced and have a considerably more vertical orientation.

Total moments about the bottom were calculated using the measured horizontal velocities and accelerations at three locations: at still water level, at the approximate location of the maximum total force, and at the crest. These were compared with the moments calculated using the procedure described in the previous section. The results are presented in Table II.

The results are quite close except for Run 26, (to be discussed later). It is apparent that the total moment which occurs at the crest due to the long moment arm is nearly the same as the total moment which occurs at the location of the maximum total force for the 0.05-foot, and the 0.1-foot pile. The inertia force becomes more important for the 0.2-foot pile since it varies directly with the square of the diameter, whereas the drag force varies with the first power of the pile diameter. Therefore, the location of the zero acceleration contour and the acceleration values are considerably more critical and this method of deriving accelerations undoubtedly is not sufficiently accurate.

The calculated values for Run 26 using the modified solitary wave equations fell considerably short of the moments derived from the measured velocities. It is believed that this is because in Run 26 the wave already is past the breaking point, and the measured value of $Y_b$ is not, therefore,

TABLE II. TOTAL MOMENTS ABOUT THE BOTTOM FOR THREE SIZES OF PILES

| Pile dia. D | Run No. | Wave per. T | Still water depth $d_m$ * | Wave ht. $H_m$* | Ht. of breaker $H_b$ | Crest elev. at brk'g $Y_b$ | Water depth at brk'g $d_b$ | Total Moments about Bottom: Computed, using meas. vel. and accelerations at wave crest | at pt. of max. force | at SWL | Calc. using modif. sol. wave theory (at crest) | Calc. using sol. wave theory (at crest) |
|---|---|---|---|---|---|---|---|---|---|---|---|---|
| ft. | | sec. | ft. | ft. | ft. | ft. | ft. | ft.-lbs. | ft.-lbs. | ft.-lbs. | ft.-lbs. | ft.-lbs. |
| 0.05 | 22 | 1.51 | 2.23 | 0.22 | 0.37 | 0.56 | 0.30 | 0.07 | 0.06 | .01 | 0.08 | |
| | 23 | 1.98 | 2.23 | 0.13 | 0.29 | 0.46 | 0.26 | 0.04 | 0.03 | .01 | 0.03 | |
| | 24 | 2.50 | 2.22 | 0.11 | 0.24 | 0.38 | 0.24 | 0.02 | 0.02 | .01 | 0.02 | |
| | 25 | 1.00 | 2.33 | 0.40 | 0.35 | 0.72 | 0.45 | 0.07 | 0.07 | .01 | 0.10 | |
| | 26 | 1.67 | 2.38 | 0.41 | — | {1.02<br>1.50 | — | 1.14 | 1.14 | .01 | {0.26<br>1.15** | |
| 0.10 | 22 | 1.51 | 2.23 | 0.22 | 0.37 | 0.56 | 0.30 | 0.14 | 0.13 | .03 | 0.15 | 0.23 |
| | 23 | 1.98 | 2.23 | 0.13 | 0.29 | 0.46 | 0.26 | 0.08 | 0.08 | .03 | 0.06 | 0.10 |
| | 24 | 2.50 | 2.22 | 0.11 | 0.24 | 0.38 | 0.24 | 0.06 | 0.04 | .03 | 0.03 | 0.05 |
| | 25 | 1.00 | 2.33 | 0.40 | 0.35 | 0.72 | 0.45 | 0.13 | 0.14 | .04 | 0.21 | 0.32 |
| | 26 | 1.67 | 2.38 | 0.41 | — | {1.02<br>1.50 | — | 2.23 | 2.23 | .03 | {0.52<br>2.30** | 0.80 |
| 0.20 | 22 | 1.51 | 2.23 | 0.22 | 0.37 | 0.56 | 0.30 | 0.25 | 0.31 | .13 | 0.30 | |
| | 23 | 1.98 | 2.23 | 0.13 | 0.29 | 0.46 | 0.26 | 0.20 | 0.26 | .11 | 0.13 | |
| | 24 | 2.50 | 2.22 | 0.11 | 0.24 | 0.38 | 0.24 | 0.13 | 0.21 | .11 | 0.07 | |
| | 25 | 1.00 | 2.33 | 0.40 | 0.35 | 0.72 | 0.45 | 0.24 | 0.29 | .17 | 0.41 | |
| | 26 | 1.67 | 2.38 | 0.41 | — | {1.02<br>1.50 | — | 4.61 | 4.61 | .13 | {1.04<br>4.60** | |

* Measured in the constant depth portion of the wave channel
** Using $Y_b = 1.5$ ft. -- see text

representative of the true wave. An attempt was made to extrapolate the profile of the original wave, from the smooth portion of the profile below the breaker and irregular crest of the wave. This extrapolation gave a steep profile and a value of $Y_b$ of 1.5 feet as compared with the measured $Y_b$ of 1.015 feet. Using the 1.5-foot value, moments were again calculated for Run 26 and the resulting values agreed quite well with those computed from the measured velocities, as seen in the table of moments. It is important to note that the field measurements in Reference (2) showed this same thing; that is, the forces exerted on the pile by a "foam line" of a certain height were considerably higher than the forces for a breaking wave of the same height.

Recent laboratory measurements by Hall(1) show that moments given in Table II are fairly reliable, but the scatter of the measurements indicate that it would be better to use the solitary wave velocity rather than 0.81 times the solitary wave velocity in computing the water particle velocities to be used in the wave force equation.

## CONCLUSIONS

It appears that the solitary wave theory should be useful for the prediction of total moments about the bottom for piles of small size in breaking waves.

## ACKNOWLEDGMENTS

The analysis of the data presented in this paper was made under a grant from the National Science Foundation. The authors wish to express their appreciation to M. M. Lincoln for preparing the illustrations.

## REFERENCES

1. HALL, M. A., Laboratory study of breaking wave forces; Univ. of California, Inst. of Engineering Research, Tech. Report, Series 95, Issue 2, 38 pp., January 1957.
2. IVERSEN, H. W., Laboratory study of breakers, Gravity Waves, National Bureau of Standards, Cir. No. 521, pp. 9-32, November 1952.
3. MORISON, J. R., JOHNSON, J. W., and O'BRIEN, M. P., Experimental studies of forces on piles, Proc. of the Fourth Conference on Coastal Engineering, Council on Wave Research, The Engineering Foundation, pp. 340-370, 1954.
4. SCHURMAN, GLEN A., Storm wave force meter, Proc. of the First Conference on Coastal Engineering Instruments, Council on Wave Research, The Engineering Foundation, pp. 166-172, 1956.
5. WIEGEL, R. L., and BEEBE, K. E., The design wave in shallow water, Journal of the Waterways Division of the ASCE, vol. 82, WW1 (Paper 910), 21 pp., March 1956.

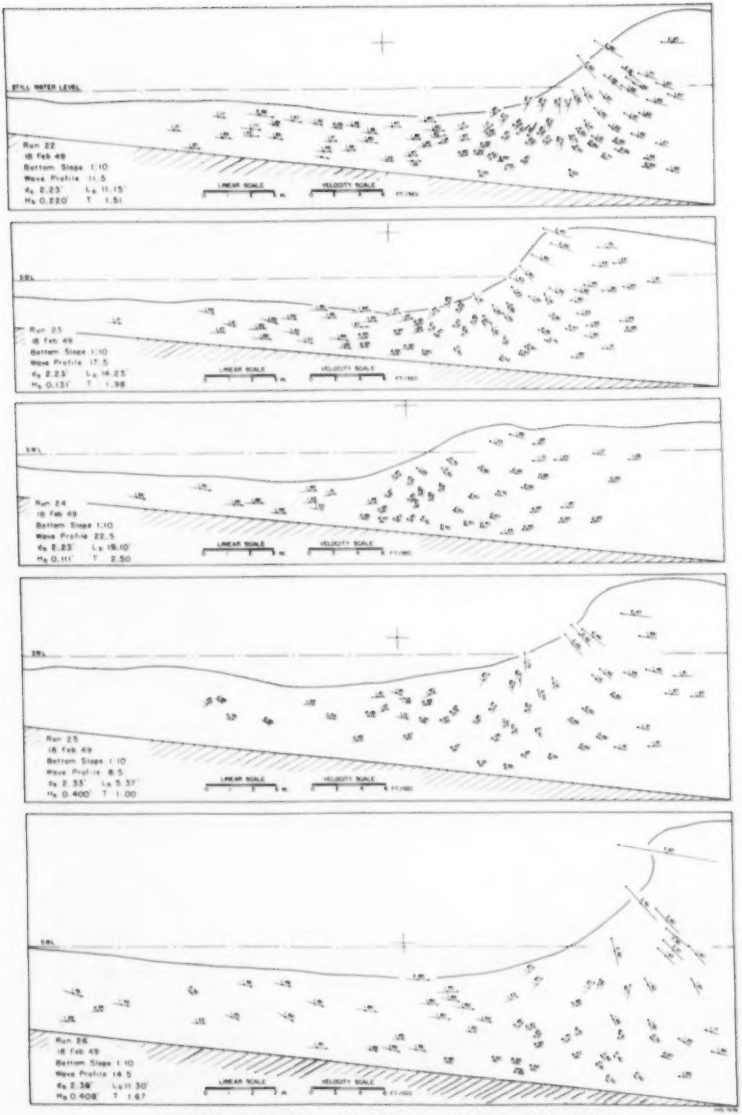


WATER PARTICLE VELOCITIES IN BREAKING WAVES

*(after Iversen)*

FIGURE 1

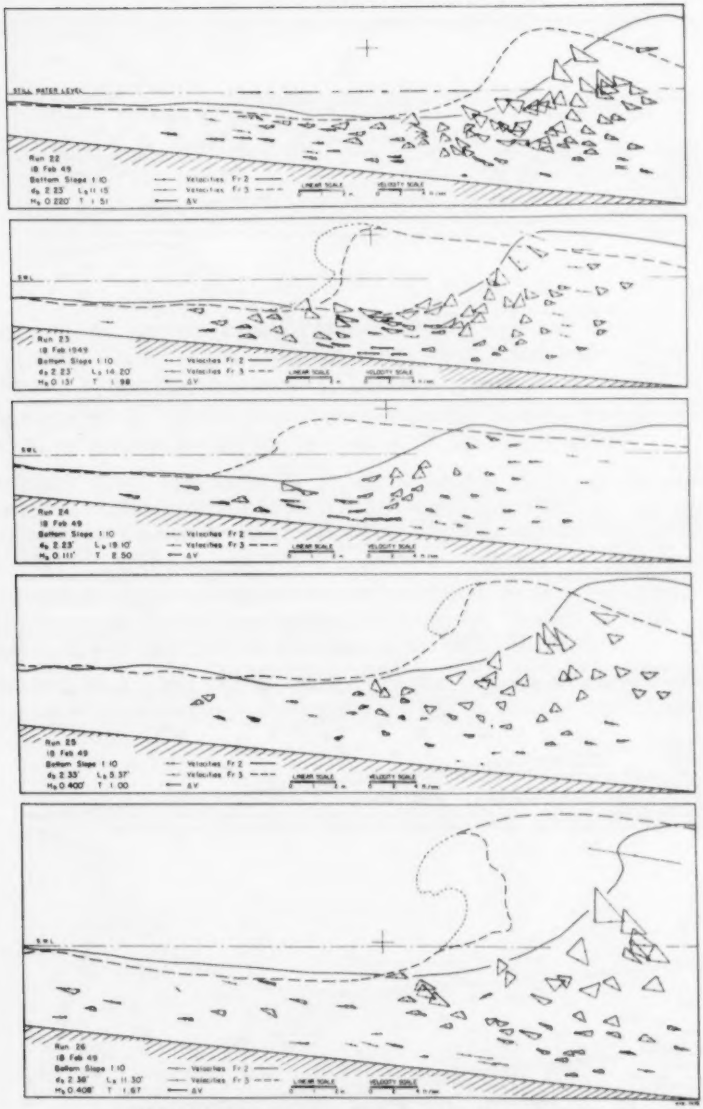


WATER PARTICLE ACCELERATIONS IN BREAKING WAVES

FIGURE 2

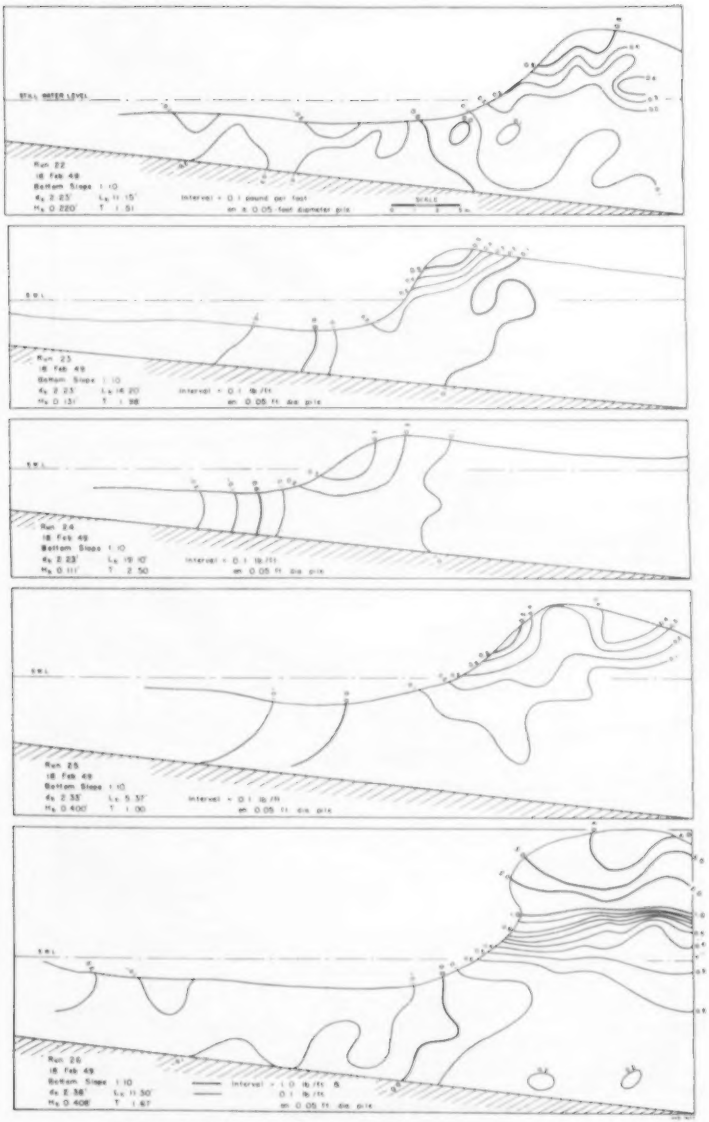


FORCE CONTOURS, 0.05-FOOT DIAMETER PILE IN BREAKING WAVES

FIGURE 3

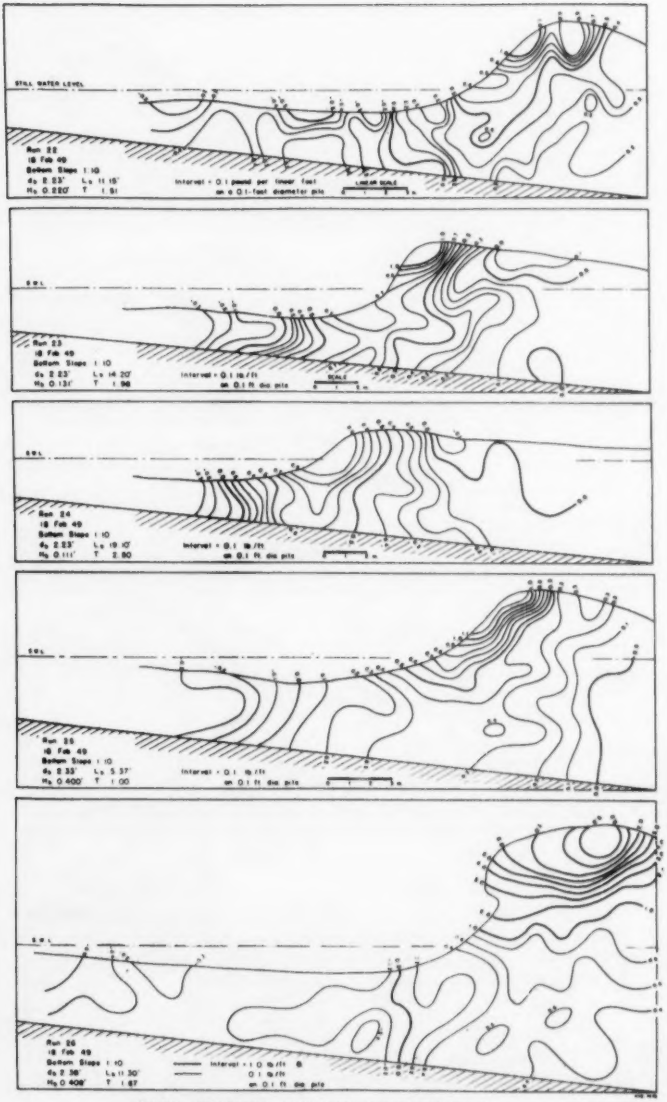


FORCE CONTOURS, 0.10-FOOT DIAMETER PILE
IN BREAKING WAVES

FIGURE 4

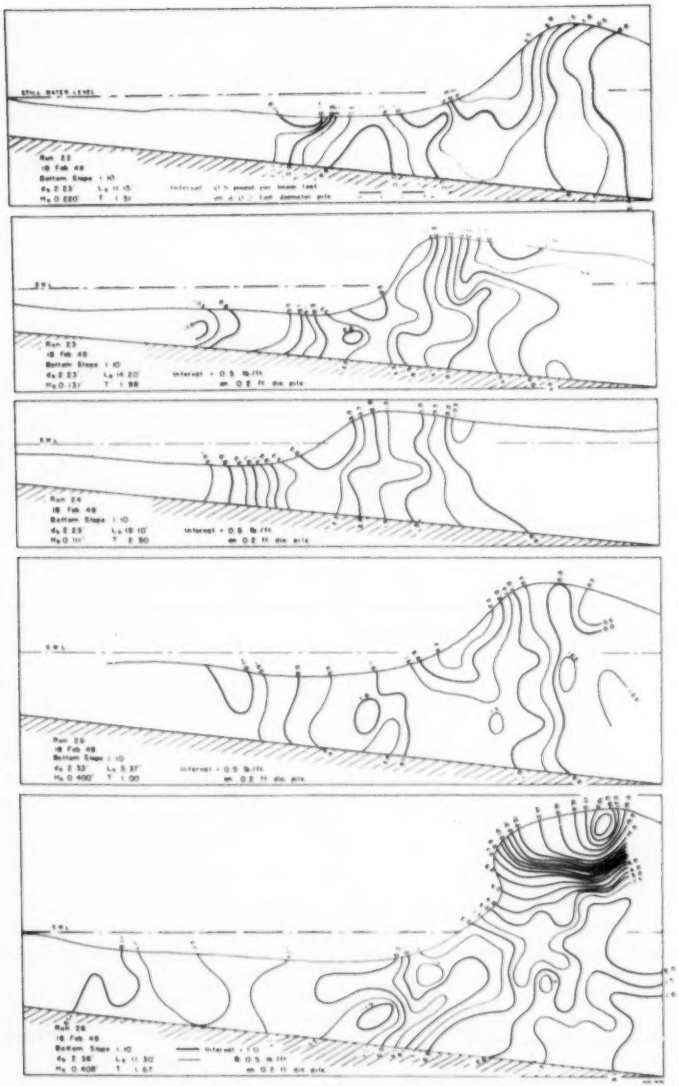

FORCE CONTOURS, 0.20-FOOT DIAMETER PILE IN BREAKING WAVES

FIGURE 5

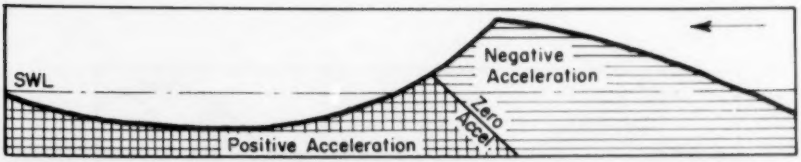


Positive and Negative Acceleration Areas

FIGURE 6

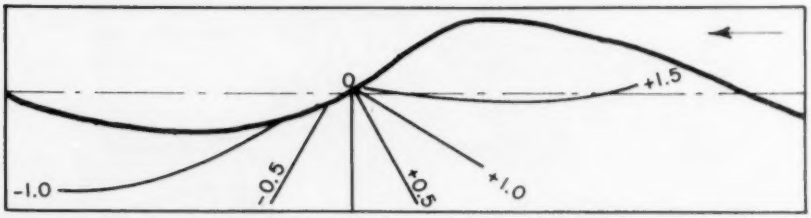


Horizontal Velocity Contours

FIGURE 7

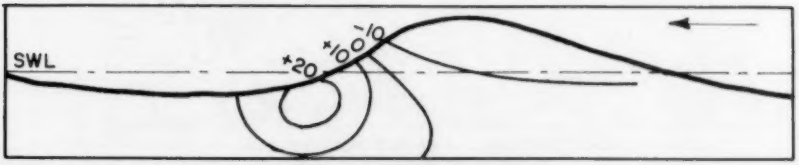


Horizontal Acceleration Distribution

FIGURE 8

Paper 1579 March, 1958 WW 2

Journal of the
WATERWAYS AND HARBORS DIVISION
Proceedings of the American Society of Civil Engineers

CONTENTS

DISCUSSION
(Proc. Paper 1579)

Page

Cellular Cofferdams and Docks, by E. M. Cummings.
(Proc. Paper 1366. September, 1957. Prior discussion:
none. Discussion closed.)
by Samuel Heyman . . . . . 1579-3
by Cevdet Z. Erzen. . . . . 1579-5

Note: Paper 1579 is part of the copyrighted Journal of the Waterways and Harbors Division, Proceedings of the American Society of Civil Engineers, Vol. 84, WW 2, March, 1958.

# CELLULAR COFFERDAMS AND DOCKS[a]

Discussion by Samuel Heyman and
Cevdet Z. Erzen

SAMUEL HEYMAN,* J.M. ASCE.—Mr. Cummings is to be complimented for presenting some new ideas on a difficult subject and for publishing the results of his tests. Additional tests on cellular cofferdams are required for determining where in the fill the actual plane of failure occurs; however, Cummings' results are a valuable addition to the available data on the behavior of cellular cofferdams.

In his paper, Cummings states that $\phi$ was determined from the force required to make the model slide. After making several tests, he divided the average horizontal force required to make the cell start to slide by the weight of the cell; this yielded the tangent of the angle of internal friction, $\phi$, of the soil. After several trials, he decided that the average angle of internal friction was $38^{\circ}\ 56'$. Cummings uses this $\phi$ value of $38^{\circ}\ 56'$ to compute the theoretical strength of the test cell and then shows how well the actual test results agree with the theoretical. This is unjustified since the angle of internal friction was determined from the test results themselves and not by an independent method.

The following analysis has been made to demonstrate two ideas. The first is that all the major methods of cellular cofferdam design become invalid at extreme, unrealistic values of $\phi$. The second is a comparison of the various design methods in the range of practical values.

To demonstrate the first idea, the resisting moment of the cohesionless fill as determined by Cummings has been compared with the resisting moment of the cohesionless fill as determined by Terzaghi.(1) Terzaghi states that the unit shearing resistance along a vertical plane of the cohesionless fill is equal to $\frac{1}{2}\ \gamma h^2\ C \tan\phi$ where C is the horizontal earth pressure coefficient. Terzaghi analyzed this force, and from the dimensions of cells which have worked satisfactorily decided that C "must be considerably greater than the active Rankine pressure" coefficient and "for the middle part of the fill in the cells ranges between 0.4 and 0.5." The author, however, in the discussion of Terzaghi's method considers it as using the active Rankine pressure along the vertical plane. In the published discussions of Terzaghi's paper,(2) Professor Krynine demonstrated (and Terzaghi approved(3)) by a Mohr's Circle analysis that this coefficient C should be equal to

a. Proc. Paper 1366, September, 1957, by E. M. Cummings.

1. Head, Sails Dept., Frederic R. Harris, Inc. New York, N. Y.

$$\frac{\cos^2 \phi}{2 - \cos^2 \phi}$$

Terzaghi's formula for the moment of resistance of the cohesionless earth fill in the cofferdam against vertical shear is

$$M_s = \frac{\gamma b h^2}{3} C \tan \phi$$

When the relationship of b = 0.85h is assumed,

$$M_s = 0.283 \gamma h^3 C \tan \phi$$

For any given cell $0.283 \gamma h^3$ is a constant; and C tan $\phi$, and therefore $M_s$, varies solely with $\phi$.

The moment of resistance of the sand as expressed by Cummings in formula 6 is equal to

$$M_s = \gamma \left( \frac{ac^2}{2} + \frac{c^3}{3} \right)$$

Substituting c = b tan $\phi$, a = h-b tan $\phi$, and Terzaghi's relationship b = 0.85h, this formula reduces to:

$$M_s = (0.283 \gamma h^3) \left[ 0.362 \tan \phi \ (3.53 - \tan \phi) \right] \tan \phi = 0.283 \gamma h^3 M \tan \phi$$

Where: $C=M= 0.362 \tan \phi \ (3.53 - \tan \phi)$

"M" will be called the Cummings Coefficient. Since both Terzaghi's and Cummings' expression of $M_s$ can be reduced to the same form, it is sufficient to compare the variation of the "C tan $\phi$" term in each case.

On the following graphs is a comparison of the various "C" coefficients that are used in the design of cofferdams. The following designations are used on the graph:

$$C=M= 0.362 \tan \phi \ (3.53 - \tan \phi), \quad C=K=\frac{\cos^2 \phi}{2-\cos^2 \phi}, \quad C=T_{min}=0.4, \quad C=T_{max}=0.5$$

and

$$C=A=\tan^2\left(45 - \frac{\phi}{2}\right)$$

The term C tan $\phi$ rather than C alone has been plotted against $\phi$ because C tan $\phi$ is the entire parameter which varies with $\phi$, and because it is consistent with the author's C tan $\phi$ presentation. As can be determined from this graph when $\phi = 90^o$, the Cummings' Coefficient "M" times tan $\phi$ approaches minus infinity. Describing Terzaghi's method the author, believing that Terzaghi's method utilizes active Rankine pressure for failure along a vertical plane through the fill, points out that when $\phi$ becomes $90^o$ "the shear, and thus the resisting moment against tilting, would be zero, as though the cells were left filled with water." Using the Cummings' method, when

$\phi = 90^{o}$ the shearing resistance of the material within the cell would be infinitely worse than plain water.

As stated above, the original formulae were not set up for such extreme values of $\phi$. In the case of Cummings' formulae the values of "a" and "c" can never be greater than "h," which would limit the value of $\phi$ to approximately $47^{o}$ using the b = 0.85h relationship. This demonstrates that all theories give impossible results for impossible $\phi$ values.

The values of C tan $\phi$ in the range of practical values of $\phi$ for a cohesionless soil are shown on the accompanying charts. As can be seen, the Cummings' design method is the least conservative for $\phi$ greater than $30^{o}$, and that using the coefficient of active pressure times the tangent of $\phi$ for shear along a vertical plane is the most conservative design method by a wide margin. For $\phi$ less than $30^{o}$ Krynine's method is less conservative than the Cummings', and at $\phi = 30^{o}$ the maximum of Terzaghi's range is within 20% of both Cummings' and Krynine's values. Because the differences in design coefficients, especially near $\phi = 30^{o}$, are smaller than the normal factor of safety used in design, cellular cofferdams have been successfully designed by the various methods discussed herein.

## REFERENCES

1. "Stability and Stiffness of Cellular Cofferdams" by Karl Terzaghi, Transactions ASCE Vol. 110 1945 P. 1083.
2. Ibid. Discussion by D. P. Krynine P. 1175.
3. Ibid. Discussion by Karl Terzaghi P. 1187.

CEVDET Z. ERZEN*—Mr. Cummings considers horizontal planes in a cellular cofferdam as the planes of failure due to shear in soil and introduces a theory based on this assumption. This concept seems justifiable when a model with 3/4 inch thick vertical planks which correspond to very stiff piles in the prototype is observed. Inasmuch as the back of the model stays straight, thus producing deflection varying linearly, considering the theories of Rankine and Coulomb there is no reason why the planes of failure in the cell must be horizontal.

The use of 3/4 inch planks in 19-1/8" x 24-1/2" x 24" cells which corresponds to very stiff piles in the prototype creates doubts as to the exact duplication of the behavior of cells with flexible sheet piles.

Dimensional analysis of such a system renders

$$u = \frac{F}{EL} f\left(\frac{F}{EL^2}, \frac{B}{EL^4}\right)$$

where

u = deflection of sheet piling
F = applied external load
B = flexural rigidity of pile
L = length of pile
E = modulus of elasticity of material

*Frederic R. Harris, Inc., New York, N. Y.

Denoting the scale factor of the model by K, there are obtained

$$K_u = \frac{K_F}{K_E K_L}, \quad K_F = K_E K_L^2, \quad K_B = K_E K_L^4$$

Taking the modulus of elasticity of white pine at 1,250,000 psi, the following are found:

$$K_E = \frac{30,000}{1,250} = 24$$

$$K_F = 24\ K_L^2$$

$$K_B = 24\ K_L^4$$

$$K_u = K_L$$

Assuming that the cofferdam is ten times the size of the model

$$K_F = 2,400$$

$$K_B = 240,000$$

$$K_u = 10$$

In other words, the line load applied on the cofferdam is

$$F = \frac{200}{2}\ (2,400) = 240 \text{ kpf}$$

The flexural rigidity of the sheet pile is found to be

$$E_p I_p = (240,000)\ \frac{1}{12}\ (12)\ (.75)^3\ E_m$$

where the subscripts p and m denote prototype and model respectively. Solving for Ip there is found:

$$I_p = \frac{10/100}{24} = 4,220 \text{ in}^4 \text{ per ft.}$$

This is equivalent to using 24 WF160 instead of the MP101 or MP102 sections which possess almost negligible moment of inertia.

Since the bending of such a heavy section is insignificant, deflection varies linearly from zero at the bottom to a maximum at top. If it were assumed that this would produce slip planes due to shear on horizontal planes, then the theory introduced in the paper would be correct. However, according to Rankine or Coulomb theory the planes of failure are different from the horizontal planes.

It is further attempted to show the existence of two zones, namely, active and passive, by means of pull-out tests on rods embedded in sand. In the opinion of this writer, the proximity of the outer rods to the boundary must be considered in evaluating the results, especially in tests indicated in Figs. 6 (b) and 7 (b) where no external force is applied. Neither the plastic nor the elastic concept of stress in circular discs can justify the substantial difference in loads in Fig. 6 (b). Therefore, it seems logical to consider the effect of the boundary on the stresses acting on the rods.

In the paper, the resisting moment of the cell against overturning forces is considered to be the sum of the resistance due to interlock friction and that due to shearing strength of the soil. Clearly, the moment of resistance of each pile is PLfb, if there exists no stress on the cross sectional area of diaphram or if this stress is constant. However, there exists bending stresses on the cross sections of the piles even when the cells are not embedded (as in the case of cells on rock), by virtue of the bending stresses in the soil which are transferred to the diaphragms through shear acting between the piles and the soil inside the cell. Therefore, the moment of resistance is not due to interlock friction acting at the ends of the diaphram, but it is due to the vertical shear at center which is some portion of the triangular area under the cell arising from the bending of the cell. Thus, this moment is

$$M_f = \frac{2}{3} \text{ Pfb} \tag{1}$$

The difference between the external moment and the above value must be resisted by shear in the soil acting on a vertical plane.

The writer has used the concept of the existence of plastic and elastic zones within a cell in the design of cofferdams. Such an analysis should be consistent with the laws of statics and Coulomb's theory. Irrespective of the dimensions of a cell there may exist an elastic zone. The forces in the plastic zone are given according to Rankine's or Coulomb's theory. Once these forces and the two zones are determined, the stresses in the elastic zone may be calculated by treating this section separately with all the known loads from the plastic zone acting on it.

The failure of the cell is possible if the maximum shearing strength of the soil in the cell is exceeded unless the overturning moment is less than the moment given by eq. (1) and also the sliding along its base is prevented. These principles may be explained by considering a cell resting on rock and holding back a fill.

In Fig. 1 (a) is shown such a cell. The area ABCDA is in a state of plastic equilibrium where the shear in the vertical and horizontal planes is zero. The active pressure on plane AB is

$$Pa = \frac{1}{2} \gamma_2 h^2 Ka$$

where subscript 2 refers to the plastic zone and similarly subscript 1 will refer to the fill outside the cell. This pressure is transmitted through the diaphragms to the back piles of the cell and is resisted by the elastic zone. If the elastic zone is ADFA, the total force acting on DF is

$$\frac{1}{2} \gamma_1 h^2 \text{ Ka} + \frac{1}{2} \gamma_2 h^2 Ka (1-\alpha_D^2)$$

and the shear on the base AF is

$$S = \frac{1}{2} \gamma_1 h^2 Ka \tag{2}$$

If G is the mid point between A and F, and assuming the shear is equally distributed between AG and GF, the total normal force on plane GJ is found from a free body diagram of forces acting on ICFGI or IGABI. Summing up forces in the X direction there is found:

$$N = \frac{1}{2}\ \gamma_1\ h^2 Ka + \frac{1}{2}\ \gamma_2\, h^2 Ka\,(1 - \alpha_j^2) - \frac{S}{2} \qquad (3)$$

where the second term is the force due to the pull in the diaphragm between G and J. The maximum shearing stress in the soil may be found from Mohr's circle of stress. For this purpose, normal and shearing stresses at mid point between G and J must be shown. The average normal stress on GJ is

$$\sigma_x = \frac{N}{GJ}$$

and the normal stress on a horizontal plane is

$$\sigma_y = \gamma_2\ \frac{h + \alpha_J h}{2}$$

The shear on plane GJ is found from the moment of the fill about the base. Since the external moment is resisted by the soil and the sheet piling, the moment due to soil is given by

$$Ms = M - M_f$$

and the vertical shear on plane GJ is

$$V = 3/2\ \frac{Ms}{b}$$

The average shear on this plane is

$$\tau = \frac{V}{GJ}$$

Knowing $\sigma x$, $\sigma y$ and $\tau$, one may obtain the maximum shear stress and the normal stress on the plane where this shear exists. These stresses may be also found from the formulae

$$\tau \max = \sqrt{(\frac{\sigma x - \sigma y}{2})^2 + \tau^2}$$

$$\sigma n = \frac{\sigma x + \sigma y}{2}$$

If $\tau \max > \sigma n \tan \phi$, then failure occurs internally and Ms becomes zero. In this case, in order that the external forces of the fill may be still resisted, the moment of the interlock friction must be greater than the external moment.

The boundaries of the elastic zone are determined from a consideration of the laws of statics. The elastic zone is not necessarily a triangle ADFA as shown in Fig. 1, but it may have the boundary AJEFA. To find this zone a free body diagram is drawn of a vertical section through H as in Fig. 1 (b) where the volume of soil HEFKH is considered separated from the sheet piles. Therefore, only the forces acting on the soil above HE and those acting on the sheet piles are considered.

Summing up the forces in the X direction there is found as the first condition

$$Pa_1\ \alpha_E^2 + Pa_2\ (\alpha_E^2 - \alpha_H^2) > P_p\,(\alpha E^2 - \alpha_H^2) \qquad (4)$$

and the second condition is that due to overturning. Taking moment about E,:

$$Pa_1 \alpha_E^2 \frac{\alpha E^h}{3} + Pa_2 \ (\alpha E^2 - \alpha H^2) \ \bar{y} >$$

$$P_p \ (\alpha_E^2 - \alpha_H^2) \ \bar{y} + Pa_2 f \ (1-\beta^2) \ \bar{x} \qquad (5)$$

where the last term is the friction force in the interlock. These are the two equations which determine the elastic zone.

As an example consider the cell shown in Fig. 7. With $\gamma$ = 91.9 pcf, h=2', $\phi$ = 38° - 56', the following are found: Tan $\phi$ = 0.81, Ka = 0.228, Kp - 4.39, $P_p$ = 803 lb., $Pa_2$ = 42 lb.

Taking $\alpha_E$ = 1 there is found $\alpha_H^2$ = 0.428. The first terms in eq. (5) is the moment of the external force about E, or according to Fig. 7

$$Ry > 2 \ (P_p - Pa_2) \ \ (\alpha E^2 - \alpha H^2) \ \bar{y}$$

$$= 2 \times 761 \times 0.572 \times .321 = 279'\#$$

which is the maximum moment that can be developed. The maximum value of R is 485# which is determined from the consideration of sliding on the base. Maximum moment of 279 ft. lb. is a good approximation to the actual test results and the curve Ry = 279 ft. lb. follows the curve obtained from tests very closely.

Shear on the bottom is R = 200 lb. Assuming this to vary according to a parabola, the shearing force within a distance of 3 inches (where the rod is located) is 13 lb. Force on the back of 2 ft. wide cell is R + $2Pa_2$ or 284 lb. The normal force at three positions of the rod are

$$N_1 = 284 - 13 = 271 \text{ lb.}$$

$$N_2 = 284 - 100 = 184 \text{ lb.}$$

$$N_3 = R + Pa_2 \ (1 - 0.75^2) - 187 = 50 \text{ lb.}$$

from which the force necessary to pull each rod becomes

$$P_1 = \frac{271}{24.5} \ \ 2.5 \times 2 \times 0.81 = 45 \text{ lb.}$$

$P_2$ = 30 lb., $P_3$ = 10 lb.

Example given in Fig. 12 is treated here for demonstration. The elastic zone starts at A and makes an angle of 27.5° with the vertical and changes to 30° as shown in Fig. 2. First, eq. (4) is used to find if there is any possibility of a failure plane through L. Here, L corresponds to point E, and B to H of Fig. 1. In eq. (4),

$$Pa_1 \ \alpha_E^2 = 96$$

$$Pa_2 \ (\alpha E^2 - \alpha H^2) = 31, \quad P_p \ (\alpha E^2 - \alpha H^2) = 426$$

since $Pa_1 \ \alpha E^2 + Pa_2 \ (\alpha E^2 - \alpha H^2) \not> P_p \ (\alpha E^2 - \alpha H^2)$

failure does not occur along BL. Similarly eqs. (4) and (5) are not satisfied for failure along ME. Therefore, the elastic zone is bounded by line ABC.

Total shear along NM is S = 147 - 75 = $72^k$ and the normal force on KG, with

$$\alpha_A^2 - \alpha_G^2 = 0.85$$

$$N = 147 + 87 \times .85 - \frac{72}{2} = 185^k$$

Therefore

$$\sigma x = \frac{185}{74} = 2.5 \text{ ksf}$$

The vertical pressure mid way between K and G is

$$\sigma y = 5.2 \text{ ksf}$$

and

$$Ms = 6098 - 623 - \frac{2}{3}\ 1306 = 4605$$

$$V = \frac{3}{2}\ \frac{Ms}{b} = 128^k$$

giving

$$\tau = \frac{128}{74} = 1.74 \text{ ksf}$$

Using these values the max shear is found to be

$$\tau \max = 2.21 \text{ ksf}$$

and

$$\sigma n = 3.8 \text{ ksf}$$

$$\tau \text{all.} = 3.85 \times 0.70 = 2.70 \text{ ksf}$$

since $\tau$ all $> \tau$ max. the soil is in a state of elastic equilibrium. However, in other cases the maximum shearing stress in the lower zone may exceed the maximum allowable shear in which case there exists a state of plastic equilibrium through the cell.

The theory given by the writer determines these zones through the use of eqs. (4) and (5) and also establishes the state of equilibrium of the lower zone - whether elastic or plastic. If the lower zone is in a plastic state, as a first condition, the external moment must be resisted by the moment of the interlock friction. The second condition of equilibrium is that due to sliding. For equilibrium the sliding forces must be less than the sum of the resisting forces and the shear on the bottom due to overburden. Finally, the equilibrium of the overturning moment of the external forces must be satisfied.

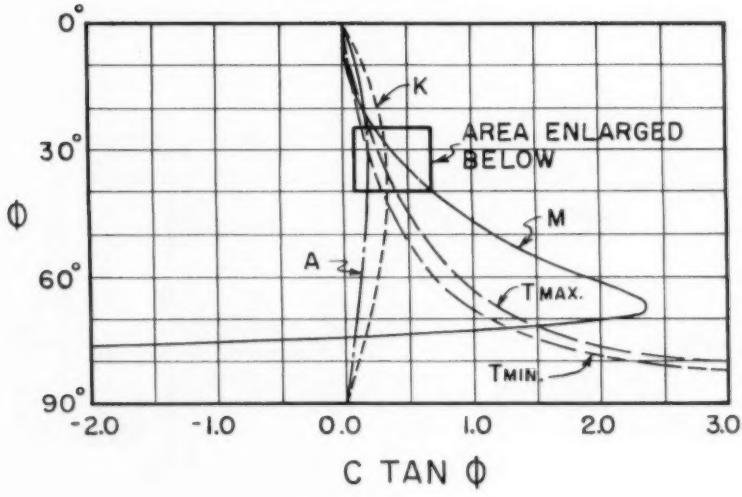


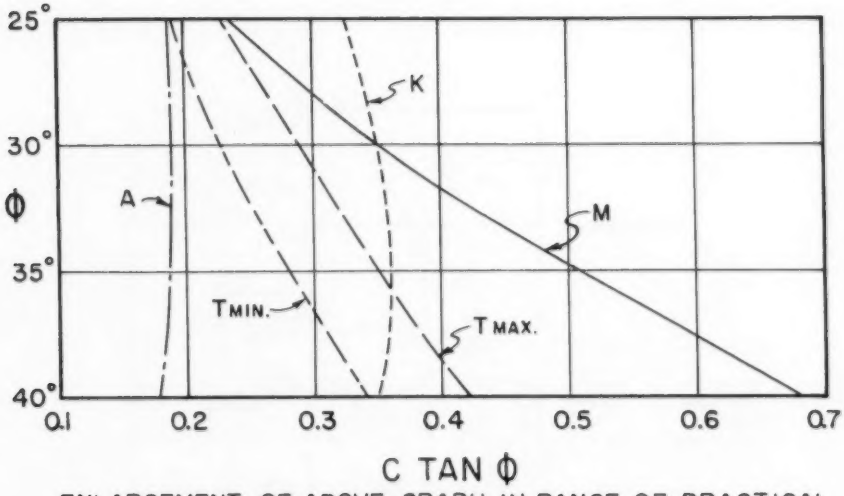


ENLARGEMENT OF ABOVE GRAPH IN RANGE OF PRACTICAL VALUES OF Φ

$M = 0.362(3.53 - \tan\Phi)\tan^2\Phi$ (CUMMINGS)

$K = \frac{\cos^2\Phi}{2 - \cos^2\Phi}\tan\Phi$ (KRYNINE)

$T_{MIN.} = 0.4\tan\Phi$, $T_{MAX.} = 0.5\tan\Phi$ (TERZAGHI'S RANGE)

$A = \tan^2(45 - \frac{\Phi}{2})\tan\Phi$

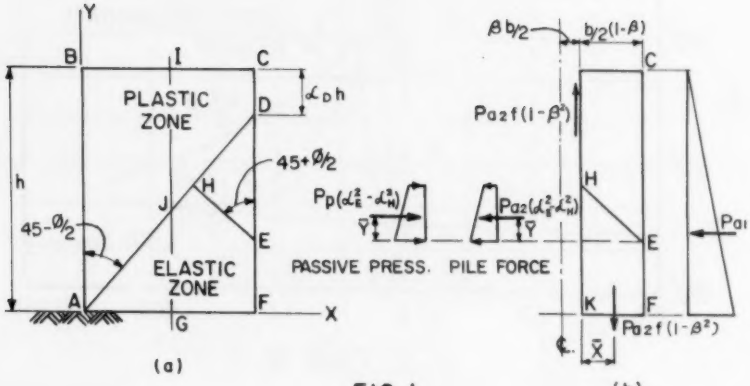
Y
B
I
C
PLASTIC ZONE
D
h
H
J
45+Ø/2
45-Ø/2
E
ELASTIC ZONE
A
F
G
X
(a)
PASSIVE PRESS.
PILE FORCE
βb/2
b/2(1-β)
H
E
K
F
(b)

FIG. 1

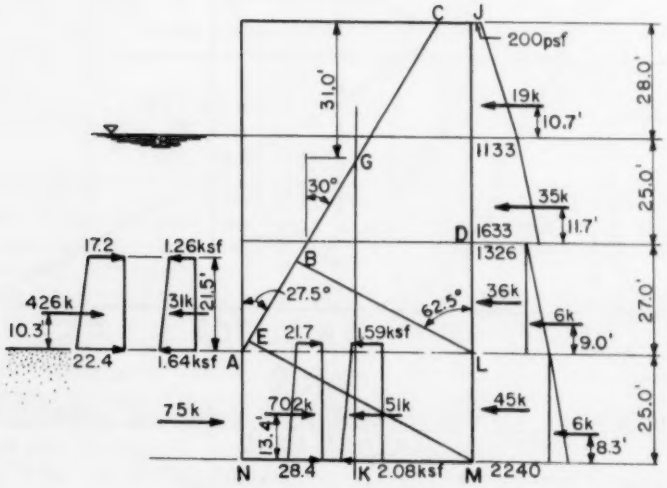
C
J
200psf
31.0'
19k
10.7'
28.0'
1133
G
30°
35k
11.7'
25.0'
D
1633
1326
17.2
1.26ksf
B
426k
10.3'
31k
21.5'
27.5°
62.5°
36k
6k
9.0'
27.0'
E
21.7
1.59ksf
22.4
1.64ksf
A
L
75k
702k
51k
45k
6k
8.3'
25.0'
13.4'
N
28.4
K 2.08ksf
M 2240

FIG. 2

## PROCEEDINGS PAPERS

The technical papers published in the past year are identified by number below. Technical-division sponsorship is indicated by an abbreviation at the end of each Paper Number, the symbols referring to: Air Transport (AT), City Planning (CP), Construction (CO), Engineering Mechanics (EM), Highway (HW), Hydraulics (HY), Irrigation and Drainage (IR), Pipeline (PL), Power (PO), Sanitary Engineering (SA), Soil Mechanics and Foundations (SM), Structural (ST), Surveying and Mapping (SU), and Waterways and Harbors (WW), divisions. Papers sponsored by the Board of Direction are identified by the symbols (BD). For titles and order coupons, refer to the appropriate issue of "Civil Engineering." Beginning with Volume 82 (January 1956) papers were published in Journals of the various Technical Divisions. To locate papers in the Journals, the symbols after the paper numbers are followed by a numeral designating the issue of a particular Journal in which the paper appeared. For example, Paper 1449 is identified as 1449 (HY 6) which indicates that the paper is contained in the sixth issue of the Journal of the Hydraulics Division during 1957.

### VOLUME 83 (1957)

MARCH: 1186(ST2), 1187(ST2), 1188(ST2), 1189(ST2), 1190(ST2), 1191(ST2), 1192(ST2)c, 1193 (PL1), 1194(PL1), 1195(PL1).

APRIL: 1196(EM2), 1197(HY2), 1198(HY2), 1199(HY2), 1200(HY2), 1201(HY2), 1202(HY2), 1203 (SA2), 1204(SM2), 1205(SM2), 1206(SM2), 1207(SM2), 1208(WW1), 1209(WW1), 1210(WW1), 1211(WW1), 1212(EM2), 1213(EM2), 1214(EM2), 1215(PO2), 1216(PO2), 1217(PO2), 1218 (SA2), 1219(SA2), 1220(SA2), 1221(SA2), 1222(SA2), 1223(SA2), 1224(SA2), 1225(PO)[c], 1226 (WW1)[c], 1227(SA2)[c], 1228(SM2)[c], 1229(EM2)[c], 1230(HY2)[c].

MAY: 1231(ST3), 1232(ST3), 1233(ST3), 1234(ST3), 1235(IR1), 1236(IR1), 1237(WW2), 1238 (WW2), 1239(WW2), 1240(WW2), 1241(WW2), 1242(WW2), 1243(WW2), 1244(HW2), 1245(HW2), 1246(HW2), 1247(HW2), 1248(WW2), 1249(HW2), 1250(HW2), 1251(WW2), 1252(WW2), 1253 (IR1), 1254(ST3), 1255(ST3), 1256(HW2), 1257(IR1)[c], 1258(HW2)[c], 1259(ST3)[c].

JUNE: 1260(HY3), 1261(HY3), 1262(HY3), 1263(HY3), 1264(HY3), 1265(HY3), 1266(HY3), 1267 (PO3), 1268(PO3), 1269(SA3), 1270(SA3), 1271(SA3), 1272(SA3), 1273(SA3), 1274(SA3), 1275 (SA3), 1276(SA3), 1277(HY3), 1278(HY3), 1279(PL2), 1280(PL2), 1281(PL2), 1282(SA3), 1283 (HY3)[c], 1284(PO3), 1285(PO3), 1286(PO3), 1287(PO3)[c], 1288(SA3)[c].

JULY: 1289(SM3), 1290(EM3), 1291(EM3), 1292(EM3), 1293(EM3), 1294(HW3), 1295(HW3), 1296 (HW3), 1297(HW3), 1298(HW3), 1299(SM3), 1300(SM3), 1301(SM3), 1302(ST4), 1303(ST4), 1304 (ST4), 1305(SU1), 1306(SU1), 1307(SU1), 1308(ST4), 1309(SM3), 1310(SU1)[c], 1311(EM3)[c], 1312 (ST4), 1313(ST4), 1314(ST4), 1315(ST4), 1316(ST4), 1317(ST4), 1318(ST4), 1319(SM3)[c], 1320 (ST4), 1321(ST4), 1322(EM3), 1323(AT1), 1324(AT1), 1325(AT1), 1326(AT1), 1327(AT1), 1328 (AT1)[c], 1329(ST4)[c].

AUGUST: 1330(HY4), 1331(HY4), 1332(HY4), 1333(SA4), 1334(SA4), 1335(SA4), 1336(SA4), 1337 (SA4), 1338(SA4), 1339(CO1), 1340(CO1), 1341(CO1), 1342(CO1), 1343(CO1), 1344(PO4), 1345 (HY4), 1346(PO4)[c], 1347(BD1), 1348(HY4)[c], 1349(SA4)[c], 1350(PO4), 1351(PO4).

SEPTEMBER: 1352(IR2), 1353(ST5), 1354(ST5), 1355(ST5), 1356(ST5), 1357(ST5), 1358(ST5), 1359(IR2), 1360(IR2), 1361(ST5), 1362(IR2), 1363(IR2), 1364(IR2), 1365(WW3), 1366(WW3), 1367(WW3), 1368(WW3), 1369(WW3), 1370(WW3), 1371(HW4), 1372(HW4), 1373(HW4), 1374 (HW4), 1375(PL3), 1376(PL3), 1377(IR2)[c], 1378(HW4)[c], 1379(IR2), 1380(HW4), 1381(WW3)[c], 1382(ST5)[c], 1383(PL3)[c], 1384(IR2), 1385(HW4), 1386(HW4).

OCTOBER: 1387(CP2), 1388(CP2), 1389(EM4), 1390(EM4), 1391(HY5), 1392(HY5), 1393(HY5), 1394(HY5), 1395(HY5), 1396(PO5), 1397(PO5), 1353(PO5), 1399(EM4), 1400(SA5), 1401(HY5), 1402(HY5), 1403(HY5), 1404(HY5), 1405(HY5), 1406(HY5), 1407(SA5), 1408(SA5), 1409(SA5), 1410(SA5), 1411(SA5), 1412(EM4), 1413(EM4), 1414(PO5), 1415(EM4)[c], 1416(PO5)[c], 1417 (HY5)[c], 1418(EM4), 1419(PO5), 1420(PO5), 1421(PO5), 1422(SA5)[c], 1423(SA5), 1424(EM4), 1425(CP2).

NOVEMBER: 1426(SM4), 1427(SM4), 1428(SM4), 1429(SM4), 1430(SM4)[c], 1431(ST6), 1432(ST6), 1433(ST6), 1434(ST6), 1435(ST6), 1436(ST6), 1437(ST6), 1438(SM4), 1439(SM4), 1440(ST6), 1441(ST6), 1442(ST6)[c], 1443(SU2), 1444(SU2), 1445(SU2), 1446(SU2), 1447(SU2), 1448(SU2)[c].

DECEMBER: 1449(HY6), 1450(HY6), 1451(HY6), 1452(HY6), 1453(HY6), 1454(HY6), 1455(HY6), 1456(HY6)[c], 1457(PO6), 1458(PO6), 1459(PO6), 1460(PO6)[c], 1461(SA6), 1462(SA6), 1463(SA6), 1464(SA6), 1465(SA6), 1466(SA6)[c], 1467(AT2), 1468(AT2), 1469(AT2), 1470(AT2), 1471(AT2), 1472(AT2), 1473(AT2), 1474(AT2), 1475(AT2), 1476(AT2), 1477(AT2), 1478(AT2), 1479(AT2), 1480(AT2), 1481(AT2), 1482(AT2), 1483(AT2), 1484(AT2), 1485(AT2)[c], 1486(BD2), 1487(BD2), 1488(PO6), 1489(PO6), 1490(BD2), 1491(BD2), 1492(HY6), 1493(BD2).

### VOLUME 84 (1958)

JANUARY: 1494(EM1), 1495(EM1), 1496(EM1), 1497(IR1), 1498(IR1), 1499(IR1), 1500(IR1), 1501(IR1), 1502(IR1), 1503(IR1), 1504(IR1), 1505(IR1), 1506(IR1), 1507(IR1), 1508(ST1), 1509(ST1), 1510(ST1), 1511(ST1), 1512(ST1), 1513(WW1), 1514(WW1), 1515(WW1), 1516(WW1), 1517(WW1), 1518(WW1), 1519(ST1), 1520(EM1)[c], 1521(IR1)[c], 1522(ST1)[c], 1523(WW1)[c], 1524(HW1), 1525(HW1), 1526(HW1)[c], 1527(HW1).

FEBRUARY: 1528(HY1), 1529(PO1), 1530(HY1), 1531(HY1), 1532(HY1), 1533(SA1), 1534(SA1), 1535(SM1), 1536(SM1), 1537(SM1), 1538(PO1)[c], 1539(SA1), 1540(SA1), 1541(SA1), 1542(SA1), 1543(SA1), 1544(SM1), 1545(SM1), 1546(SM1), 1547(SM1), 1548(SM1), 1549(SM1), 1550(SM1), 1551(SM1), 1552(SM1), 1553(PO1), 1554(PO1), 1555(PO1), 1556(PO1), 1557(SA1)[c], 1558(HY1)[c], 1559(SM1)[c].

MARCH: 1560(ST2), 1561(ST2), 1562(ST2), 1563(ST2), 1564(ST2), 1565(ST2), 1566(ST2), 1567(ST2), 1568(WW2), 1569(WW2), 1570(WW2), 1571(WW2), 1572(WW2), 1573(WW2), 1574(PL1), 1575(PL1), 1576(ST2)[c], 1577(PL1), 1578(PL1)[c], 1579(WW2)[c].

---

c. Discussion of several papers, grouped by divisions.

# AMERICAN SOCIETY OF CIVIL ENGINEERS

## OFFICERS FOR 1958

### PRESIDENT

LOUIS R. HOWSON

### VICE-PRESIDENTS

*Term expires October, 1958:*
FRANCIS S. FRIEL
NORMAN R. MOORE

*Term expires October, 1959:*
WALDO G. BOWMAN
SAMUEL B. MORRIS

### DIRECTORS

*Term expires October, 1958:*
JOHN P. RILEY
CAREY H. BROWN
MASON C. PRICHARD
ROBERT H. SHERLOCK
R. ROBINSON ROWE
LOUIS E. RYDELL
CLARENCE L. ECKEL

*Term expires October, 1959:*
CLINTON D. HANOVER, Jr.
E. LELAND DURKEE
HOWARD F. PECKWORTH
FINLEY B. LAVERTY
WILLIAM J. HEDLEY
RANDLE B. ALEXANDER

*Term expires October, 1960:*
PHILIP C. RUTLEDGE
WESTON S. EVANS
TILTON E. SHELBURNE
CRAIG P. HAZELET
DONALD H. MATTERN
JOHN E. RINNE

### PAST PRESIDENTS

*Members of the Board*

ENOCH R. NEEDLES

MASON G. LOCKWOOD

---

EXECUTIVE SECRETARY
WILLIAM H. WISELY

TREASURER
CHARLES E. TROUT

ASSISTANT SECRETARY
E. LAWRENCE CHANDLER

ASSISTANT TREASURER
CARLTON S. PROCTOR

---

# PROCEEDINGS OF THE SOCIETY

HAROLD T. LARSEN
*Manager of Technical Publications*

PAUL A. PARISI
*Editor of Technical Publications*

FRANCIS J. SCHNELLER, JR.
*Assistant Editor of Technical Publications*

---

### COMMITTEE ON PUBLICATIONS

HOWARD F. PECKWORTH, *Chairman*
PHILIP C. RUTLEDGE, *Vice-Chairman*

E. LELAND DURKEE
TILTON E. SHELBURNE
R. ROBINSON ROWE
LOUIS E. RYDELL